June 2019

In Vitro Evaluation of Ovarian Cancer Tumorigenesis as a Function of Quinone Oxidoreducatse-1 and Cell Phenotype

Milcah S. Jackson
Louisiana State University and Agricultural and Mechanical College

IN VITRO EVALUATION OF OVARIAN CANCER TUMORIGENESIS AS A FUNCTION OF QUINONE OXIDOREDUCTASE-1 AND CELL PHENOTYPE

A Dissertation

Submitted to the Graduate Faculty of the
Louisiana State University and
Agricultural and Mechanical College
in partial fulfillment of the
requirements for the degree of
Doctor of Philosophy

in

The Department of Chemistry

by
Milcah S. Jackson
B.A., University of Mississippi, 2014
August 2019

This dissertation is dedicated to my loving grandmother:

Easter C. Jordan (May 5, 1930-July 27, 2012)

And to

My parents, Brenda and Ricky

My sisters and brothers;

Their unconditional love and unwavering support

Of me as I embarked upon this journey

Is greatly appreciated.

ACKNOWLEDGEMENTS

First and foremost, I would like to thank my advisor, Prof. Robin L. McCarley, for the support and encouragement he has provided throughout my graduate studies. Under his leadership, I was allowed to decide how I would answer my research questions which, in turn, has molded me into an independent researcher. He is one of the most intelligent and well-rounded people I have ever met, and I'm thankful to have had him as my advisor.

I would also like to acknowledge my committee members, Prof. Samuel D. Gilman and Prof. Kermit Murray, for their support and advice throughout my time here at LSU. I would also like to thank Prof. Martha Littlefield for her willingness to serve as the dean's representative on my dissertation committee.

To my McGroup family, both past and present, I would like to thank you all for your continued support, advice, and friendship. I would like to thank former McGroup member, Dr. Bijeta Prasai, for her patience and guidance at the start of my graduate career. I would also like to give thanks to Dr. Zhenhua Shen, who never hesitated to assist me with any task or answer my questions no matter how ridiculous they were. I would also like to give special thanks to Shaniqua Hayes for never hesitating to assist me, even if it meant traveling to campus on a Saturday morning to let me back into the lab after locking myself out. She is a great friend, and I am forever indebted to her.

Finally, to my mom, Brenda; older brother, Ricky Jr.; my sisters, Avondra, Lindsay, and Amber; my new friends, Stephanie, Kwan and Ashley; my forever friends, Natasha, Ty'Neshia, Jalesa, Brittany, and Marquisha; and my NOBCChE family; thank you all for your support, encouragement, for being confidants, providing comfort in times of sadness, and for always reminding me that I have made it this far because I worked hard for it.

TABLE OF CONTENTS

LIST OF TABLES

LIST OF FIGURES

LIST OF SCHEMES

LIST OF ABBREVIATIONS AND SYMBOLS

ALDH	Aldehyde dehydrogenase
ALDHA1	Aldehyde dehydrogenase isozyme-1
ARE	Antioxidant response elements
ATCC	American Type Culture Collection
AZQ	Diaziquone
BAX	BCL2 apoptosis regulator
BCA	Bicinchoninic acid assay
BCL-2	B-cell lymphoma-2
BRCA 1	Breast cancer type 1
BRCA 2	Breast cancer type 2
BSA	Bovine serum albumin
CAM	Cell adhesion molecule
CD	Cluster differentiation
CD133	Prominin-1
cDNA	Complementary deoxyribonucleic acid
cm^3	Cubic centimeter
CSC	Cancer stem cells
Ct	Threshold cycle
CXRC-4	Chemokine receptor type 4
DAPI	4,6-diamidino-2-phenylindole
DCPIP	2,6-dichlorophenolindophenol
DIC	Differential interference contrast

DNA	Deoxyribonucleic acid
ECM	Extracellular matrix
EDTA	Ethylenediaminetetraacetic acid
EMT	Epithelial-to-mesenchymal transition
EO9	Indoloquinone
EpCAM	Epithelial cell adhesion molecule
ERK 1	Extracellular signal-regulated kinase 1
ERK 2	Extracellular signal-regulated kinase 2
ELDA	Extreme limited dilution assay
FAD	Flavin adenine dinucleotide
FADH	Reduced flavin adenine dinucleotide
FBS	Fetal bovine serum
FGF	Fibroblast growth factors
GLUT1	Glucose transporter 1
GLUT2	Glucose transporter 2
GSH	Glutathione
GSSH	Oxidized glutathione
H_2O_2	Hydrogen peroxide
HA	Hyaluronic acid
HGSOC	High-grade serous ovarian carcinoma
HIF	Hypoxia-inducible factor
HO-1	Heme oxygenase-1
HRP	Horseradish peroxidase

HSP	Heat shock proteins
LAS X	Leica application suite X
MET	Mesenchymal-to-epithelial transition
ICC	Immunocytochemistry
IF	Immunofluorescence
Keap 1	Kelch-like ECH-associated protein 1
MMC	Mitomycin C
MCTS	Multicellular tumor spheroids
MLL-ENL	Mixed-lineage leukemia-eleven nineteen leukemia
MOZ-TIF2	Monocytic leukemia zinc finger-transcription intermediary factor 2
NADH	Reduced nicotinamide adenine dinucleotide
NAD(P)H	Reduced nicotinamide adenine dinucleotide phosphate
NFκB	Nuclear factor kappa-light-chain-enhancer of activated B cells
NFDM	Non-fat dry milk
Nrf2	Nuclear Factor Erythroid related factor-2
NSCLC	Non-small cell lung cancer cells
NQO1	NAD(P)H:quinone oxidoreductase isozyme-1
OC	Ovarian cancer
O_3	Ozone
$\cdot O_2^-$	Superoxide radical
$\cdot OH$	Hydroxyl radical
PAX5	B-cell-specific activator protein
PBS	Phosphate-buffered saline

PBST	Phosphate-buffered saline-0.1% tween-20
PCAF	p300/CBP-associated factor
PFA	Paraformaldehyde
PI3K/AKT	Phosphoinositide 3-kinase/Protein kinase B
pRb	Retinoblastoma protein
Q_3	Quinone substrate
RIPA	Radioimmunoprecipitation assay
RNA	Ribonucleic acid
RNS	Reactive nitrogen species
ROS	Reactive oxygen species
RT-qPCR	Real-time quantitative polymerase chain reactions
SDS-PAGE	Sodium dodecyl sulphate-polyacrylamide gel electrophoresis
TBR	Target-to-background
TBST	Tris-buffered saline-0.1% tween-20 solution
TIFF	Tagged image file format
TGFβ–1	Transforming growth factor β–1
UV/Vis	Ultraviolet-visible
VEGF	Vascular endothelial growth factor
WEHI	Walter and Eliza Hall Institute
WT	Wildtype
ZEB1	Zinc-finger E-box binding homeobox 1
β–lap	β–lapchapone
ΔCt	Relative fold change in gene expression

λ_{em}	Emission wavelength

ABSTRACT

In vitro multicellular spheroids are attractive model systems for assessing genetic and epigenetic changes that occur in diseased tissues. Understanding how such alterations in gene and subsequent protein expression affect disease progression and metastasis, drug resistance, and recurrence is of great interest in cancer research. In this regard, examining expression and activity of proteins, such as those with cytoprotective ability that are overexpressed in cancer cells, in addition to cell phenotype (i.e., stem-like, epithelial, mesenchymal, or mixed), are two ways to evaluate genetic and epigenetic changes. Moreover, determining the impact that cytoprotective proteins and cell phenotype have on tumor formation would be beneficial to clinicians and drug developers, as this would provide suitable targets for diagnostic testing and anti-cancer therapies. One such cytoprotective protein is human NAD(P)H:quinone oxidoreductase-1 (NQO1), due to its overexpression in diseased tissues. To this end, the goal of this research is to determine if the expression and activity of NQO1 and cell phenotype in human tumor-derived ovarian cancer cell lines influences in vitro spheroid formation. Therefore, in this work will be detailed, characterization of four ovarian cell lines as a function of (**1**) NQO1 activity and expression in two-dimensional monolayers in addition to proliferative ability; (**2**) spheroid formation under anchorage-independent culture conditions and subsequent NQO1 expression and activity in said spheroids; and (**3**) the phenotype as determined from presence of cancer stem cell markers and epithelial-to-mesenchymal transition in monolayer and spheroid culture.

CHAPTER 1
INTRODUCTION

1.1 Research Goals and Aims

Understanding ovarian cancer (OC) metastasis is crucial for the development of more effective diagnostics and targeted therapies. More specifically, identifying factors that may be aiding in its progression, chemo-resistant nature, and ultimately recurrence, is significant. In this regard, taking a closer look at changes in expression and activity of cytoprotective enzymes, as well as changes in the phenotypic nature of ovarian cancer cells prior to and after treatment with chemotherapeutics, could be beneficial to clinicians. Research of this nature could also be useful in understanding key features associated with cancerous tissues like tumorigenesis and angiogenesis.

Human NAD(P)H:quinone oxidoreductase isozyme-1 (NQO1) is one cytoprotective enzyme of interest. Primarily located in the cytosol, it catalyzes the two-electron reduction of quinone substrates to hydroquinones.[1] This process ensures that semiquinone radical formation, which can be detrimental to the cells, is bypassed. Due to its overexpression in several cancerous tissues (e.g., pancreatic, breast, lung, colorectal, and ovarian), both its presence and activity toward substrates renders it beneficial for diagnostic testing and chemotherapy.[2-7] One such diagnostic technique is the use of NQO1-activatable fluorescent probes, such as those developed in the McCarley research group, which exploit the enzyme's reductive abilities, allowing visual detection of NQO1 presence in cancerous tissues.[8-14] Moreover, the enzyme could also play a significant role in the

formation, progression, and survival of solid tumors, thus again making it a target for chemotherapeutics like β-lapchapone (β-lap) and Mitomycin C (MMC).[15-17]

Aside from NQO1, research has shown that cancer cells can undergo phenotypic transitions like those observed during embryonic development. Solid tumor tissues are generally composed of cells with a more epithelial morphology, which is associated with less invasive cells. In contrast, as the cancer starts to metastasize, the expression of epithelial-associated biomolecules decreases, while increased expression of more invasive, mesenchymal cells is found.[16, 18-19] Mesenchymal cells are characterized as having an elongated morphology, similar to fibroblasts, and increased motility, thus allowing the cells to travel to distant sites within the body. It has been suggested that such plasticity in cancer cells is driven by a population of cancer stem cells (CSC), which could be controlling the adaptive nature of the cells prior to and after treatment.[20-21]

My research goal is to investigate ovarian cancer tumorigenesis as a function of oxidoreductase activity/expression and the cell phenotype. My first aim was to identify the presence of NQO1 in ovarian cancer cell monolayers of different origin (i.e., location in peritoneal cavity, stage of cancer, and treated/untreated) using traditional biochemical techniques such as western blotting, immunocytochemistry/immunofluorescence (ICC/IF), real-time quantitative polymerase chain reaction (RT-qPCR). After evaluating enzyme expression, I went on to examine its activity using an established spectrometric method which exploits its reductive capability. Furthermore, I used a novel near-infrared, “ON-ON” fluorescent probe, **Q_3NTCY**, developed by Dr. Zhenhua Shen during his time in the McCarley research group, for the visualization of NQO1 in ovarian cancer cells in two-dimensional and three-dimensional cultures. This probe offers the advantage of both the

probe and reporting moiety being fluorescent, but at different wavelengths. This quality is significant because it allows for detection of unreacted probe, as well as the reporting moiety that is released upon NQO1-initiated cleavage.

After determining expression and activity of NQO1 in cell monolayers, I then sought to evaluate its influence on the ability of cells to form three-dimensional multicellular tumor spheroid (MCTS) mimics under non-adherent culture conditions. By altering culture conditions, I was able to work with a system that better mimics solid tumors within the body, as cell monolayers are primarily composed of proliferating cells. MCTS offer the advantage of providing a heterogeneous population of cells with layers of proliferating, quiescent, or necrotic cells, each with differing levels of enzymatic expression and activeness due to interaction with oxygen and other nutrients needed for survival. Using this method would also highlight which cell lines can form spheroids under these conditions, which could then be related back to NQO1 expression/activity in cell monolayers. Moreover, due the cell lines being of different origin, it would allow them to be further categorized based on their sphere forming abilities.

Finally, I evaluated the phenotypic nature of cell monolayers and MCTSs, which could potentially be driven by the presence of cancer stem cells or stem-like cells. If CSC are found to be present in populations of the studied ovarian cancer cells, they could be the driving force behind chemoresistance, as well as phenotypic nature (e.g., non-invasive vs invasive) of the cancer cell lines. It is possible that cells undergo phenotypic transitions between 2D and 3D culture, which could yield more information about the behavior of such cells within the body. The epithelial-to-mesenchymal transition (EMT) describes the loss of cellular polarity and adherent nature observed in solid tumors and the emergence

of elongated cells with increased motility and invasive characteristics.[18-20, 22] It has also been suggested that a hybrid subtype of cells exist that exhibit features related to both epithelial and mesenchymal cells, indicating that these cells could be completely plastic in nature.

1.2 Cancer and Statistics

Cancer is defined as uncontrolled proliferation of cells in the body, whose cellular functions have been altered, thus causing them not to behave in the same manner as normal cells. Cancer-related deaths account for more than double the amount caused by AIDS, malaria, and tuberculosis, combined. In the United States, it is the second most prevalent cause of death after heart disease. It is estimated that in 2018 alone, roughly 1.7 million new cancer cases will arise, and 609,640 cancer-related deaths will occur.[23-24] While one specific cause of cancer has yet to be identified, researchers suggest that non-modifiable factors like genetics, hormones, and immune functions, as well as lifestyle choices (e.g., smoking vs not smoking, body weight, and diet) all influence disease onset and progression.[25] Although it has been suggested that by altering one's lifestyle choices, roughly 50% of cancers can be treated, it is critical that researchers identify ways to target and treat cancers related to changes at the cellular level.

In Figure 1.1 is a proposed mechanism depicting the spread of cancer in the body. It suggests that DNA mutation occurs leading to the disease initiation, followed by promotion, also referred to as clonal expansion, into the tissue, and finally progression/metastasis, which signifies that invasion of other tissues has occurred.[25] This process is thought to be driven by cellular mutations brought on by the changes in the

DNA or the cellular environment. Due to rapid proliferation, these mutated cells can then begin to proliferate and eventually give rise to progenitor cells that can go on to produce tumors.[25] Tumors are defined as growths that are either benign or localized at certain area in the tissues, or malignant, meaning that they can shed cells into neighboring tissues and the blood stream.[25-26] Malignant tumors can result in poor patient prognosis and resistance to chemotherapeutics due to constant changes to the cells' DNA.[25-26]

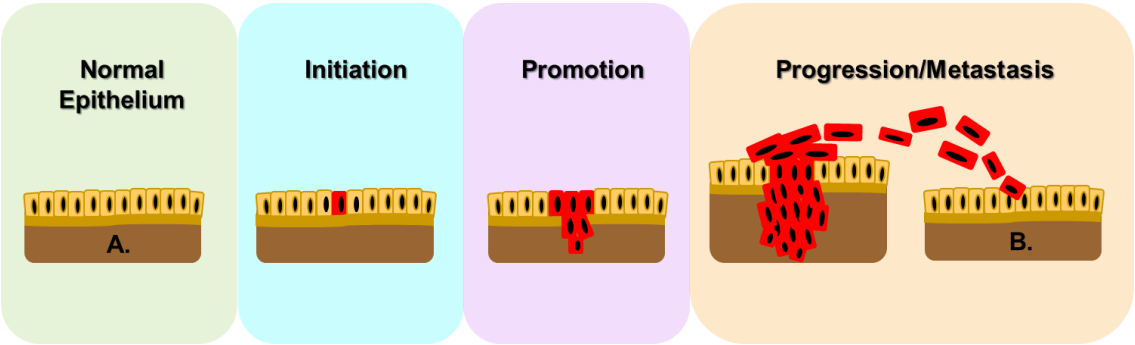

Figure 1.1. The evolution of cancer from normal epithelium to metastasis.

1.2.1 Ovarian Cancer and Statistics

Currently only three of the four most common types of cancer in the U.S. (i.e., lung, colorectal, and breast) affect both men and women. However, OC is ranked fifth in cancer-related deaths in women and has the highest mortality rate of cancers involving the female reproductive system. The American Cancer Society estimates that in 2018, over 22,000 women will have been diagnosed with OC, and over 14,000 women will die from it.[27] While it is more prominent in women over the age of 63, it is not uncommon for younger women to develop the disease. One key reason ovarian cancer is so lethal is that the disease is asymptomatic until it enters the advanced stages. Moreover, most cancers

typically spread to distant sites through the bloodstream, but it has been found that ovarian cancer metastasizes via clumps of shed cells in the peritoneal cavity, as demonstrated in Figure 1.2.

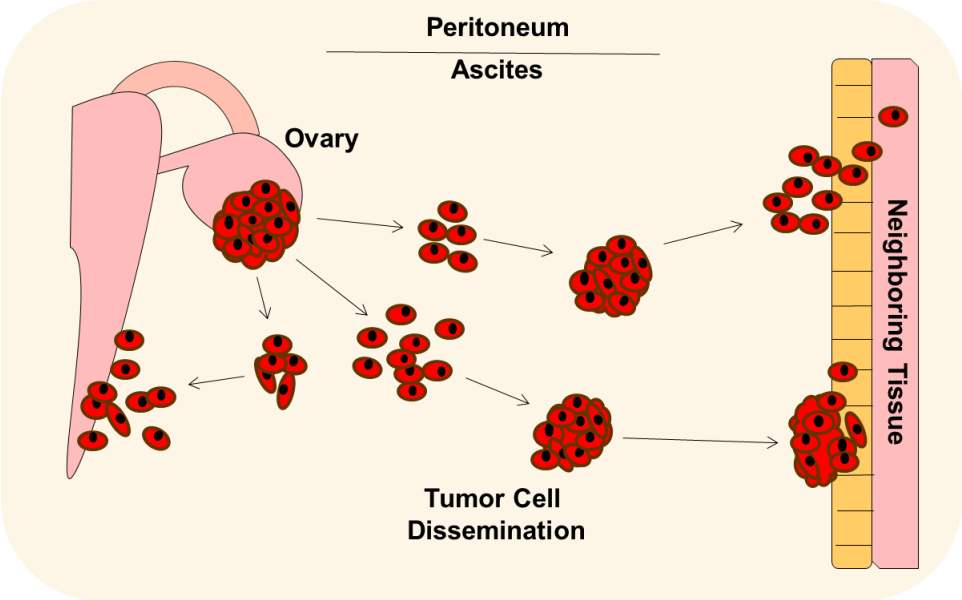

Figure 1.2. Proposed pathway of ovarian cancer metastasis.

Ovarian cancer can be divided into three types: epithelial, germ cell, and sex cord-stromal, with epithelial ovarian cancer being the source of roughly 90% of cases.[24] Epithelial ovarian cancer can further be split into four subtypes: serous, endometrioid, mucinous, and clear cell—all of which are characterized as diseases with different biological pathways, risks, and treatments.[23-24, 27] Serous OC accounts for over 50% of epithelial ovarian cancer cases. It has been shown to affect both ovaries, be highly aggressive, undetectable at early stages, and linked to poor patient survival.[24] More recently, it has been suggested that serous-grade ovarian cancer may originate in the uterine tubes and then disseminate to the ovaries and other sites within the peritoneal

cavity.[24, 28-30] Both mucinous and clear-cell carcinomas account for 6% of all OC cases of epithelial origin, while endometrioid carcinomas account for 10%.[24, 27] Endometrioid and clear-cell carcinomas are thought to derive from the lining of the uterus, and mucinous ovarian carcinomas from either the ovaries or the fallopian tube–peritoneal junction.[24, 27]

Aside from the epithelial subtype of OC, the two types of non-epithelial ovarian cancer, namely, germ-cell and sex cord-stromal, account for only about 5% of ovarian cancer cases.[24] Germ-cell carcinomas are derived from eggs in the ovary and are more common in younger women. On the contrary, sex cord carcinomas and stromal sarcomas are associated with several different cells (i.e., Leydig cells, Sertoli cells, and granulosa), as well as the tissues supporting the ovaries. Moreover, sex cord-stromal carcinomas are prevalent in women over the age of 50.[31] Because both types of non-epithelial ovarian cancer are rare, it is difficult for clinicians and physicians to diagnose them in the early stages. Furthermore, both are believed to be associated with hormonal and genetic changes in the body, and symptoms vary from irregular bleeding to development of male physical characteristics.[32-35]

1.2.2 Cancer Hallmarks and Metabolism

A simplified explanation of cancer's onset and progression was provided in Section 1.1. In this section, a more detailed review of major hallmarks of cancer and its metabolism will be provided. In 2000, Hanahan and Weinberg described cancer cells as having defects in regulatory systems that control normal cell homeostasis and proliferation.[36-37] They went on to suggest that six alterations in a cell's physiology result in malignancy, including a growth signal autonomy, bypassing antigrowth cues, avoiding

apoptosis, unrestricted proliferation, angiogenic switches, and finally invasion and metastasis, as depicted Figure 1.3.[36-37] Normal cells often take cues from the cell's microenvironment on when to undergo or halt mitosis. On the contrary, cancer cells have been found be less dependent on these environmental cues, due to their ability to synthesize their own growth factors. Moreover, due to overexpression of growth factor receptors on the surface of cancer cells, it has been suggested that low levels of their respective ligands can elicit a response leading to increased proliferation. In addition, cancerous cells have been found to switch the type of cell surface receptors that are expressed, which can lead to major changes in the way they behave.

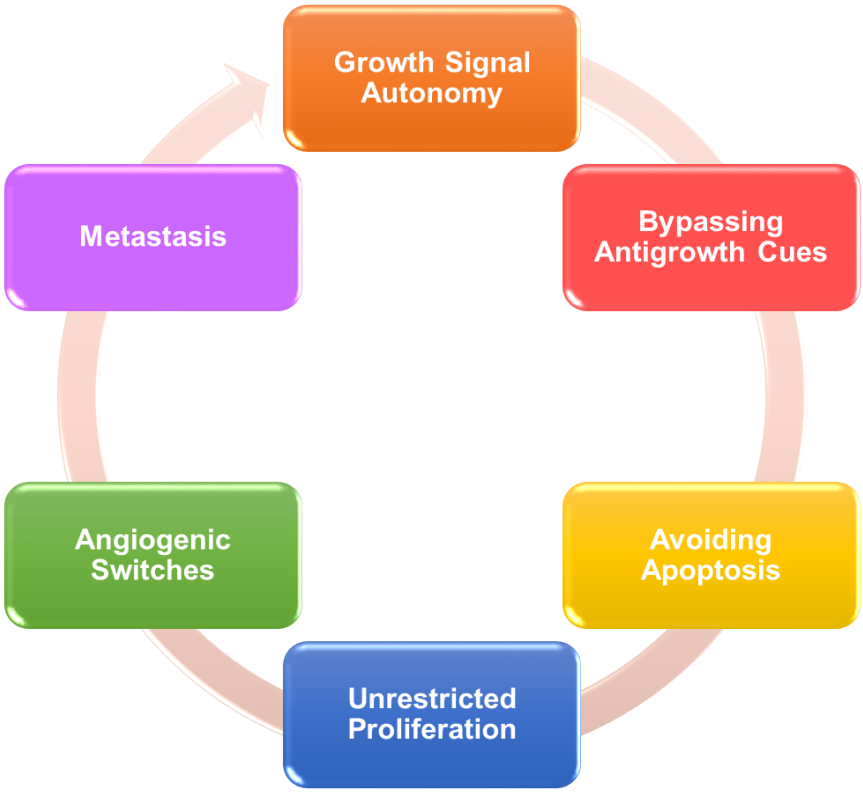

Figure 1.3. The six hallmarks of cancer.

Growth factor autonomy leads to cancerous cells being able to hijack certain signaling pathways that govern transcription factors favoring antiproliferation. For example, the retinoblastoma protein (pRb) is both a tumor suppressing protein and cell cycle regulator. Hypophosphorylation of pRb alters the function of E2F transcription factors—major contributors to cell cycle progression—resulting in cell cycle arrest and decreased proliferation.[37-38] However, cancer cells tend to block pRb's influence on E2F genes through several mechanisms, leading to enhanced proliferation.[37-38] Aside from altering cell cycle regulatory systems, cancerous cells can avoid apoptosis, or programmed cell death. This evasion of apoptosis has been linked to decreased expression or mutations in tumor suppressor gene p53. Also, overexpression and interaction of oncogenes like BCL-2 and myc, led to antiapoptotic events in lymphomas and serum-deprived fibroblasts.[37, 39-40] Therefore, it is plausible that unrestricted proliferation in cancer cells results in part from the combination of growth factor autonomy, bypassing antigrowth cues, and evading apoptosis.

In normal cells, the amount of times cells can undergo division and replication to produce a new progeny is often limited. Cellular senescence is the first barrier against uncontrolled growth. It is the process by which proliferative ability ceases, yet the cells remain viable.[41] However, some cells can bypass senescence, resulting in the second barrier—termed crisis—occurring, leading to widespread cell death. When viable cells emerge from the crisis phase, they are considered immortalized as they have evaded cell death.[41] Studies have shown that cancer cells are considered immortal due to their ability to bypass senescence and/or escape the crisis phase.[41-42] This ability has been largely associated with increased telomere presence at the ends of chromosomes, essentially

protecting the DNA from erosion that could potentially lead to death.[41-42] Therefore, proliferative ability leading to the generation of a new progeny is dependent on the telomeric presence. Cancer cells have been shown to exhibit increased telomerase, the enzyme responsible for adding more telomeres to chromosomal DNA, activity and expression not observed in normal cells.[41]

While the factors discussed above are key to cancer progression, angiogenesis—the growth of new blood vessels—ensures that oxygen and other nutrients are constantly supplied to tumors.[36-37, 43] It has been shown that angiogenic-activators, like vascular endothelial growth factor (VEGF) and fibroblast growth factors (FGF), are often found at elevated levels in cancerous tumor tissues, while proteins that act as inhibitors of the two are downregulated.[36-37, 44] Expression of VEGF and FGFs allow tumor tissues to recruit endothelial cells, which line blood vessels, thus giving them access to nutrients found in the blood supply.[45] Acquiring more oxygen and nutrients from the blood stream provides cancer cells with support for their rapid metabolism, thus ensuring their survival and synthesis of other nutrients.

However, tumors generally expand rapidly leading to slower diffusion of oxygen and nutrients from the bloodstream, resulting in a hypoxic environment and stabilization of hypoxia inducible factor (HIF).[46-47] HIF induces the production of glucose transporters (GLUT1 and GLUT2) and has been linked to angiogenesis by activating VEGF.[46-48] In fact, this environmental shift favors glycolysis in lieu of aerobic respiration via the mitochondria and was first described by Otto Warberg.[49] However, it is important to note that mitochondrial respiration still occurs, but the pathway is not as advantageous to highly proliferative cancerous cells. Moreover, enhanced HIF expression is influenced by

both glycolysis and mitochondrial respiration, due to highly reactive species that lead to stress being produced by both pathways.[50-51] It has been suggested that tumors take advantage of the hypoxic conditions, because they will lead to enhanced glucose transport and consumption, as well as allow for more glycolytic intermediates to be produced, thereby generating a wide variety of macromolecules essential for tumor growth and development.[43-45, 50] Also, glycolysis results in the formation of an abundance of lactate, an anaerobic product of the pathway, regardless of the amount of oxygen present. Increased lactate production is often counteracted by increasing the rate of glycolysis—which again can lead to the production of more HIF.[47, 50, 52]

Another nutrient that is found at elevated levels in tumor cells is glutamine. Glutamine is an essential amino acid involved in the synthesis of a variety of nitrogen-containing compounds from nucleotides to non-essential amino acids.[43] It has also been found to have a role in the transport of essential amino acids including leucine, tyrosine, and tryptophan to name a few. Due to their roles in biosynthesis of diverse nutrients needed for survival and maintenance, it is not surprising that both glucose and glutamine have been found to be overexpressed in tumorous tissues in comparison to normal tissues. It has also been suggested that growth factors in nutrient-deprived cells and the ECM enable increased uptake of glucose into cancerous cells.[44, 52]

1.2.3 Cellular Plasticity and Heterogeneity in Cancer

Cancer is a multidimensional disease. It arises from the various intrinsic and extrinsic alternations that occur within and around diseased cells that lead to heterogeneity and tumorigenesis. Moreover, these changes result in mixed populations

of cells with varying degrees of tumorigenic potential. Intrinsic changes affect cellular genetics, epigenetics, and influence which cells are capable of initiating tumorigenesis.[53] Genetic mutations have been implicated as driving forces in disease onset, progression, and recurrence. It has also been shown that identifying mutant genes is beneficial for both diagnostics and targeted therapies. For example, clinicians look for mutations in breast cancer 1 or 2 genes (BRCA1 and BRCA 2, respectively) to diagnose early onset breast cancer.[53-54] Unlike genetic alterations, epigenetic changes that occur in cancer are not the result of mutations or deletions in the DNA sequence, but instead are changes in what genetic information manifests in cells, which is directly linked to the structure of chromatin.[55-59] This type of variability is associated with changes in level of DNA methylation and modifications to histones and microRNA expression. Research has also shown that epigenetic mutations have the potential to be reversed.

On the contrary, extrinsic factors, specifically the changes in the cellular microenvironment that encompasses the extracellular matrix (ECM), blood vessels, and supporting cells (i.e., fibroblasts and immune cells), impact the behavior of cancer cells.[53] In cancerous tissues, changes in the microenvironment can lead to uncontrolled proliferation, invasiveness, and act as a chemoattractant for stromal cells.[60-61] It can also be posited that changes within the microenvironment impact epigenetic aberration due to the cell monitoring which genes are expressed when conditions surrounding it change. Moreover, the notion of epigenetic modulation in response to changes in the microenvironment suggests that both the intrinsic and extrinsic factors work together to influence the aggressive phenotype exhibited by most cancers.

1.2.4 Epithelial-to-Mesenchymal Transition (EMT)

In the last section, intrinsic and extrinsic alterations that affect the heterogeneity and tumorigenic nature of cancer cells were introduced. One important concept was that variations within the cell (i.e., genetic and epigenetic) and in the microenvironment influence the phenotypic nature of the cancer cell, and ultimately metastasis. In recent years, researchers have suggested that epithelial cells exhibit a high level of plasticity and switch their phenotype in response to intrinsic or extrinsic cues. This phenomenon is referred to as EMT, or epithelial-to-mesenchymal transition, which is an important process in early embryonic development.[18-19, 62] EMT refers to the loss of epithelial characteristics, like cell-cell interactions and polarity, and the acquisition of mesenchymal characteristics, including an elongated shape, like that of fibroblasts, and enhanced migratory ability as depicted in Figure 1.4. In addition to EMT, the reverse reaction, the mesenchymal-to-epithelial transition (MET) is also required.

In most cancers, this process is marked by the loss of or decreased expression of epithelial markers (e.g., E-cadherin, occludin, and keratin) and increased expression of mesenchymal markers, such as vimentin, N-cadherin, and vitronectin).[63-64] In addition, the transition between the two phenotypes is also associated with alterations in expression of several transcription factors (e.g., Snail, Twist, Slug, and β-catenin) and activations of kinases (e.g., PI3K/AKT, NFκB, and ERK 1 and 2).[64-65] Moreover, increased expression of collagen IV and fibronectin in the ECM has also been found to be related to the occurrence of EMT.[22, 64] It is when cells acquire a mesenchymal phenotype that they start to exhibit more aggressive and invasive behaviors, and as a result, influence cancer progression. Both pathways are needed for migration and invasion at distant sites,

survival, and metastatic dissemination.[18-19, 62, 65-66] Research has also shown that each pathway increases cancer cell survival and induces resistance to anti-cancer agents.

Figure 1.4. Epithelial-to-mesenchymal transition (EMT).

1.2.5 Cancer Stem Cell Theory

The plastic nature of cancer cells is thought to be the result of a small population of cells with stem-like qualities, dubbed cancer stem cells. Like normal stem cells, CSC can self-renew, initiate tumor growth, and differentiate into progenies that may not exhibit stem-like qualities.[26, 53] Research on acute myeloid leukemia supported the CSC theory in that cells with leukemia-initiating cells differentiated, proliferated, and regenerated in a manner similar to that of hematopoietic cells.[67-68] Traditionally, this hierarchy is referred to as the CSC theory, which states that CSC can undergo either symmetric or asymmetric division.[53] Symmetric division would result in self-renewal; thus, all daughter cells would be identical to the parent cells. Alternatively, asymmetric division would result in a progeny composed of non-CSC with phenotypes that are modulated in part by changes within the microenvironment. This small subset of CSC is believed to be the driving force

behind tumor recurrence, drug resistance, and metastasis in cancer; even though non-CSC make up most established tumors.[53]

In recent years, researchers have suggested that the traditional CSC theory is not as straightforward as previously presumed. Moreover, epigenetic changes can potentially result in CSC shutting down genes associated with stemness and initiate lineage-specification genes. Considering the impact epigenetic change has on the behavior of a given population of cells, the modified CSC theory posits that some non-CSC can reacquire the CSC phenotype, thus suggesting that the pathway from CSC to non-CSC is bidirectional.[53] The new theory expands upon the idea that plasticity in cancer is an attribute shared by both CSC and non-CSC. One instance of the modified CSC theory in action involves transcription factor PAX5, which is required for the differentiation of lymphoid progenitor cells. Once PAX5 was silenced, mature B-cells dedifferentiated back to their progenitors.[69-70] Moreover, it has been found that some non-CSC can acquire a stem-like phenotype due to overexpression of oncogenes like the BMI1 polycomb ring oncogene or oncogene fusion proteins, such as MOZ-TIF2 and MLL-ENL.[71-73] Both CSC models are displayed in Figure 1.5.

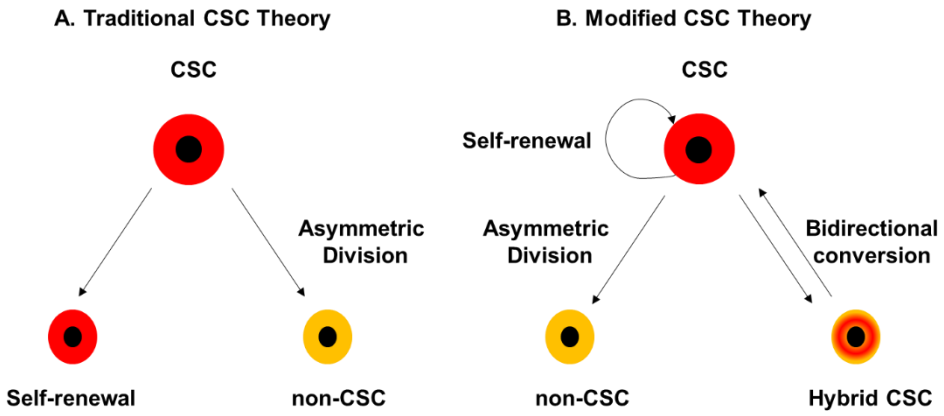

Figure 1.5. Models of the Cancer Stem Theory (CSC). (A) Traditional CSC theory and (B) Modified CSC theory.

Several molecules have been identified as CSC markers in cancer. Cluster differentiation (CD) markers are a family of glycoproteins located on the cell surface with roles in various cellular functions. While several CD markers have been suggested to be involved with stemness, two of the most widely studied markers, CD133 and CD44, will be highlighted. CD133, or Prominin-1, is a transmembrane protein found in human hematopoietic stem cells and several cancerous tissues (colon, pancreatic, ovarian, and gall bladder) with roles in tumorigenesis, metastasis, self-renewal, resistance, and apoptosis.[74-77] It has been found to be upregulated by both intracellular and extracellular factors such as hypoxia, transforming growth factor β1 (TGFβ1), and microRNAs.[56, 75-79] CD44 is a surface glycoprotein associated with a family of cell adhesion molecules (CAM).[64] It has been found to bind with ECM components like laminin and fibronectin, cytokines, and a variety of growth factors, rendering it useful in cell signaling; thus, it is not uncommon for CD44 to be overexpressed on the cell surface, particularly in cancerous tissues.[80-81] One of the key functions of CD44 is its role as a cell surface receptor for hyaluronic acid (HA), which has roles in wound healing, immune response, and blood vessel formation. Like CD133, CD44 has also been found to influence tumor progression, metastasis, and resistance to anti-cancer agents.[80, 82-83]

Aside from CD markers, aldehyde dehydrogenase (ALDH), an enzyme involved in cellular detoxification, has also been implicated as CSC marker.[84-85] It has been found that ALDH is linked to drug resistance, differentiation, and angiogenesis. It has been found to be overexpressed in non-small cell lung cancer cells (NSCLC), yielding them highly tumorigenic and capable of self-renewal.[86] Epithelial cell adhesion molecule (EpCAM) is a transmembrane glycoprotein that is expressed in both normal epithelia and

stem cells. It has also been found to be heterogeneously overexpressed in cancerous tissues. It has been identified as a CSC marker in breast, colon, and pancreatic cancers, due to its roles in cell proliferation, differentiation, and signaling.[87-90]

1.2.6 EMT and CSC in OC

Earlier in the chapter, EMT and the CSC theory were introduced. However, this section will focus specifically on EMT and CSC exhibited in OC. It has been found that normal ovarian surface epithelium exhibits a mixed phenotype, being that it expresses both epithelial and mesenchymal features. However, it is keratin, not E-cadherin, that is prominently expressed alongside vimentin in these tissues.[91] Also, N-cadherin, an adhesion molecule associated a mesenchymal phenotype, has also been found to be present in normal ovarian surface epithelia.[92-93] Moreover, it has been shown that E-cadherin expression is increased in inclusion cysts and inner layers of epithelia, which are areas where malignancy is thought to occur.[64, 94] The assumption that E-cadherin presence may be associated with diseased tissues was further supported by studies showing that the marker had enhanced expression in primary ovarian neoplasms.[64, 95] These findings suggest that initially, malignant tissues are composed of cells with an epithelial phenotype, and as the cancer advances it is repressed in favor of a more mesenchymal phenotype. The shift from a mixed phenotype in normal ovarian epithelia to either primarily epithelial or mesenchymal in early or advanced staged malignancies, respectively, suggests that EMT is significant feature of OC.

Moreover, it is postulated that phenotypic transitions in conjunction with the cellular microenvironment influence the tumorigenic nature of OC cells. Ovarian cancer cells

exclusively expressing a noninvasive, epithelial phenotype with intact cell junctions could form MCTS in non-adherent culture with or without ECM components.[16] Conversely, cells expressing the more invasive, mesenchymal phenotype became epithelial-like under anchorage-independent conditions indicating MET took place.[16] Moreover, those same cells expressed a hybrid phenotype, with mesenchymal cells on the outer layer and epithelial cells in the inner regions of the spheroids.[16] The shifts in phenotype presented in these studies support the claim that cancer progression, and ultimately metastasis, is due to the cell's ability to switch on or off certain gene expression in response to environmental cues.

Aside from EMT, extensive research conducted to determine the role of CSC in OC has led to a collection of putative molecules thought to define ovarian CSC.[96] It has been proposed that the aggressiveness of ovarian cancer is due to transformations and dysfunction related to stem cells in the ovary due to isolated tumorigenic clones differentiating to form in vitro spheroids despite tissue-specific differentiation being arrested.[97] Similarly, Cioffi et al. found that ovarian cancer cells possessing two distinct biomarkers, CD133 and CXCR4, were capable of forming microtumors with high efficiency.[98] CD133 is a widely studied OC CSC marker due to its expression being linked to tumor formation both in vitro and in vivo.[96, 99-102] In addition to CD133, studies by two independent research groups have shown that aldehyde dehydrogenase isozyme-1 (ALDHA1) to be a prevalent marker in ovarian cancer stem cells.[102-103] In fact, the work suggests that cells positively expressing both markers were highly tumorigenic and promoted angiogenesis. Other markers that have been found to be present in CSC of OC are CD44 and CD117, and like CD133 and ALDH, were found to be involved in tumor

initiation and propagation in vivo.[64, 84, 96, 102] In addition to tumor initiation, these markers have been found to promote angiogenesis, and be involved in promoting resistance to chemotherapeutic agents.

1.3 Reactive Oxygen Species (ROS) and Cancer

Reactive oxygen species (ROS) are defined as highly reactive oxygen free radicals like superoxide ($^{\cdot}O_2^-$) or hydroxyl ($^{\cdot}OH$), as well as non-radicals like hydrogen peroxide (H_2O_2) or ozone (O_3) that can be converted into radicals.[104] Mitochondria and NAD(P)H oxidase are major producers of ROS within the cell, while pollutants like smoke are exogeneous ROS producers.[105] At low levels, ROS can be beneficial for cell signaling and protein regulation due to antioxidant response systems that help maintain a homeostasis in the cell.[105-106] However, excessive ROS has been linked to several diseases, including cancer, diabetes, and cardiovascular disease.

Damage to DNA, proteins, and lipids is likely to be the result of oxidative stress brought on by increased ROS. DNA damage, particularly mutations, resulting from ROS has roles in carcinogenesis, tumorigenesis, angiogenesis and induction of a malignant phenotype breast, lung, and colon cancer.[46, 107] Also, it has been found that ROS signaling pathways promote enhanced proliferation, invasion, and survival in cancerous cells. It has been noted that the invasive behavior observed in breast cancer cells was due to the accumulation of HIF1α resulting from increased ROS.[107] Likewise, superoxide presence in ovarian cancer cells led to increased proliferation and malignant tumor growth in vitro and in vivo, respectively.[108] Pancreatic cancer cells have been found to avoid apoptosis due to the generation of ROS by NADPH oxidase isoform 4, thus making them highly

resistant to chemotherapy.[109] The role of ROS in drug resistance will be discussed later in this chapter.

1.3.1 Antioxidant Response: Nuclear Factor Erythroid related factor-2 (Nrf2)

In the last section, ROS and the impact it has on cancer onset and progression was introduced, as well as how cells have a system in place to regulate it. One way to combat ROS is using transcription factors that initiate the production of antioxidants like glutathione (GSH), ascorbic acid, and vitamin C.[110] In addition, cytoprotective enzymes whose purpose is to catalyze reactions that work to maintain homeostasis are also essential in the fight against ROS. Nuclear factor erythroid-related factor-2 (Nrf2) is responsible for inducing the transcription of several cellular detoxifying genes associated with metabolizing enzymes and drug transporters.[110] Moreover, it also regulates the transcription of cellular detoxifying enzymes, like NQO1 and heme oxygenase (HO-1), as well as key antioxidants, like glutathione.[111] Aside from activating antioxidant genes, Nrf2 has also been found to have roles in anti-inflammation, as well as mitochondrial biogenesis and autophagy.[112-113] Literature states that Nrf2 expression is regulated by the Kelch-like ECH-associated protein 1, Keap 1, which causes the degradation of Nrf2 in the cytoplasm.[110] However, when cells are under oxidative stress, the Keap 1-Nrf2 complex is disrupted, resulting in Nrf2 translocation to the nucleus where it activates gene transcription of antioxidant response elements (ARE).[110] This process is depicted in Figure 1.6.

In addition to oxidative stress, it has also been found that miRNAs and several other transcription factors have some regulatory influence on this pathway. Studies have shown

that miR-200a, which regulates Keap 1 gene expression, inhibits the interaction of Keap1 and Nrf2. Moreover, when there is increased expression of miR-200a, Keap1 expression is decreased. In breast cancer cells overexpressing Nrf2, decreased tumor formation under anchorage-independent conditions was observed. miRNAs have also been found to target Nrf2 in oesophageal cancer and blood borne diseases, like sickle cell anemia and lymphoma. However, miRNA-controlled regulation of Nrf2 is not apparent in all cancers. In fact, it has been suggested that loss-of-function mutations in Keap 1 can also disrupt the Keap 1-Nrf2 interaction, leading to hyper-activation of Nrf2, and thus enhanced transcription of ARE. Epigenetic aberrations to Keap1, specifically hypermethylation, have also resulted in enhanced Nrf2 presence in cells.

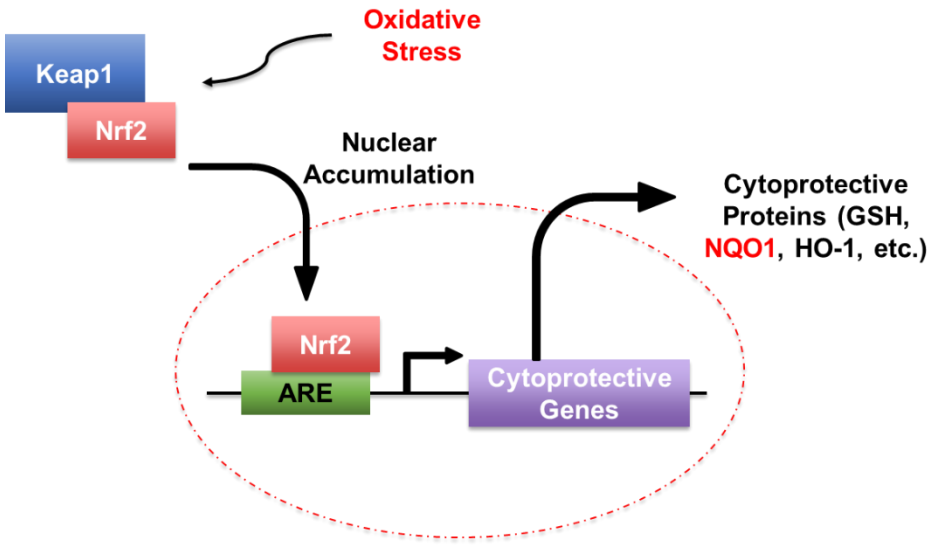

Figure 1.6. Oxidative stress disrupts the Keap1-Nrf2 complex, leading to nuclear accumulation of Nrf2. Nrf2 then binds to ARE leading to the production of multiple detoxifying enzymes.

Nrf2 has also been found to activate various genes that are associated with cancer cell proliferation and death. Studies have shown that Nrf2 is capable of binding to the

ARE region of the Notch1 gene, resulting in increased proliferation and an aggressive phenotype.[114] Nrf2 has also been found to be involved in EMT, due to E-cadherin binding to it (i.e., Nrf2), thus preventing nuclear accumulation and subsequent ARE gene transcription.[115-116] However, when zinc-finger E-box binding homeobox 1 (ZEB1) is upregulated during EMT, ZEB1 suppresses E-cadherin, leading to enhanced expression of N-cadherin and other mesenchymal markers, and subsequently more Nrf2 activity. In Figure 1.7 is depicted alternate mechanisms for Nrf2 accumulation in the nucleus as a function of ZEB1 inhibition of E-cadherin and miR-200a acting on Keap1.

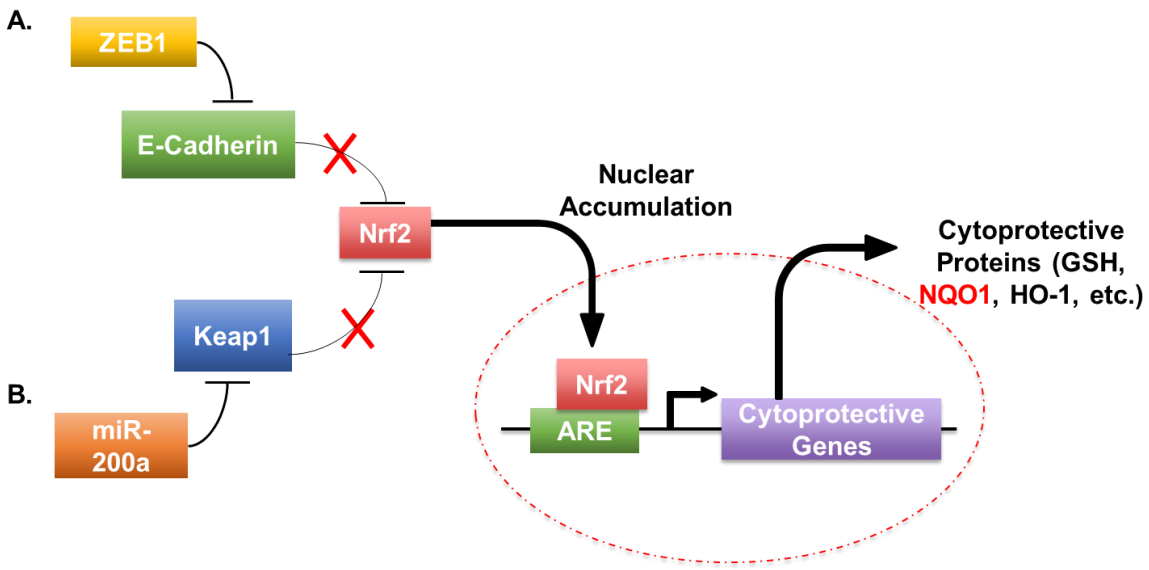

Figure 1.7. Nrf2 nuclear translocation by way of (A) ZEB1 inhibition of E-cadherin and (B) miR-200a inhibition of Keap1.

1.3.2 Human NAD(P)H:Quinone Oxidoreductase Isozyme-1 (NQO1)

Primarily localized in the cytosol, NQO1 catalyzes the two-electron reduction of quinones to hydroquinones in the presence of cofactor NAD(P)H to prevent the

production of semiquinone radicals.[116] Its active site is in a non-covalent binding pocket for FAD between two identical monomers. To be specific, when cofactor NAD(P)H is present, NQO1 will bind to it, and hydride transfer will occur from NAD(P)H to the FAD^+ housed in the active site of the enzyme yielding $NAD(P)^+$ and FADH, respectively. FADH will then donate a proton to a bound quinone substrate, thereby reducing it and reestablishing the oxidized FAD. Because NQO1 has two identical active sites, this process occurs twice. Figure 1.8 illustrates this process.

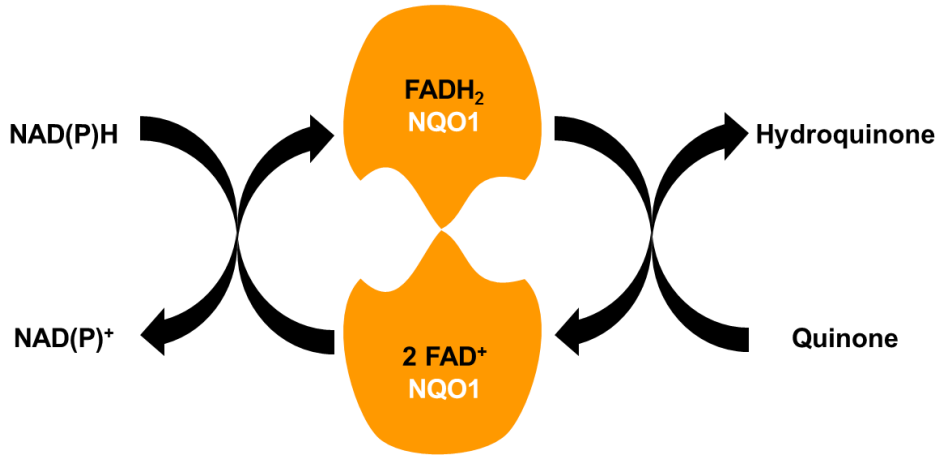

Figure 1.8. NQO1 reduction of quinones to hydroquinones.

NQO1 is described as a protective agent within the cells, owing to its acting against oxidative stress and neoplasia.[1, 116] NQO1 also has bioreductive functions, such as converting DNA alkylating quinones into highly cytotoxic species resulting in the development of antitumor drugs.[15] Two of the most notable DNA alkylating quinones, β-lap and MMC, which can be converted into highly cytotoxic species upon reaction by NQO1, have been exploited in several studies.[7, 17, 117] For example, β-lap has been shown to reduce inflammation and neoplasia, as well as act as an analgesic.[17] Several groups

have worked to several additional anticancer agents like indoloquinone EO9 and Diaziquone (AZQ), which can also act as substrates that exploit the enzyme's bioreductive properties.[118] In addition, NQO1 serves as a superoxide scavenger, as well as a stabilizer of tumor suppressor genes.[119-121] Other functions of the enzyme include protection of proteins from 20S proteoseomal degradation, acting as a mRNA binding protein, and being involved in the plasma membrane redox cycling process.[116]

Despite its detoxification and bioreductive properties, NQO1 has been found to be overexpressed in several cancerous tissues.[3, 5, 7, 122] Cui and colleagues found that poor prognosis in advanced stage serous ovarian carcinomas was associated with elevated levels of NQO1 in tumor tissues.[4] Due to its increased expression in the initial stages of ovarian cancer, NQO1 may be aiding in the progression of the disease rather than preventing it.[4] In another study, high NQO1 expression was associated with tumorigenesis in NSCLC cells because upon repression of the enzyme, cells proliferative and tumorigenic abilities decreased.[123] Moreover, NQO1 inhibition was found to be accompanied by increased ROS, which as mentioned in an earlier section, could result in increased glucose metabolism and angiogenesis due to HIFα being overexpressed.

1.3.3 NQO1-Activatable Fluorescent Probes

Due to its role in combating oxidative stress, as a bioreductive agent, and more recently as a poor prognostic factor in cancer, NQO1 has been found to be an excellent therapeutic target. In addition, the enzyme is overexpressed 5- to 200- fold in cancerous tissues in comparison to neighboring tissues of solid tumors derived from lung, breast, and pancreatic cancers.[2, 6, 17, 123-124] Several groups have worked to develop anticancer

agents like MMC, β-lap, indoloquinone EO9 and AZQ, which act as substrates that exploit the enzyme's bioreductive properties. Overexpression of NQO1 has also rendered it an excellent target for fluorescence-guided visualization of cancer, which is of great interest to the McCarley research group. The McCarley group has synthesized several fluorescently-silent probes equipped with quinone species serving as NQO1 substrates. These probes become activated via reduction of the quinone substrates by NQO1, leading to the release of highly fluorescent reporting moieties with emissions in the visible and NIR regions of the electromagnetic spectrum. Scheme 1 is a generic depiction of the proposed mechanism of NQO1 activation of fluorescent probes. Using this technology, the McCarley lab has successfully distinguished between NQO1-postive and negative cells and/or tissues via fluorescence microscopy with high target-to-background ratios (TBR). To date, these highly specific and selective NQO1-activatable probes have been used to visualize enzyme localization in human colon, pancreatic, lung, and ovarian cancer cells.[8-14] A complete list of developed NQO1-activable probes produced in the McCarley lab is provided in Table 1.1.

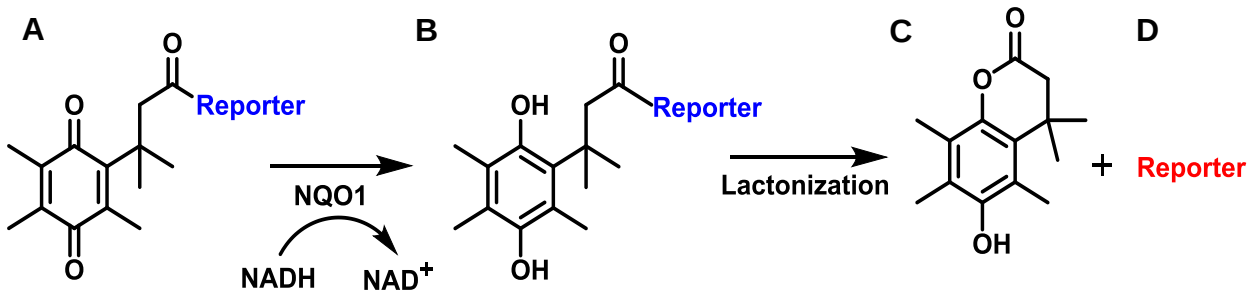

Scheme 1.1. (**A**) Fluorescently-silent probe is reduced by NQO1 in presence of NADH to from a (**B**) hydroquinone, which can then undergo lactonization to produce (**C**) lactone and (**D**) fluorescent reporter.

Table 1.1: NQO1-activatable probes developed in the McCarley lab

Probes	Application
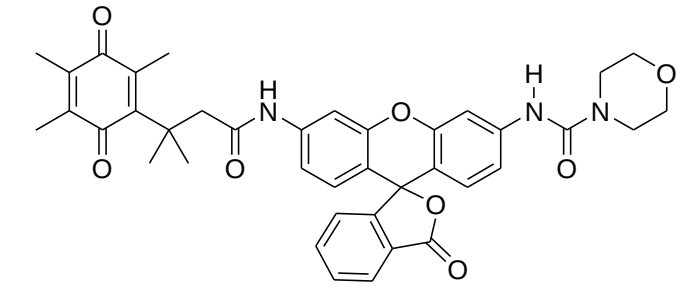	Fluorescence detection of 5×10^{-5} g NQO1 in aqueous solution.[13]
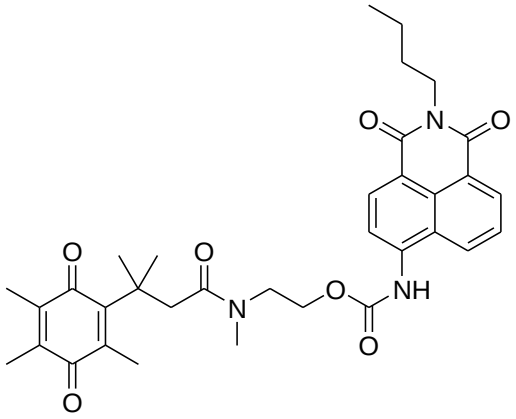	Visualization of NQO1 activity via fluorescence microscopy in human carcinomas of various origins.[14]
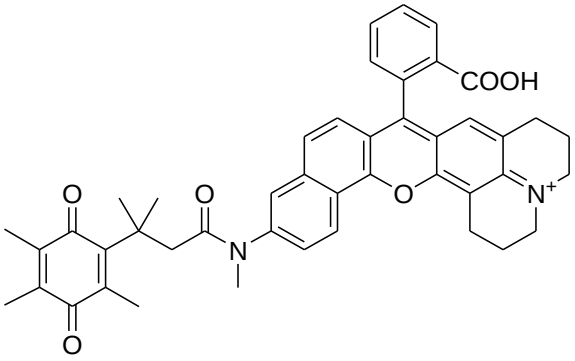	Visualization of NQO1 activity via fluorescence microscopy in tumor-derived human NSCLC and colorectal cells.[10]
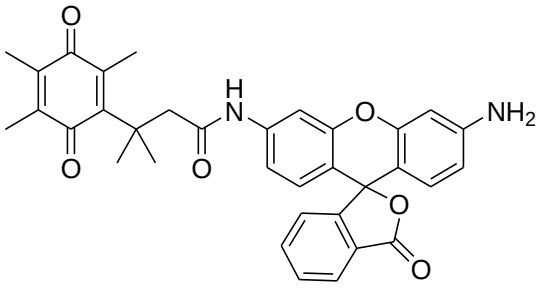	Visualization of NQO1 activity via fluorescence microscopy in tumor-derived human colorectal and ovarian cancer cells.[8]

(Table cont'd.)

Probes	Application
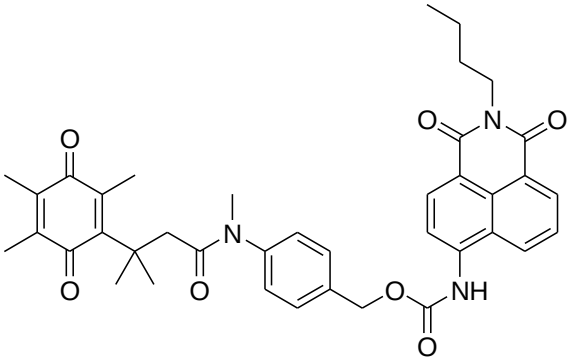	Visualization of NQO1 activity via fluorescence microscopy in tumor-derived human NSCLC and colorectal cancer cells.[9]
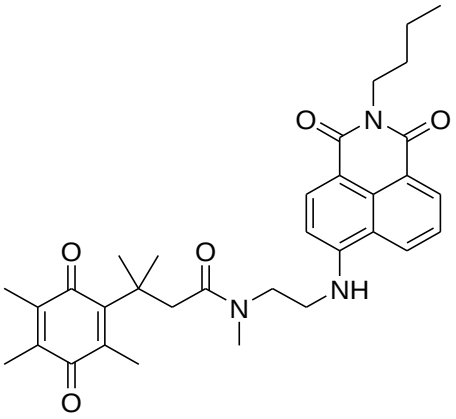	Visualization of NQO1 activity via fluorescence microscopy in tumor-derived NSCLC, colorectal, and ovarian cancer cells.[11]
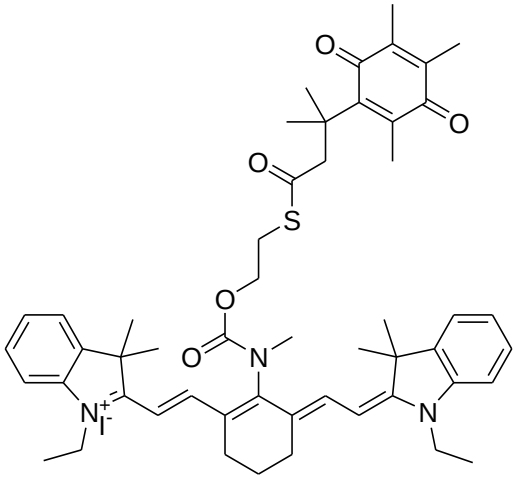	Visualization of NQO1 activity via fluorescence microscopy in tumor-derived NSCLC, colorectal, and ovarian cancer cells in vitro and ovarian cancer in vivo.[12]

1.3.4 Additional Cytoprotective Enzymes

In addition to NQO1, Nrf2 translocation to the nucleus and subsequent transcription produces several other cytoprotective enzymes. One of these is heme oxygenase-1 (HO-

1), whose role in ROS, cell growth, and chemoresistance has been widely studied.[111] HO-1 is responsible for catalyzing the oxidation of heme into ferritin, biliverdin/bilirubin, and carbon monoxide.[110-111] While the first two products of this process are antioxidants, carbon monoxide has antiapoptotic properties. HO-1 is present in low levels in the cell unless its expression is induced by stressors. It is considered as a major effector of cellular responses mediated by Nrf2. Moreover, like NQO1, HO-1 has been associated with aggressiveness, survival, and poor prognosis in several cancers.[125-128] It has also been linked to resistance to chemo- and radiation therapies.[128-129] Also, it has been found that if the enzymes expression is inhibited, cancerous tissues become sensitive to therapy.[127, 130]

Nrf2 is also responsible for the transcription of enzymes required for de novo synthesis and redox homeostasis of glutathione (GSH), which has been described as one of the most important antioxidants in the body. More specifically, Nrf2 regulates the transcription of glutathione reductase, which is responsible for reducing oxidized glutathione (GSSH) to GSH, thereby modifying GSH redox state.[110] GSH modulates cellular redox signaling, proliferation, and death. Like HO-1 and NQO1, GSH works to remove toxic ROS and reactive nitrogen species (RNS) from the cell to maintain homeostasis. GSH is also involved in recycling other antioxidants as well as acting against inflammation.[112] It serves as a cofactor for gluthathione peroxidases, gluthathione-*S*-transferases, and glutaredoxins; all of which are antioxidant enzymes.[110] However, glutathione levels have been found to increase in cancer cells after treatment with chemotherapeutics. Godwin and colleagues observed that ovarian cancer cells with a wide range of resistance to cisplatin also had increased levels of GSH compared to parental cell lines.[131] In the same

study, it was found that enzymes involved in the synthesis of GSH showed increased expression in highly cisplatin-resistant cells.[131]

1.4 Treatment, Resistance, and Recurrence

While surgery and radiation treatment are often the first lines of defense, not all tumors are amendable to them, due to some of the diseased tissue still being present after treatment. As a result, several systemic drugs like cisplatin, paclitaxel, and doxorubicin, to name a few, are employed. However, the use of anti-cancer drugs is correlated with two forms of resistance: intrinsic and acquired. Intrinsic resistance is observed in patients that do not display sensitivity to anti-cancer therapy after initial treatment, whereas acquired resistance manifests in patients that were once sensitive to therapy but become resistant to it overtime.[53] Intrinsic resistance is thought to be the result of genetic changes, such as mutations in genes associated with growth factors, oncogenes, cytokines, and signaling pathways. For example, mutations in tumor suppressor gene p53 were found to be associated with resistance to cisplatin and doxorubicin in NSCLC and breast cancer, respectively.[132-133] Regardless of the form of resistance, it is important to understand the changes occurring within the cells remaining after initial treatment.

Mounting evidence suggests that acquired drug resistance is due in part to EMT taking place in cancer cells, thereby leading to the development of metastatic disease.[21] Several studies have demonstrated that cancerous cells of epithelial origin are often sensitive to anticancer agents; however, acquisition of a mesenchymal phenotype has been linked to increased resistance. This was evident in studies where transcription factors Snail and Slug, which induce EMT, were all upregulated in cells showing resistance to cisplatin in

lung, head and neck squamous, and ovarian cancer cells.[71, 134-136] Moreover, researchers found that after repressing both transcription factors, the cells became re-sensitized to the drug. Silencing of Snail resulted in tumor and immunosuppression melanoma and induced apoptosis in an Adriamycin-resistant melanoma.[137]

Resistance and subsequent recurrence are thought to be the result of tumor dormancy, a period after initial treatment where proliferation is halted, and cells lie in a state of mitotic arrest. Dormant cells are believed to be CSC capable of inducing EMT, which then circulate locally or through the bloodstream to distant sites where they will later invade.[138] Because they can survive in a highly stressed environment, these cells are considered highly resistant to chemotherapy. Resultantly, EMT and CSC are often studied in tandem, due to phenotypic transitions occurring in diseased cells resulting in the acquisition of epithelial, mesenchymal, or a mixture of the two along with stemlike features during relapse.[64, 138] For example, circulating tumor cells have been found to exhibit behaviors mirroring cells undergoing EMT as well as CSC.[138] A study by Mani and colleagues supports EMT and CSC being studied together.[139] The work details how breast cancer cells overexpressing EMT- promoting transcription factors, snail and twist, were found to also highly express CSC marker CD44.[21, 139] Moreover, these cells exhibited a malignant phenotype and could produce mammospheres in vitro.

1.4.1 Cisplatin Resistance

The remaining section will focus on reviewing specific genetic and epigenetic aberrations that occur after initial or prolonged exposure to the chemotherapeutic drug cisplatin. Treatment with chemotherapeutics in ovarian cancer often results in acquired

resistance after initial exposure as evident by over 70% of women experiencing recurrence 6-18 months after initial treatment.[140-142] Research suggests that mutations in genes like p53, which is linked to DNA repair and cellular apoptosis, may be involved in acquired resistance to chemotherapeutic drugs.[132] Furthermore, Perego et al. found that resistance to cisplatin in ovarian cancer is linked to mutations in the p53 gene that inhibit its ability to activate bax, an apoptotic gene.[143-144] Likewise, research conducted by Parker et al. and Masuda et al. suggests that cisplatin resistance in OC is associated with increased DNA repair of lesions and decreased drug accumulation.[145-146]

Aside from altering the rate at which DNA lesions are repaired and reducing overall drug accumulation, drug resistance, particularly resistance to cisplatin has been found to be linked to several other genetic and epigenetic changes within cells. Extensive research has been conducted to probe the effect that cisplatin has on diseased tissues. It has been associated with endocytic defects, which can be linked to reduced uptake of the drug.[147-148] Other studies have shown that cisplatin resistance is related to heat shock proteins (HSPs), which work to ensure that cells are protected against DNA damage and apoptosis resulting from an influx of oxidant species.[144] It has been suggested that the upregulation of HSPs in cisplatin resistant cells could mean cell defense reactions may be comprised.[144] Research has shown that ovarian, breast, and colon cancer cells, with established resistance to cisplatin, have increased expression of several heat shock proteins.[149-151] Epigenetic alterations like enhanced chromatin condensation, DNA hypermethylation resulting in gene silencing, and increased histone acetylation have all been suggested to be associated with cisplatin resistance.[144, 152-154]

Furthermore, several transcription factors have been linked to increased resistance to cisplatin and other anti-cancer therapeutics. Some of these include activating transcription factor 4, zinc-finger factor 143, nuclear transcription factor-κB, mitochondrial transcription factor A, and CCAAT-binding transcription factor 2.[144] Another transcription factor, p300/CBP-associated factor (PCAF), whose function is to initiate cell cycle arrest and/or apoptosis via regulation of p53, p73, and BAX, has been shown to be overexpressed in cisplatin resistant P/CDP6 and Hela/CP4 cells.[155] It is also involved in acetylating and stabilizing transcription factors E2F1 in response to DNA damage, meaning it could be aiding in cellular survival in cells that overexpress it. In addition to PCAF, Nrf2 and the cytoprotective genes (e.g., NQO1) it transcribes, have also been linked to cisplatin resistance.[15, 111, 156-157]

1.5 References

1. Ross, D.; Kepa, J. K.; Winski, S. L.; Beall, H. D.; Anwar, A.; Siegel, D., NAD (P) H: quinone oxidoreductase 1 (NQO1): chemoprotection, bioactivation, gene regulation and genetic polymorphisms. *Chemico-Biological Interactions* **2000,** *129* (1-2), 77-97.

2. Winski, S. L.; Koutalos, Y.; Bentley, D. L.; Ross, D., Subcellular Localization of NAD(P)H:quinone Oxidoreductase 1 in Human Cancer Cells. *Cancer Research* **2002,** *62* (5), 1420.

3. Siegel, D.; Ross, D., Immunodetection of NAD (P) H: quinone oxidoreductase 1 (NQO1) in human tissues1. *Free Radical Biology and Medicine* **2000,** *29* (3-4), 246-253.

4. Cui, X.; Li, L.; Yan, G.; Meng, K.; Lin, Z.; Nan, Y.; Jin, G.; Li, C., High expression of NQO1 is associated with poor prognosis in serous ovarian carcinoma. *BMC Cancer* **2015,** *15* (1), 244.

5. Lewis Anne, M.; Ough, M.; Hinkhouse Marilyn, M.; Tsao, M.-S.; Oberley Larry, W.; Cullen Joseph, J., Targeting NAD(P)H:quinone oxidoreductase (NQO1) in pancreatic cancer. *Molecular Carcinogenesis* **2005,** *43* (4), 215-224.

6. Marín, A.; López de Cerain, A.; Hamilton, E.; Lewis, A. D.; Martinez-Peñuela, J. M.; Idoate, M. A.; Bello, J., DT-diaphorase and cytochrome B5 reductase in human lung and breast tumours. *British Journal Of Cancer* **1997,** *76*, 923.

7. Traver, R. D.; Horikoshi, T.; Danenberg, K. D.; Stadlbauer, T. H.; Danenberg, P. V.; Ross, D.; Gibson, N. W., NAD (P) H: quinone oxidoreductase gene expression in human colon carcinoma cells: characterization of a mutation which modulates DT-diaphorase activity and mitomycin sensitivity. *Cancer Research* **1992,** *52* (4), 797-802.

8. Best, Q. A.; Prasai, B.; Rouillere, A.; Johnson, A. E.; McCarley, R. L., Efficacious fluorescence turn-on probe for high-contrast imaging of human cells overexpressing quinone reductase activity. *Chemical Communications* **2017,** *53* (4), 783-786.

9. Hettiarachchi, S. U.; Prasai, B.; McCarley, R. L., Detection and Cellular Imaging of Human Cancer Enzyme Using a Turn-On, Wavelength-Shiftable, Self-Immolative Profluorophore. *Journal of the American Chemical Society* **2014,** *136* (21), 7575-7578.

10. Best, Q. A.; Johnson, A. E.; Prasai, B.; Rouillere, A.; McCarley, R. L., Environmentally Robust Rhodamine Reporters for Probe-based Cellular Detection of the Cancer-linked Oxidoreductase hNQO1. *ACS Chemical Biology* **2016,** *11* (1), 231-240.

11. Prasai, B.; Silvers, W. C.; McCarley, R. L., Oxidoreductase-Facilitated Visualization and Detection of Human Cancer Cells. *Analytical Chemistry* **2015,** *87* (12), 6411-6418.

12. Shen, Z.; Prasai, B.; Nakamura, Y.; Kobayashi, H.; Jackson, M. S.; McCarley, R. L., A Near-Infrared, Wavelength-Shiftable, Turn-on Fluorescent Probe for the Detection and Imaging of Cancer Tumor Cells. *ACS Chemical Biology* **2017,** *12* (4), 1121-1132.

13. Silvers, W. C.; Payne, A. S.; McCarley, R. L., Shedding light by cancer redox—human NAD (P) H: quinone oxidoreductase 1 activation of a cloaked fluorescent dye. *Chemical Communications* **2011,** *47* (40), 11264-11266.

14. Silvers, W. C.; Prasai, B.; Burk, D. H.; Brown, M. L.; McCarley, R. L., Profluorogenic Reductase Substrate for Rapid, Selective, and Sensitive Visualization and Detection of Human Cancer Cells that Overexpress NQO1. *Journal of the American Chemical Society* **2013,** *135* (1), 309-314.

15. Siegel, D.; Yan, C.; Ross, D., NAD(P)H:quinone oxidoreductase 1 (NQO1) in the sensitivity and resistance to antitumor quinones. *Biochemical Pharmacology* **2012,** *83* (8), 1033-1040.

16. Gardi, N. L.; Deshpande, T.; Kamble, S.; Budhe, S.; Bapat, S. A., Discrete Molecular Classes of Ovarian Cancer Suggestive of Unique Mechanisms of Transformation and Metastases. *Clinical Cancer Research* **2013**.

17. Yang, Y.; Zhou, X.; Xu, M.; Piao, J.; Zhang, Y.; Lin, Z.; Chen, L., β-lapachone suppresses tumour progression by inhibiting epithelial-to-mesenchymal transition in NQO1-positive breast cancers. *Scientific Reports* **2017,** *7* (1), 2681.

18. Chaffer, C. L.; San Juan, B. P.; Lim, E.; Weinberg, R. A., EMT, cell plasticity and metastasis. *Cancer and Metastasis Reviews* **2016,** *35* (4), 645-654.

19. Nieto, M. A.; Huang, Ruby Y.-J.; Jackson, Rebecca A.; Thiery, Jean P., EMT: 2016. *Cell* **2016,** *166* (1), 21-45.

20. Dave, B.; Mittal, V.; Tan, N. M.; Chang, J. C., Epithelial-mesenchymal transition, cancer stem cells and treatment resistance. *Breast Cancer Research* **2012,** *14* (1), 202.

21. Singh, A.; Settleman, J., EMT, cancer stem cells and drug resistance: an emerging axis of evil in the war on cancer. *Oncogene* **2010,** *29*, 4741.

22. Turley, E. A.; Veiseh, M.; Radisky, D. C.; Bissell, M. J., Mechanisms of Disease: epithelial–mesenchymal transition—does cellular plasticity fuel neoplastic progression? *Nature clinical practice. Oncology* **2008,** *5* (5), 280-290.

23. Siegel, R. L.; Miller, K. D.; Jemal, A., Cancer statistics, 2018. *CA: A Cancer Journal for Clinicians* **2018,** *68* (1), 7-30.

24. Society, A. C. Cancer Facts & Figures 2018. https://www.cancer.org/content/dam/cancer-org/research/cancer-facts-and-statistics/annual-cancer-facts-and-figures/2018/cancer-facts-and-figures-2018.pdf (accessed May 3).

25. Institute, N. C. What is Cancer? https://www.cancer.gov/about-cancer/understanding/what-is-cancer (accessed May 3).

26. Meacham, C. E.; Morrison, S. J., Tumour heterogeneity and cancer cell plasticity. *Nature* **2013,** *501*, 328.

27. Torre, L. A.; Trabert, B.; DeSantis, C. E.; Miller, K. D.; Samimi, G.; Runowicz, C. D.; Gaudet, M. M.; Jemal, A.; Siegel, R. L., Ovarian cancer statistics, 2018. *CA: A Cancer Journal for Clinicians* **2018,** *68* (4), 284-296.

28. Kurman, R. J.; Shih, I.-M., The dualistic model of ovarian carcinogenesis: revisited, revised, and expanded. *The American Journal of Pathology* **2016,** *186* (4), 733-747.

29. Kurman, R., Origin and molecular pathogenesis of ovarian high-grade serous carcinoma. *Annals of Oncology* **2013,** *24* (suppl_10), x16-x21.

30. Meyn, A.; Lim, B., A paradigm shift in the origin of ovarian cancer: the ovary is no longer to blame. *BJOG: An International Journal of Obstetrics & Gynaecology* **2017,** *124* (6), 859-859.

31. Schultz, K. A. P.; Harris, A. K.; Schneider, D. T.; Young, R. H.; Brown, J.; Gershenson, D. M.; Dehner, L. P.; Hill, D. A.; Messinger, Y. H.; Frazier, A. L., Ovarian sex cord-stromal tumors. *Journal of Oncology Practice* **2016,** *12* (10), 940-946.

32. Walker, A.; Ross, R.; Haile, R.; Henderson, B., Hormonal factors and risk of ovarian germ cell cancer in young women. *British Journal of Cancer* **1988,** *57* (4), 418.

33. Heravi-Moussavi, A.; Anglesio, M. S.; Cheng, S.-W. G.; Senz, J.; Yang, W.; Prentice, L.; Fejes, A. P.; Chow, C.; Tone, A.; Kalloger, S. E., Recurrent somatic DICER1 mutations in nonepithelial ovarian cancers. *New England Journal of Medicine* **2012,** *366* (3), 234-242.

34. Shah, S. P.; Köbel, M.; Senz, J.; Morin, R. D.; Clarke, B. A.; Wiegand, K. C.; Leung, G.; Zayed, A.; Mehl, E.; Kalloger, S. E., Mutation of FOXL2 in granulosa-cell tumors of the ovary. *New England Journal of Medicine* **2009,** *360* (26), 2719-2729.

35. Van Nieuwenhuysen, E.; Lambrechts, S.; Lambrechts, D.; Leunen, K.; Amant, F.; Vergote, I., Genetic changes in nonepithelial ovarian cancer. *Expert Review of Anticancer Therapy* **2013,** *13* (7), 871-882.

36. Hanahan, D.; Weinberg, R. A., Hallmarks of cancer: the next generation. *Cell* **2011,** *144* (5), 646-674.

37. Hanahan, D.; Weinberg, R. A., The hallmarks of cancer. *Cell* **2000,** *100* (1), 57-70.

38. Weinberg, R. A., The retinoblastoma protein and cell cycle control. *Cell* **1995,** *81* (3), 323-330.

39. McDonnell, T. J.; Korsmeyer, S. J., Progression from lymphoid hyperplasia to high-grade malignant lymphoma in mice transgenic for the t (14; 18). *Nature* **1991,** *349* (6306), 254.

40. Strasser, A.; Harris, A. W.; Bath, M. L.; Cory, S., Novel primitive lymphoid tumours induced in transgenic mice by cooperation between myc and bcl-2. *Nature* **1990,** *348* (6299), 331.

41. Shay, J. W.; Wright, W. E., Senescence and immortalization: role of telomeres and telomerase. *Carcinogenesis* **2005,** *26* (5), 867-874.

42. Kim, N. W.; Piatyszek, M. A.; Prowse, K. R.; Harley, C. B.; West, M. D.; Ho, P. L.; Coviello, G. M.; Wright, W. E.; Weinrich, S. L.; Shay, J. W., Specific association of human telomerase activity with immortal cells and cancer. *Science* **1994,** *266* (5193), 2011.

43. Folkman, J., Role of angiogenesis in tumor growth and metastasis. *Seminars in Oncology* **2002,** *29* (6, Supplement 16), 15-18.

44. Pavlova, Natalya N.; Thompson, Craig B., The Emerging Hallmarks of Cancer Metabolism. *Cell Metabolism* **2016,** *23* (1), 27-47.

45. Carmeliet, P.; Jain, R. K., Angiogenesis in cancer and other diseases. *Nature* **2000,** *407*, 249.

46. Wan, J.; Chai, H.; Yu, Z.; Ge, W.; Kang, N.; Xia, W.; Che, Y., HIF-1α effects on angiogenic potential in human small cell lung carcinoma. *Journal of Experimental & Clinical Cancer Research* **2011,** *30* (1), 77.

47. Marin-Hernandez, A.; Gallardo-Perez, J. C.; Ralph, S. J.; Rodriguez-Enriquez, S.; Moreno-Sanchez, R., HIF-1α Modulates Energy Metabolism in Cancer Cells by Inducing Over-Expression of Specific Glycolytic Isoforms. *Mini Reviews in Medicinal Chemistry* **2009,** *9* (9), 1084-1101.

48. Chan, D. A.; Sutphin, P. D.; Nguyen, P.; Turcotte, S.; Lai, E. W.; Banh, A.; Reynolds, G. E.; Chi, J.-T.; Wu, J.; Solow-Cordero, D. E.; Bonnet, M.; Flanagan, J. U.; Bouley, D. M.; Graves, E. E.; Denny, W. A.; Hay, M. P.; Giaccia, A. J., Targeting GLUT1 and the Warburg Effect in Renal Cell Carcinoma by Chemical Synthetic Lethality. *Science Translational Medicine* **2011,** *3* (94), 94ra70.

49. Koppenol, W. H.; Bounds, P. L.; Dang, C. V., Otto Warburg's contributions to current concepts of cancer metabolism. *Nature Reviews Cancer* **2011,** *11*, 325.

50. Kim, J.-w.; Tchernyshyov, I.; Semenza, G. L.; Dang, C. V., HIF-1-mediated expression of pyruvate dehydrogenase kinase: A metabolic switch required for cellular adaptation to hypoxia. *Cell Metabolism* **2006,** *3* (3), 177-185.

51. Semenza, G. L., HIF-1: upstream and downstream of cancer metabolism. *Current Opinion in Genetics & Development* **2010,** *20* (1), 51-56.

52. Grassian, A. R.; Coloff, J. L.; Brugge, J. S., Extracellular Matrix Regulation of Metabolism and Implications for Tumorigenesis. *Cold Spring Harbor Symposia on Quantitative Biology* **2011,** *76*, 313-324.

53. Marjanovic, N. D.; Weinberg, R. A.; Chaffer, C. L., Cell plasticity and heterogeneity in cancer. *Clinical Chemistry* **2012**, clinchem. 2012.184655.

54. Boehm, J. S.; Hahn, W. C., Towards systematic functional characterization of cancer genomes. *Nature Reviews Genetics* **2011,** *12* (7), 487.

55. Berdasco, M.; Esteller, M., Aberrant Epigenetic Landscape in Cancer: How Cellular Identity Goes Awry. *Developmental Cell* **2010,** *19* (5), 698-711.

56. You, H.; Ding, W.; Rountree, C. B., Epigenetic regulation of cancer stem cell marker CD133 by transforming growth factor-β. *Hepatology* **2010,** *51* (5), 1635-1644.

57. Jones, P. A.; Baylin, S. B., The Epigenomics of Cancer. *Cell* **2007,** *128* (4), 683-692.

58. Sandoval, J.; Esteller, M., Cancer epigenomics: beyond genomics. *Current Opinion in Genetics & Development* **2012,** *22* (1), 50-55.

59. Rodríguez-Paredes, M.; Esteller, M., Cancer epigenetics reaches mainstream oncology. *Nature Medicine* **2011,** *17*, 330.

60. Hynes, R. O., The extracellular matrix: not just pretty fibrils. *Science* **2009,** *326* (5957), 1216-1219.

61. Lu, P.; Takai, K.; Weaver, V. M.; Werb, Z., Extracellular matrix degradation and remodeling in development and disease. *Cold Spring Harbor Perspectives in Biology* **2011**, a005058.

62. Nieto, M. A., The Ins and Outs of the Epithelial to Mesenchymal Transition in Health and Disease. *Annual Review of Cell and Developmental Biology* **2011,** *27* (1), 347-376.

63. Zeisberg, M.; Neilson, E. G., Biomarkers for epithelial-mesenchymal transitions. *The Journal of Clinical Investigation* **2009,** *119* (6), 1429-1437.

64. Strauss, R.; Li, Z.-Y.; Liu, Y.; Beyer, I.; Persson, J.; Sova, P.; Möller, T.; Pesonen, S.; Hemminki, A.; Hamerlik, P.; Drescher, C.; Urban, N.; Bartek, J.; Lieber, A., Analysis of Epithelial and Mesenchymal Markers in Ovarian Cancer Reveals Phenotypic Heterogeneity and Plasticity. *PLOS ONE* **2011,** *6* (1), e16186.

65. Nieto, M. A., Context-specific roles of EMT programmes in cancer cell dissemination. *Nature Cell Biology* **2017,** *19*, 416.

66. Thiery, J. P.; Acloque, H.; Huang, R. Y. J.; Nieto, M. A., Epithelial-Mesenchymal Transitions in Development and Disease. *Cell* **2009,** *139* (5), 871-890.

67. Bonnet, D.; Dick, J. E., Human acute myeloid leukemia is organized as a hierarchy that originates from a primitive hematopoietic cell. *Nature Medicine* **1997,** *3*, 730.

68. Lapidot, T.; Sirard, C.; Vormoor, J.; Murdoch, B.; Hoang, T.; Caceres-Cortes, J.; Minden, M.; Paterson, B.; Caligiuri, M. A.; Dick, J. E., A cell initiating human acute myeloid leukaemia after transplantation into SCID mice. *Nature* **1994,** *367*, 645.

69. Cobaleda, C.; Schebesta, A.; Delogu, A.; Busslinger, M., Pax5: the guardian of B cell identity and function. *Nature Immunology* **2007,** *8*, 463.

70. Cobaleda, C.; Jochum, W.; Busslinger, M., Conversion of mature B cells into T cells by dedifferentiation to uncommitted progenitors. *Nature* **2007,** *449*, 473.

71. Yu, C.-C.; Lo, W.-L.; Chen, Y.-W.; Huang, P.-I.; Hsu, H.-S.; Tseng, L.-M.; Hung, S.-C.; Kao, S.-Y.; Chang, C.-J.; Chiou, S. H., Bmi-1 Regulates Snail Expression and Promotes Metastasis Ability in Head and Neck Squamous Cancer-Derived ALDH1 Positive Cells. *Journal of Oncology* **2011,** *2011*, 16.

72. Huntly, B. J. P.; Shigematsu, H.; Deguchi, K.; Lee, B. H.; Mizuno, S.; Duclos, N.; Rowan, R.; Amaral, S.; Curley, D.; Williams, I. R.; Akashi, K.; Gilliland, D. G., MOZ-TIF2, but not BCR-ABL, confers properties of leukemic stem cells to committed murine hematopoietic progenitors. *Cancer Cell* **2004,** *6* (6), 587-596.

73. Cozzio, A.; Passegué, E.; Ayton, P. M.; Karsunky, H.; Cleary, M. L.; Weissman, I. L., Similar MLL-associated leukemias arising from self-renewing stem cells and short-lived myeloid progenitors. *Genes & Development* **2003,** *17* (24), 3029-3035.

74. Hess, D. A.; Wirthlin, L.; Craft, T. P.; Herrbrich, P. E.; Hohm, S. A.; Lahey, R.; Eades, W. C.; Creer, M. H.; Nolta, J. A., Selection based on CD133 and high aldehyde dehydrogenase activity isolates long-term reconstituting human hematopoietic stem cells. *Blood* **2006,** *107* (5), 2162.

75. Griguer, C. E.; Oliva, C. R.; Gobin, E.; Marcorelles, P.; Benos, D. J.; Lancaster, J. R., Jr.; Gillespie, G. Y., CD133 Is a Marker of Bioenergetic Stress in Human Glioma. *PLOS ONE* **2008,** *3* (11), e3655.

76. Ma, S.; Tang, K. H.; Chan, Y. P.; Lee, T. K.; Kwan, P. S.; Castilho, A.; Ng, I.; Man, K.; Wong, N.; To, K.-F.; Zheng, B.-J.; Lai, P. B. S.; Lo, C. M.; Chan, K. W.; Guan, X.-Y., miR-130b Promotes CD133+ Liver Tumor-Initiating Cell Growth and Self-Renewal via Tumor Protein 53-Induced Nuclear Protein 1. *Cell Stem Cell* **2010,** *7* (6), 694-707.

77. Li, Z., CD133: a stem cell biomarker and beyond. *Experimental Hematology & Oncology* **2013,** *2* (1), 17.

78. Hashimoto, O.; Shimizu, K.; Semba, S.; Chiba, S.; Ku, Y.; Yokozaki, H.; Hori, Y., Hypoxia Induces Tumor Aggressiveness and the Expansion of CD133-Positive Cells in a Hypoxia-Inducible Factor-1α-Dependent Manner in Pancreatic Cancer Cells. *Pathobiology* **2011,** *78* (4), 181-192.

79. Soeda, A.; Park, M.; Lee, D.; Mintz, A.; Androutsellis-Theotokis, A.; McKay, R. D.; Engh, J.; Iwama, T.; Kunisada, T.; Kassam, A. B.; Pollack, I. F.; Park, D. M., Hypoxia promotes expansion of the CD133-positive glioma stem cells through activation of HIF-1α. *Oncogene* **2009,** *28*, 3949.

80. Ponta, H.; Sherman, L.; Herrlich, P. A., CD44: From adhesion molecules to signalling regulators. *Nature Reviews Molecular Cell Biology* **2003,** *4*, 33.

81. Morath, I.; Hartmann, T. N.; Orian-Rousseau, V., CD44: More than a mere stem cell marker. *The International Journal of Biochemistry & Cell Biology* **2016,** *81*, 166-173.

82. Orian-Rousseau, V., CD44, a therapeutic target for metastasising tumours. *European Journal of Cancer* **2010,** *46* (7), 1271-1277.

83. Orian-Rousseau, V., CD44 Acts as a Signaling Platform Controlling Tumor Progression and Metastasis. *Frontiers in Immunology* **2015,** *6*, 154.

84. Landen, C. N.; Goodman, B. W.; Katre, A. A.; Steg, A. D.; Nick, A. M.; Stone, R.; Miller, L.; Vivas-Mejia, P. E.; Jennings, N. B.; Gershenson, D. M.; Bast, R. C.; Coleman, R. L.; Lopez-Berestein, G.; Sood, A. K., Targeting Aldehyde Dehydrogenase Cancer Stem Cells in Ovarian Cancer. *Molecular Cancer Therapeutics* **2010**.

85. Ma, I.; Allan, A. L., The Role of Human Aldehyde Dehydrogenase in Normal and Cancer Stem Cells. *Stem Cell Reviews and Reports* **2011,** *7* (2), 292-306.

86. Jiang, F.; Qiu, Q.; Khanna, A.; Todd, N. W.; Deepak, J.; Xing, L.; Wang, H.; Liu, Z.; Su, Y.; Stass, S. A., Aldehyde dehydrogenase 1 is a tumor stem cell-associated marker in lung cancer. *Molecular Cancer Research* **2009,** *7* (3), 330-338.

87. Dalerba, P.; Dylla, S. J.; Park, I.-K.; Liu, R.; Wang, X.; Cho, R. W.; Hoey, T.; Gurney, A.; Huang, E. H.; Simeone, D. M.; Shelton, A. A.; Parmiani, G.; Castelli, C.; Clarke, M. F., Phenotypic characterization of human colorectal cancer stem cells. *Proceedings of the National Academy of Sciences* **2007,** *104* (24), 10158.

88. Tayama, S.; Motohara, T.; Narantuya, D.; Li, C.; Fujimoto, K.; Sakaguchi, I.; Tashiro, H.; Saya, H.; Nagano, O.; Katabuchi, H., The impact of EpCAM expression on response to chemotherapy and clinical outcomes in patients with epithelial ovarian cancer. *Oncotarget* **2017,** *8* (27), 44312-44325.

89. Al-Hajj, M.; Wicha, M. S.; Benito-Hernandez, A.; Morrison, S. J.; Clarke, M. F., Prospective identification of tumorigenic breast cancer cells. *Proceedings of the National Academy of Sciences* **2003,** *100* (7), 3983.

90. Li, C.; Heidt, D. G.; Dalerba, P.; Burant, C. F.; Zhang, L.; Adsay, V.; Wicha, M.; Clarke, M. F.; Simeone, D. M., Identification of Pancreatic Cancer Stem Cells. *Cancer Research* **2007,** *67* (3), 1030.

91. Wong, A. S.; Auersperg, N., Normal ovarian surface epithelium. In *Ovarian Cancer*, Springer: 2002; pp 161-183.

92. Soler, A. P.; Knudsen, K.; Tecson-Miguel, A.; McBrearty, F.; Han, A.; Salazar, H., Expression of E-cadherin and N-cadherin in surface epithelial-stromal tumors of the ovary distinguishes mucinous from serous and endometrioid tumors. *Human Pathology* **1997,** *28* (6), 734-739.

93. Patel, I. S.; Madan, P.; Getsios, S.; Bertrand, M. A.; MacCalman, C. D., Cadherin switching in ovarian cancer progression. *International Journal of Cancer* **2003,** *106* (2), 172-177.

94. Sundfeldt, K.; Piontkewitz, Y.; Ivarsson, K.; Nilsson, O.; Hellberg, P.; Brännströ, M.; Janson, P. O.; Enerbäck, S.; Hedin, L., E-cadherin expression in human epithelial ovarian cancer and normal ovary. *International Journal of Cancer* **1997,** *74* (3), 275-280.

95. Hudson, L. G.; Zeineldin, R.; Stack, M. S., Phenotypic plasticity of neoplastic ovarian epithelium: unique cadherin profiles in tumor progression. *Clinical & Experimental Metastasis* **2008,** *25* (6), 643-655.

96. Burgos-Ojeda, D.; Rueda, B. R.; Buckanovich, R. J., Ovarian cancer stem cell markers: Prognostic and therapeutic implications. *Cancer Letters* **2012,** *322* (1), 1-7.

97. Bapat, S. A.; Mali, A. M.; Koppikar, C. B.; Kurrey, N. K., Stem and Progenitor-Like Cells Contribute to the Aggressive Behavior of Human Epithelial Ovarian Cancer. *Cancer Research* **2005,** *65* (8), 3025.

98. Cioffi, M.; D'Alterio, C.; Camerlingo, R.; Tirino, V.; Consales, C.; Riccio, A.; Ieranò, C.; Cecere, S. C.; Losito, N. S.; Greggi, S.; Pignata, S.; Pirozzi, G.; Scala, S., Identification of a distinct population of CD133+CXCR4+ cancer stem cells in ovarian cancer. *Scientific Reports* **2015,** *5*, 10357.

99. Ferrandina, G.; Martinelli, E.; Petrillo, M.; Prisco, M. G.; Zannoni, G.; Sioletic, S.; Scambia, G., CD133 antigen expression in ovarian cancer. *BMC Cancer* **2009,** *9* (1), 221.

100. FERRANDINA, G.; BONANNO, G.; PIERELLI, L.; PERILLO, A.; PROCOLI, A.; MARIOTTI, A.; CORALLO, M.; MARTINELLI, E.; RUTELLA, S.; PAGLIA, A.; ZANNONI, G.; MANCUSO, S.; SCAMBIA, G., Expression of CD133-1 and CD133-2 in ovarian cancer. *International Journal of Gynecological Cancer* **2008,** *18* (3), 506-514.

101. Curley, M. D.; Therrien, V. A.; Cummings, C. L.; Sergent, P. A.; Koulouris, C. R.; Friel, A. M.; Roberts, D. J.; Seiden, M. V.; Scadden, D. T.; Rueda, B. R., CD133 expression defines a tumor initiating cell population in primary human ovarian cancer. *Stem Cells* **2009,** *27* (12), 2875-2883.

102. Kryczek, I.; Liu, S.; Roh, M.; Vatan, L.; Szeliga, W.; Wei, S.; Banerjee, M.; Mao, Y.; Kotarski, J.; Wicha Max, S.; Liu, R.; Zou, W., Expression of aldehyde dehydrogenase and CD133 defines ovarian cancer stem cells. *International Journal of Cancer* **2011,** *130* (1), 29-39.

103. Silva, I. A.; Bai, S.; McLean, K.; Yang, K.; Griffith, K.; Thomas, D.; Ginestier, C.; Johnston, C.; Kueck, A.; Reynolds, R. K.; Wicha, M. S.; Buckanovich, R. J., Aldehyde Dehydrogenase in Combination with CD133 Defines Angiogenic Ovarian Cancer Stem Cells That Portend Poor Patient Survival. *Cancer Research* **2011**.

104. Lushchak, V. I., Free radicals, reactive oxygen species, oxidative stress and its classification. *Chemico-Biological Interactions* **2014,** *224*, 164-175.

105. Schieber, M.; Chandel, Navdeep S., ROS Function in Redox Signaling and Oxidative Stress. *Current Biology* **2014,** *24* (10), R453-R462.

106. Finkel, T., Signal transduction by reactive oxygen species. *The Journal of Cell Biology* **2011,** *194* (1), 7-15.

107. Brown, N. S.; Bicknell, R., Hypoxia and oxidative stress in breast cancer Oxidative stress-its effects on the growth, metastatic potential and response to therapy of breast cancer. *Breast Cancer Research* **2001,** *3* (5), 323.

108. Hu, Y.; Rosen, D. G.; Zhou, Y.; Feng, L.; Yang, G.; Liu, J.; Huang, P., Mitochondrial manganese-superoxide dismutase expression in ovarian cancer role in cell proliferation and response to oxidative stress. *Journal of Biological Chemistry* **2005,** *280* (47), 39485-39492.

109. Natarajan, S. K.; Becker, D. F., Role of apoptosis-inducing factor, proline dehydrogenase, and NADPH oxidase in apoptosis and oxidative stress. *Cell Health and Cytoskeleton* **2012,** *2012* (4), 11.

110. Pall, M. L.; Levine, S., Nrf2, a master regulator of detoxification and also antioxidant, anti-inflammatory and other cytoprotective mechanisms, is raised by health promoting factors. *Sheng Li Xue Bao* **2015,** *67* (1), 1-18.

111. Furfaro, A.; Traverso, N.; Domenicotti, C.; Piras, S.; Moretta, L.; Marinari, U.; Pronzato, M.; Nitti, M., The Nrf2/HO-1 axis in cancer cell growth and chemoresistance. *Oxidative Medicine and Cellular Longevity* **2016,** *2016*.

112. Harvey, C. J.; Thimmulappa, R. K.; Singh, A.; Blake, D. J.; Ling, G.; Wakabayashi, N.; Fujii, J.; Myers, A.; Biswal, S., Nrf2-regulated glutathione recycling independent of biosynthesis is critical for cell survival during oxidative stress. *Free Radical Biology and Medicine* **2009,** *46* (4), 443-453.

113. Walker, A.; Singh, A.; Tully, E.; Woo, J.; Le, A.; Nguyen, T.; Biswal, S.; Sharma, D.; Gabrielson, E., Nrf2 signaling and autophagy are complementary in protecting breast cancer cells during glucose deprivation. *Free Radical Biology and Medicine* **2018,** *120*, 407-413.

114. Wakabayashi, N.; Shin, S.; Slocum, S. L.; Agoston, E. S.; Wakabayashi, J.; Kwak, M.-K.; Misra, V.; Biswal, S.; Yamamoto, M.; Kensler, T. W., Regulation of Notch1 Signaling by Nrf2: Implications for Tissue Regeneration. *Science Signaling* **2010,** *3* (130), ra52.

115. Kim, W. D.; Kim, Y. W.; Cho, I. J.; Lee, C. H.; Kim, S. G., E-cadherin inhibits nuclear accumulation of Nrf2: implications for chemoresistance of cancer cells. *J Cell Science* **2012**, jcs. 095422.

116. Dinkova-Kostova, A. T.; Talalay, P., NAD (P) H: quinone acceptor oxidoreductase 1 (NQO1), a multifunctional antioxidant enzyme and exceptionally versatile cytoprotector. *Archives of Biochemistry and Biophysics* **2010,** *501* (1), 116-123.

117. Seow, H. A.; Penketh, P. G.; Belcourt, M. F.; Tomasz, M.; Rockwell, S.; Sartorelli, A. C., Nuclear overexpression of NAD (P) H: quinone oxidoreductase 1 in Chinese hamster ovary cells increases the cytotoxicity of mitomycin C under aerobic and hypoxic conditions. *Journal of Biological Chemistry* **2004,** *279* (30), 31606-31612.

118. Belinsky, M.; Jaiswal, A. K., NAD (P) H: quinone oxidoreductase 1 (DT-diaphorase) expression in normal and tumor tissues. *Cancer and Metastasis Reviews* **1993,** *12* (2), 103-117.

119. Beyer, R. E.; Segura-Aguilar, J.; Di Bernardo, S.; Cavazzoni, M.; Fato, R.; Fiorentini, D.; Galli, M. C.; Setti, M.; Landi, L.; Lenaz, G., The role of DT-diaphorase in the maintenance of the reduced antioxidant form of coenzyme Q in membrane systems. *Proceedings of the National Academy of Sciences* **1996,** *93* (6), 2528-2532.

120. Asher, G.; Lotem, J.; Kama, R.; Sachs, L.; Shaul, Y., NQO1 stabilizes p53 through a distinct pathway. *Proceedings of the National Academy of Sciences* **2002,** *99* (5), 3099-3104.

121. Siegel, D.; Bolton, E. M.; Burr, J. A.; Liebler, D. C.; Ross, D., The reduction of α-tocopherolquinone by human NAD (P) H: quinone oxidoreductase: the role of α-tocopherolhydroquinone as a cellular antioxidant. *Molecular Pharmacology* **1997,** *52* (2), 300-305.

122. Phillips, R. M.; de la Cruz, A.; Traver, R. D.; Gibson, N. W., Increased activity and expression of NAD (P) H: quinone acceptor oxidoreductase in confluent cell cultures and within multicellular spheroids. *Cancer Research* **1994,** *54* (14), 3766-3771.

123. Madajewski, B.; Boatman, M. A.; Chakrabarti, G.; Boothman, D. A.; Bey, E. A., Depleting Tumor-NQO1 Potentiates Anoikis and Inhibits Growth of NSCLC. *Molecular Cancer Research* **2015**.

124. Lister, A.; Nedjadi, T.; Kitteringham, N. R.; Campbell, F.; Costello, E.; Lloyd, B.; Copple, I. M.; Williams, S.; Owen, A.; Neoptolemos, J. P.; Goldring, C. E.; Park, B. K., Nrf2 is overexpressed in pancreatic cancer: implications for cell proliferation and therapy. *Molecular Cancer* **2011,** *10* (1), 37.

125. Wang, J.; Zhang, M.; Zhang, L.; Cai, H.; Zhou, S.; Zhang, J.; Wang, Y., Correlation of Nrf2, HO-1, and MRP3 in Gallbladder Cancer and Their Relationships to

Clinicopathologic Features and Survival. *Journal of Surgical Research* **2010,** *164* (1), e99-e105.

126. Barrera, L. N.; Rushworth, S. A.; Bowles, K. M.; MacEwan, D. J., Bortezomib induces heme oxygenase-1 expression in multiple myeloma. *Cell Cycle* **2012,** *11* (12), 2248-2252.

127. Do, M. T.; Kim, H. G.; Khanal, T.; Choi, J. H.; Kim, D. H.; Jeong, T. C.; Jeong, H. G., Metformin inhibits heme oxygenase-1 expression in cancer cells through inactivation of Raf-ERK-Nrf2 signaling and AMPK-independent pathways. *Toxicology and Applied Pharmacology* **2013,** *271* (2), 229-238.

128. Jozkowicz, A.; Was, H.; Dulak, J., Heme oxygenase-1 in tumors: is it a false friend? *Antioxidants & Redox Signaling* **2007,** *9* (12), 2099-2118.

129. Nowis, D.; Legat, M.; Grzela, T.; Niderla, J.; Wilczek, E.; Wilczynski, G.; Głodkowska, E.; Mrowka, P.; Issat, T.; Dulak, J., Heme oxygenase-1 protects tumor cells against photodynamic therapy-mediated cytotoxicity. *Oncogene* **2006,** *25* (24), 3365.

130. Berberat, P. O.; Dambrauskas, Z.; Gulbinas, A.; Giese, T.; Giese, N.; Künzli, B.; Autschbach, F.; Meuer, S.; Büchler, M. W.; Friess, H., Inhibition of heme oxygenase-1 increases responsiveness of pancreatic cancer cells to anticancer treatment. *Clinical Cancer Research* **2005,** *11* (10), 3790-3798.

131. Godwin, A. K.; Meister, A.; Dwyer, P. J.; Huang, C. S.; Hamilton, T. C.; Anderson, M. E., High resistance to cisplatin in human ovarian cancer cell lines is associated with marked increase of glutathione synthesis. *Proceedings of the National Academy of Sciences* **1992,** *89* (7), 3070.

132. Aas, T.; Børresen, A.-L.; Geisler, S.; Smith-Sørensen, B.; Johnsen, H.; Varhaug, J. E.; Akslen, L. A.; Lønning, P. E., Specific P53 mutations are associated with de novo resistance to doxorubicin in breast cancer patients. *Nature Medicine* **1996,** *2*, 811.

133. Rusch, V.; Klimstra, D.; Venkatraman, E.; Oliver, J.; Martini, N.; Gralla, R.; Kris, M.; Dmitrovsky, E., Aberrant p53 expression predicts clinical resistance to cisplatin-based chemotherapy in locally advanced non-small cell lung cancer. *Cancer Research* **1995,** *55* (21), 5038-5042.

134. Haslehurst, A. M.; Koti, M.; Dharsee, M.; Nuin, P.; Evans, K.; Geraci, J.; Childs, T.; Chen, J.; Li, J.; Weberpals, J.; Davey, S.; Squire, J.; Park, P. C.; Feilotter, H., EMT transcription factors snail and slug directly contribute to cisplatin resistance in ovarian cancer. *BMC Cancer* **2012,** *12* (1), 91.

135. Kaufhold, S.; Bonavida, B., Central role of Snail1 in the regulation of EMT and resistance in cancer: a target for therapeutic intervention. *Journal of Experimental & Clinical Cancer Research* **2014,** *33* (1), 62.

136. Kajita, M.; McClinic, K. N.; Wade, P. A., Aberrant expression of the transcription factors snail and slug alters the response to genotoxic stress. *Molecular and Cellular Biology* **2004,** *24* (17), 7559-7566.

137. Kudo-Saito, C.; Shirako, H.; Takeuchi, T.; Kawakami, Y., Cancer metastasis is accelerated through immunosuppression during Snail-induced EMT of cancer cells. *Cancer Cell* **2009,** *15* (3), 195-206.

138. Mitra, A.; Mishra, L.; Li, S., EMT, CTCs and CSCs in tumor relapse and drug-resistance. *Oncotarget* **2015,** *6* (13), 10697-10711.

139. Mani, S. A.; Guo, W.; Liao, M.-J.; Eaton, E. N.; Ayyanan, A.; Zhou, A. Y.; Brooks, M.; Reinhard, F.; Zhang, C. C.; Shipitsin, M., The epithelial-mesenchymal transition generates cells with properties of stem cells. *Cell* **2008,** *133* (4), 704-715.

140. Markman, M., Combination versus sequential cytotoxic chemotherapy in recurrent ovarian cancer: Time for an evidence-based comparison. *Gynecologic Oncology* **2010,** *118* (1), 6-7.

141. McGuire, W. P.; Hoskins, W. J.; Brady, M. F.; Kucera, P. R.; Partridge, E. E.; Look, K. Y.; Clarke-Pearson, D. L.; Davidson, M., Cyclophosphamide and cisplatin compared with paclitaxel and cisplatin in patients with stage III and stage IV ovarian cancer. *New England Journal of Medicine* **1996,** *334* (1), 1-6.

142. Sherman-Baust, C. A.; Becker, K. G.; Wood Iii, W. H.; Zhang, Y.; Morin, P. J., Gene expression and pathway analysis of ovarian cancer cells selected for resistance to cisplatin, paclitaxel, or doxorubicin. *Journal of Ovarian Research* **2011,** *4* (1), 21.

143. Perego, P.; Giarola, M.; Righetti, S. C.; Supino, R.; Caserini, C.; Delia, D.; Pierotti, M. A.; Miyashita, T.; Reed, J. C.; Zunino, F., Association between Cisplatin Resistance and Mutation of p53 Gene and Reduced Bax Expression in Ovarian Carcinoma Cell Systems. *Cancer Research* **1996,** *56* (3), 556.

144. Shen, D.-W.; Pouliot, L. M.; Hall, M. D.; Gottesman, M. M., Cisplatin Resistance: A Cellular Self-Defense Mechanism Resulting from Multiple Epigenetic and Genetic Changes. *Pharmacological Reviews* **2012**.

145. Masuda, H.; Ozols, R. F.; Lai, G.-M.; Fojo, A.; Rothenberg, M.; Hamilton, T. C., Increased DNA Repair as a Mechanism of Acquired Resistance to cis-Diamminedichloroplatinum(II) in Human Ovarian Cancer Cell Lines. *Cancer Research* **1988,** *48* (20), 5713.

146. Parker, R. J.; Eastman, A.; Bostick-Bruton, F.; Reed, E., Acquired cisplatin resistance in human ovarian cancer cells is associated with enhanced repair of cisplatin-DNA lesions and reduced drug accumulation. *The Journal of Clinical Investigation* **1991,** *87* (3), 772-777.

147. Chauhan, S. S.; Liang, X. J.; Su, A. W.; Pai-Panandiker, A.; Shen, D. W.; Hanover, J. A.; Gottesman, M. M., Reduced endocytosis and altered lysosome function in cisplatin-resistant cell lines. *British Journal Of Cancer* **2003,** *88*, 1327.

148. Liang, X.-J.; Mukherjee, S.; Shen, D.-W.; Maxfield, F. R.; Gottesman, M. M., Endocytic Recycling Compartments Altered in Cisplatin-Resistant Cancer Cells. *Cancer Research* **2006,** *66* (4), 2346.

149. Arts Henriette, J. G.; Hollema, H.; Lemstra, W.; Willemse Pax, H. B.; De Vries Elisabeth, G. E.; Kampinga Harm, H.; Van der Zee Ate, G. J., Heat-shock-protein-27(HSP27) expression in ovarian carcinoma: Relation in response to chemotherapy and prognosis. *International Journal of Cancer* **1999,** *84* (3), 234-238.

150. Vargas-Roig Laura, M.; Gago Francisco, E.; Tello, O.; Aznar Juan, C.; Ciocca Daniel, R., Heat shock protein expression and drug resistance in breast cancer patients treated with induction chemotherapy. *International Journal of Cancer* **1998,** *79* (5), 468-475.

151. Belfi, C. A.; Chatterjee, S.; Gosky, D. M.; Berger, S. J.; Berger, N. A., Increased Sensitivity of Human Colon Cancer Cells to DNA Cross-Linking Agents after GRP78 Up-Regulation. *Biochemical and Biophysical Research Communications* **1999,** *257* (2), 361-368.

152. Wang, Q.-E.; Han, C.; Milum, K.; Wani, A. A., Stem cell protein Piwil2 modulates chromatin modifications upon cisplatin treatment. *Mutation Research/Fundamental and Molecular Mechanisms of Mutagenesis* **2011,** *708* (1), 59-68.

153. Chang, X.; Monitto, C. L.; Demokan, S.; Kim, M. S.; Chang, S. S.; Zhong, X.; Califano, J. A.; Sidransky, D., Identification of hypermethylated genes associated with cisplatin resistance in human cancers. *Cancer Research* **2010**, 0008-5472. CAN-09-3427.

154. Miyamoto, N.; Izumi, H.; Noguchi, T.; Nakajima, Y.; Ohmiya, Y.; Shiota, M.; Kidani, A.; Tawara, A.; Kohno, K., Tip60 is regulated by circadian transcription factor clock and is involved in cisplatin resistance. *Journal of Biological Chemistry* **2008,** *283* (26), 18218-18226.

155. Hirano, G.; Izumi, H.; Kidani, A.; Yasuniwa, Y.; Han, B.; Kusaba, H.; Akashi, K.; Kuwano, M.; Kohno, K., Enhanced Expression of PCAF Endows Apoptosis Resistance in Cisplatin-Resistant Cells. *Molecular Cancer Research* **2010**.

156. Cho, J.-M.; Manandhar, S.; Lee, H.-R.; Park, H.-M.; Kwak, M.-K., Role of the Nrf2-antioxidant system in cytotoxicity mediated by anticancer cisplatin: implication to cancer cell resistance. *Cancer Letters* **2008,** *260* (1-2), 96-108.

157. Singh, A.; Misra, V.; Thimmulappa, R. K.; Lee, H.; Ames, S.; Hoque, M. O.; Herman, J. G.; Baylin, S. B.; Sidransky, D.; Gabrielson, E.; Brock, M. V.; Biswal, S., Dysfunctional KEAP1–NRF2 Interaction in Non-Small-Cell Lung Cancer. *PLOS Medicine* **2006,** *3* (10), e420.

CHAPTER 2
EVALUATION OF NAD(P)H:QUINONE OXIDOREDUCTASE ISOZYME-1 EXPRESSION AND ACTIVITY, AND CELLULAR PHENOTYPE IN HUMAN OVARIAN CANCER CELL MONOLAYERS

2.1 Introduction

Increasing evidence has been found suggesting that major detoxification pathways may be involved in cancer progression, chemoresistance, and ultimately recurrence. As detailed in Chapter 1, the Keap1/Nrf2/ARE pathway drives the production of cytoprotective enzymes and antioxidants in response to oxidative stress.[1] However, aberrant mutations in the genes that regulate this pathway can lead to overproduction or underproduction of detoxifying proteins.[1] In addition, it has been suggested that abnormalities in this pathway can result in increased ROS, drug resistance, and even tumor formation.[2-5] Thus, assessing the level of influence cytoprotective proteins associated with the Keap1/Nrf2/ARE pathway have on cancer progression and survival is would beneficial to cancer researchers and clinicians.

One way to probe the influence of detoxifying pathways on cancer progression and resistance is to monitor expression and subsequent activity of the cytoprotective species that are generated as a result of it. NAD(P)H:quinone oxidoreductase isozyme-1 (NQO1), a cytoprotective enzyme whose generation is directly influenced by the Keap1/Nrf2/ARE pathway, has garnered attention due to its detoxifying and bioreductive capabilities within the cell.[6] As mentioned in Chapter 1, NQO1 combats ROS brought on by changes in the cellular environment by ensuring that semiquinone radical production is minimized.[6] In Scheme 2.1 is illustrated the reduction of 1,4-benzoquinone by a one-electron

reductase (A) and NQO1 (B). Moreover, it has been found to be involved in generation of antioxidants such as ubiquinone and vitamin E.

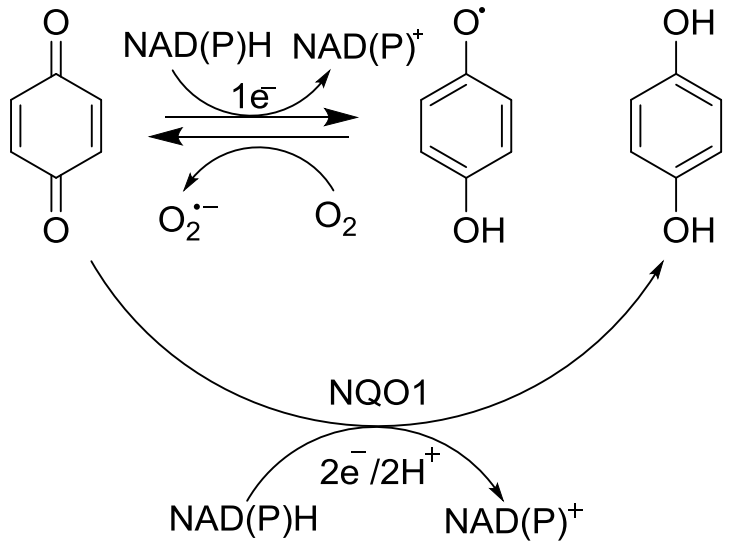

Scheme 2.1. Reduction of quinone by reductases. (A) Reduction by a one-electron reductase (e.g., cytochrome p450) in the presence of NAD(P)H cofactor yields a semiquinone radical. (B) Two-electron reduction of the quinone species by NQO1 in the presence of NAD(P)H cofactor enables A to be bypassed, thereby yielding a hydroquinone.

Unfortunately, NQO1 expression and activity provides benefits to both healthy and diseased cells. The 2-electron reductase has been found to be highly expressed, up to 200-fold, in pancreatic, colorectal, lung, breast, gastrointestinal, and ovarian cancer tumor tissues, in comparison to their normal counterparts.[7-12] These findings have led to a surge in anti-tumor drugs that are bioactivated by NQO1 to produce highly toxic species that can combat disease.[13-15] In addition to anti-tumor drug development, diseased cell imaging strategies based on NQO1 reduction of quinone-based agents have become extensive since the pioneering work of the McCarley group. The LSU team has created

NQO1-activatable fluorescent probes that enable visualization of diseased tissues overexpressing the enzyme, over a broad range of emission energies.[16-23] Such probes enable active NQO1 to be observed in live and subsequently fixed cells upon reduction of a quinone probe substrate that leads to the release of a highly fluorescent reporter, thus enabling visualization of NQO1-bearing cancer cells with confocal or widefield microscopies.

To gain knowledge concerning NQO1 expression and activity levels in often-studied ovarian cancer cell lines derived from patients at various disease and treatment timelines, NQO1 expression and activity was examined in several high-grade serous ovarian carcinoma (HGSOC) cell lines using traditional biochemical techniques and a NQO1-activated fluorescent probe, Q_3NTCY, developed by former McCarley group member, Dr. Zhenhua Shen.[24] In addition, culture time-dependent analysis of cellular proliferation, which is likely to affected by both the presence and activeness of NQO1, as well as the level of invasiveness of a cell line, was assayed.

2.2 Experimental

2.2.1 Cell Culture

Human ovarian carcinoma cell lines OVCAR-5, OVCAR-8, and SHIN-3, gifts from Dr. Hisataka Kobayashi at the United States National Institutes of Health, National Cancer Institute, Center for Cancer Research were used for the studies presented in this chapter. Human ovarian carcinoma cell line OVCAR-3 was purchased from American Type Culture Collection (ATCC). All cell lines were cultured in either DMEM or RPMI-1640 medium purchased from the ATCC, which was supplemented with 10% fetal bovine

serum (FBS; ATCC), 10 IU/mL penicillin, and 10 μg/mL streptomycin (Life Technologies), unless stated otherwise. Bovine insulin (1 μg/mL) was an additional supplement for OVCAR-3 cells. Cells were cultured in 75 cm^2 treated tissue culture flasks at 37 °C under 5% CO_2 in a humidified incubator.

2.2.2 Protein Quantification

To determine the total protein concentration in cell monolayers for each cell line, bulk protein was extracted. Briefly, cells were grown in treated tissue culture 6-well plates (Fisher Scientific), and each day over a 7-day period, cells were dissociated with trypsin-EDTA (Fisher Scientific). Following centrifugation at 900 rpm for 7 minutes at 4 °C, the supernatant was removed, and 300 μL of radioimmunoprecipitation assay (RIPA, ThermoFisher) buffer with 1 mM phenylmethylsulfonyl fluoride (Sigma) and protease inhibitor cocktail (Sigma) were added to pelleted cells. The suspended cells were incubated on ice for 20 minutes with periodic vortexing to achieve homogeneity within the solution. The solution was then centrifuged at 18,000 × *g* for 20 minutes at 4 °C. The supernatant was obtained and aliquoted into sterile Eppendorf tubes at −80 °C until use. Total protein content was quantified using the well-established BCA assay.

2.2.3 Western Blot

NQO1 expression was measured in 25–30 μg protein samples, each corresponding to the number of days that cells were cultured prior to protein extraction. Samples were analyzed using sodium dodecyl sulphate-polyacrylamide gel electrophoresis (SDS-PAGE) using 4–20% polyacrylamide gels (Bio-Rad). 10 μL of Kaleidoscope Pre-Stained Standard marker was used to track proteins. Samples were

diluted in 2X Laemmli sample buffer containing 2-mercaptoethanol at a 1:1 ratio. Protein separation was conducted at 100 V for 65 minutes in running buffer (1X Tris/Glycine/SDS in deionized water) followed by protein transfer onto nitrocellulose membranes in transfer buffer (1X Tris-Glycine and 20% methanol).

Following transfer, the nitrocellulose membrane was blocked with 5% non-fat dry milk (NFDM) for one hour before being washed with tris-buffered saline with 0.1% tween-20 (TBST) solution. Simultaneously, working concentrations of the mouse anti-NQO1 monoclonal antibody and rabbit anti-β-actin monoclonal antibody were added to each membrane. All antibodies used in this work were purchased from Cell Signaling Technologies. Upon antibody addition, membranes were incubated overnight at 4 °C with gentle shaking. The following day, the membrane was washed with PBS 3X in 10-minute intervals. Next, both anti-mouse IgG and anti-rabbit IgG, HRP-linked secondary antibodies (Cell Signaling Technologies) were added to the membranes for 1 hour at room temperature with gentle shaking. All antibodies were made at a 1:1000 dilution in a 1% NFDM. Super Signal West Pico Plus chemiluminescent substrate (Fisher Scientific) was prepared based on the manufacturer's protocol, and it was slowly pipetted onto the membranes several times over a period of roughly 2 minutes. Membranes were imaged using a Bio-Rad ChemiDoc MP system with an exposure time of 300 seconds at 60 second intervals. Raw images were saved in tagged image file format (TIFF) files, and band analysis was performed using Fiji/ImageJ software.

2.2.4 RNA Purification and Real-Time Quantitative PCR (RT-qPCR)

Total RNA from cell lines was extracted and purified for analysis using Direct-zol RNA MicroPrep kit (Zymo Research) according to the manufacturer's instructions. RNA was quantified spectrometrically using an Epoch microplate reader (BioTek). Total RNA was reversed transcribed to cDNA using TaqMan Reverse Transcriptase reaction mix provided in the High Capacity RNA-to-cDNA Kit (Applied Biosystems) according to the supplier's instructions. The cDNA was diluted 1:10 in nuclease-free water and 2 μL was used as a template to perform RT-PCR in a 25 μL reaction. B-actin was used as an endogenous control (Applied Biosystems, UK) in single-plexed PCR reactions on an ABI ViiA-7 (qPCR) Detection System (Applied Biosystems) with fast thermocycling conditions (50 °C for 2 minutes, 95 °C for 2 minutes, then 40 cycles at 95 °C for 1 second and 60 °C for 20 seconds), using Taqman Fast Advanced PCR Master Mix (Applied Biosystems). To confirm the modulated expression of the selected target gene and endogenous control, TaqMan 20x gene expression primers and probes (Applied Biosystems) for NQO1-Hs00168547_m1 and ACTB-Hs99999903_m1 were used. All PCR reactions were performed in triplicate.

2.2.5 NQO1 Activity via Spectrometric Analysis/Enzyme Kinetics

NQO1 activity was assayed spectrometrically by measuring the absorbance at 600 nm for the dicoumarol-sensitive reduction of the quinone substrate 2,6-dichlorophenolindophenol (DCPIP). The assay buffer consisted of 200 μM NADH and 0.014% BSA in 25 mM of Tris-HCl at pH 7.4 with or without 20 μM dicoumarol, a known NQO1 inhibitor. A fraction of lysate was added to 0.75 mL of assay buffer to give a final

protein concentration of 5 μg in a 2-mL plastic cuvette. To start the reaction, 0.75 mL of 80 μM DCPIP in assay buffer was added, bringing the final volume to 1.5 mL. Enzymatic activity was determined based on NQO1 ability to reduce the DCPIP substrate at 600 nm in the presence and absence of the dicoumarol inhibitor. Each measurement was carried out using a Cary 50 UV/Vis spectrometer over a 2 to 10-minute timeframe depending on the cell line being assayed. Dicoumarol-sensitive NQO1 activity is then calculated by subtracting the activity of an assay with dicoumarol from the corresponding assay without dicoumarol. Finally, activity is recorded in units of *nmol /mg/min*.

2.2.6 Immunocytochemistry/Immunofluorescence (ICC/IF)

OVCAR-5, OVCAR-8, SHIN-3, and OVCAR-3 cell monolayers were cultured overnight in a 16-well chambered slide (LabTek) at 37 °C. The following day, cells were washed with ice cold PBS for 5 minutes to remove excess media. Samples were then treated with 200 μL of cold 4% PFA for 15 minutes in the dark at room temperature. Once the fixation step was completed, samples were washed with PBS for 5 minutes. Samples were then permeabilized with 1% PBST for 15 minutes at 37°C. 200 μL 3% BSA blocking buffer was prepared in PBST and added to each well. The slides were then incubated for 1 hour at room temperature. Simultaneously, a working concentration mouse anti-NQO1 primary antibody was prepared in 1% BSA in PBST at 1:200 dilutions. The antibody solution was added at the volume of 200 μL per well. The slides were incubated at 4 ºC for 1 hour with shaking. Next, the primary antibody solution was removed, and samples were washed with PBST 3 times for 10 minutes each. The secondary antibody was prepared in 1% PBST solution. AlexaFluor-488 conjugated anti-mouse antibody (ThermoFisher) and

prepared at 1:500 dilutions. The samples were incubated with secondary for 1 hour at room temperature, after which they were washed 3 times with PBS. The separating chamber and polymer coating were then removed from the slides and they were mounted with ProLong Gold Diamond Anti-fade mountant with DAPI for nuclear colocalization (ThermoFisher).

Stained cells were excited at 488 nm or 633 using white light laser with spectral emission collected between 495-520 nm and 650-750 nm, respectively. The pinhole was set at 1 Airy Unit (53.1 μm). The DAPI nuclear stain was excited at 405 nm by an argon laser with spectral emission collected between 410-483 nm. Each image was frame and line averaged 4 and 2 times, respectively, at a scan speed of 8000 Hz. An Apo plan 20X 0.3 NA objective was used. Image analysis was performed using LAS X and Fiji/Image J software.

2.2.7 Visualization of NQO1 Activity via Fluorescent Probe Q_3NTCy

OVCAR-5, OVCAR-8, SHIN-3, and OVCAR-3 cells at a concentration of 2×10^5 cell/mL were cultured overnight onto 22 × 22 mm sterile glass coverslips (Corning) in treated tissue culture 6-well plates containing RPMI-1640 medium supplemented with 10 % FBS, 10 IU/mL penicillin, and 10 μg/mL streptomycin. The following day, cell media was removed, and cells were washed with PBS before warmed RPMI-1640 medium without phenol red was added to each well. A 5 μM concentration of **Q_3NTCy** probe was added to each well and incubated at 37 °C for 20 minutes. Following probe exposure, the culture medium was removed, and cells were washed with PBS 3X before 2 mL of 4% PFA was added to the wells. After fixation, cell-coated coverslips were then bonded to

Colormark Plus Precleaned Microscope Slides with ProLong Gold Antifade mountant with DAPI (ThermoFisher). Slides were left to dry overnight in the dark at room temperature.

Confocal images were collected using a Leica TCS SP8 laser-scanning confocal microscope. The TCy reporter that was released from the **Q_3NTCy** probe upon exposure to NQO1 was imaged using a white light laser. The TCy reporter was excited at 633 nm with spectral emission was collected between 650–750 nm using hybrid detectors. The pinhole was set at 1 Airy Unit (53.1 μm). The DAPI nuclear stain was excited at 405 nm by an argon laser with spectral emission collected between 410-483 nm. Each image was frame and line averaged 4 and 2 times, respectively, at a scan speed of 8000 Hz. An Apo plan 20X 0.3 NA objective was used. Image analysis was performed using LAS X and Fiji/Image J software.

2.3 Results and Discussion

2.3.1 NQO1 Expression in OC Monolayers

OVCAR-3, OVCAR-5, and OVCAR-8 cells were preselected for this study due to it being shown that they more closely reflect the behavior of HGSOC.[25] SHIN-3 cells are not as common as the previously mentioned cell lines but were derived from an ovarian serous cystadenocarinoma.[26] It was also important to note that the patients from which these cells were obtained may or may not have underwent chemotherapy prior to debulking surgery, which could have an effect on the presence of NQO1. In addition, it has been reported that OVCAR-3 cells were NQO1-expressing, however, its expression in relation to that of other cell lines has yet to be determined.[27-28] Therefore, NQO1

expression in these cell lines was assessed using traditional western blotting, ICC/IF, and RT-qPCR on monolayer cultures of each cell line.

Western blot analysis of cell monolayers (Figure 2.1.A) revealed that NQO1 expression was effectively undetectable in OVCAR-8, and only faint expression was observed in OVCAR-3 cells. These findings were in stark contrast to those of OVCAR-5 and SHIN-3 cells, which showed expression of the enzyme. ICC/IF was incorporated to qualitatively observe localization of enzyme. ICC/IF analysis, to an extent, corroborated results from western blot analysis. Each cell line displayed expression of NQO1, with OVCAR-8 cells yielding the lowest fluorescence intensity (Figure 2.1.B). However, the fluorescence intensity of stained OVCAR-3 was comparable to that of OVCAR-5 and SHIN-3. The lower overall expression of NQO1 in OVCAR-8 and OVCAR-3 was attributed to the cells being subjected to chemotherapy prior to their removal from the patient, whereas SHIN-3 and OVCAR-5 cells were extracted prior to administration of anticancer agents.[26, 29]

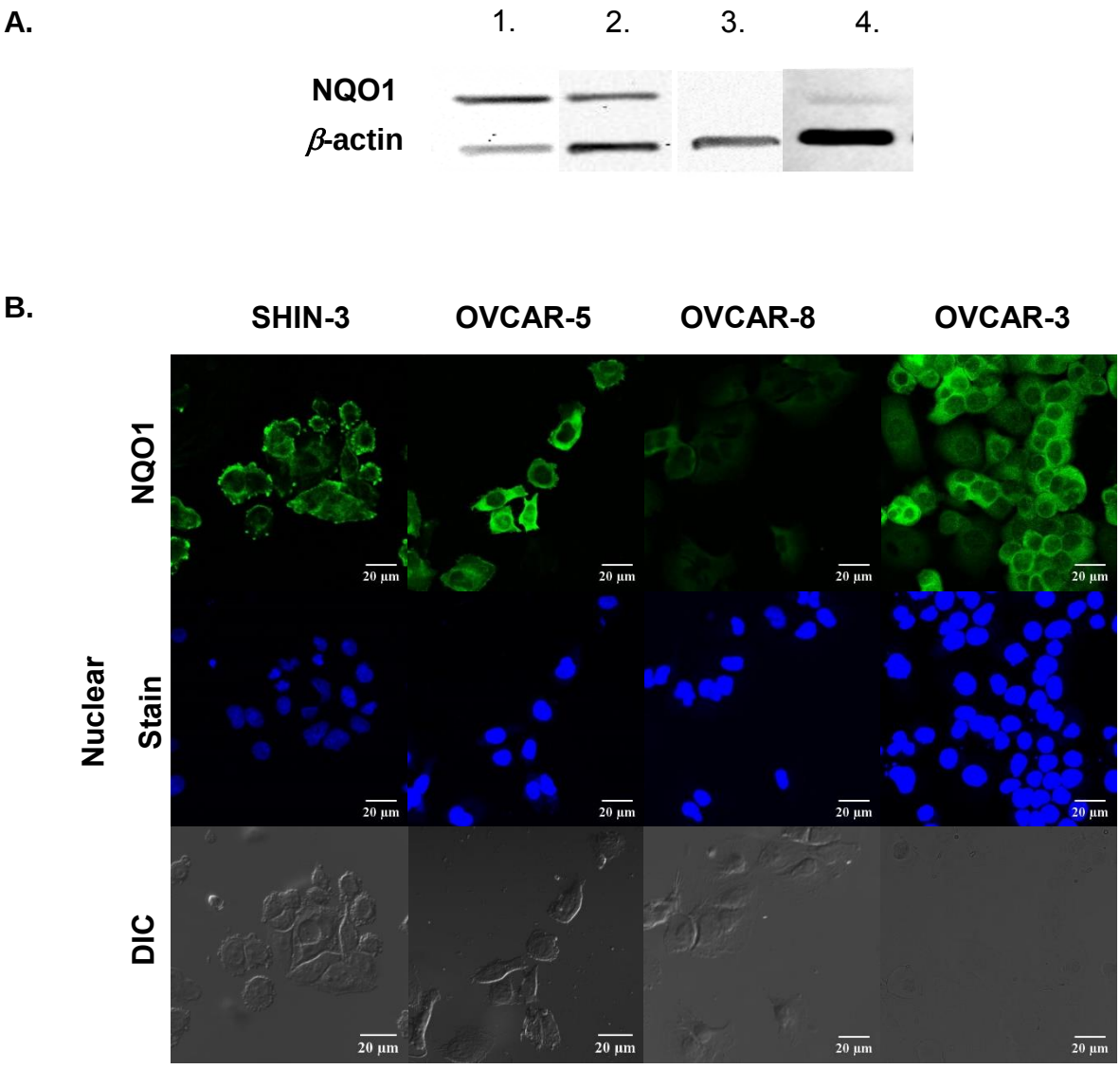

Figure 2.1. (A) Protein bands representative of NQO1 expression obtained from 25-30 μg protein using western blot for ovarian cancer cell monolayers, where SHIN-3, OVCAR-5, OVCAR-8, and OVCAR-3 are respectively labeled as 1-4. **(B)** Immunocytochemistry (immunofluorescence) performed on ovarian cancer cells stained with anti-NQO1 mouse primary antibody and an AlexaFluor-488 mouse secondary antibody. Images were obtained using 488-nm excitation and 490–515 nm emission for NQO1 detection. Nuclear colocalization was achieved with DAPI stain.

Because ICC/IF revealed NQO1 expressed in in OVCAR-8 and OVCAR-3 cells, but bulk lysates assessed via western blot did not, RT-qPCR was conducted to determine expression of NQO1 using a cDNA template derived from each cell line. Specifically, RT-qPCR was used in presence/absence mode to evaluate the expression of the NQO1 gene. The qPCR data revealed that each ovarian cancer cell line studied indeed expressed NQO1. Further examination of the Ct values, or the number of cycles to reach a defined threshold, revealed that neither cell line displayed a statistically significant difference in the number of cycles needed to amplify NQO1 and the β-actin (Figure 2.2). Moreover, in RT-qPCR the difference in Ct value (ΔCt) between the target gene, NQO1, and the endogenous control, β-actin, allows normalized gene expression of the target to be evaluated. In practice, a more negative the ΔCt means increased expression of the target gene. Taking this information into consideration, the ΔCt values obtained in this study depicting the relative gene expression of NQO1 in each cell line are displayed in Figure 2.2.

The relative gene expression of NQO1 between cell lines supported earlier findings regarding NQO1 protein expression indicating a direct relationship between NQO1 gene and protein levels in each cell line. It was determined that SHIN-3 and OVCAR-5 have the highest relative gene expression of NQO1 followed by OVCAR-3, and OVCAR-8 has the lowest. However, it was observed that the error bars representative of OVCAR-5 and SHIN-3 overlapped, thus a *t*-test was performed to determine how insignificant the difference in NQO1 gene expression was between the two cell lines and the calculated *p*-value was 0.7.

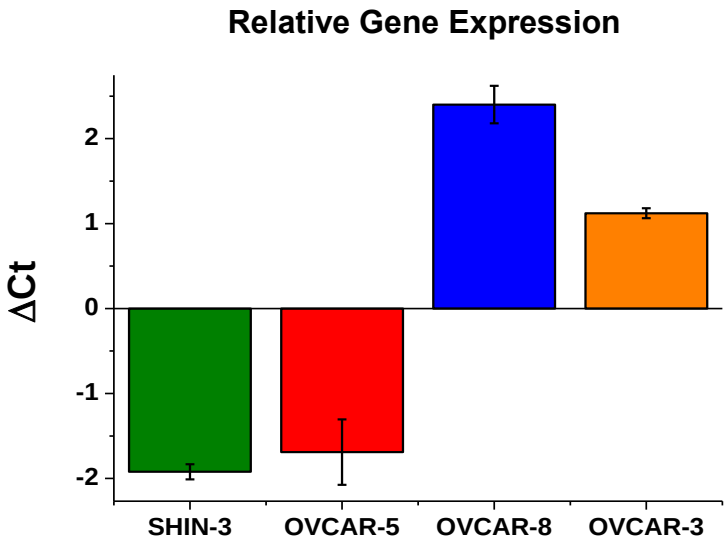

Figure 2.2. Relative gene expression of NQO1 (ΔCt_{mean}) in OC cell monolayers. All values represent gene expression normalized to □-actin.

2.3.2 Spectrometric Determination NQO1 Activity

An established spectrometric method incorporating a quinone substrate, DCPIP, enabled the enzyme catalytic ability to be quantified over a 7-day period (Figure 2.3). It was found that NQO1 activity increased in each cell line over the 7-day period, peaking around the fourth day of culture. However, OVCAR-5, OVCAR-8, and OVCAR-3 cells show a steady decline in activity starting at the fifth day of culture. NQO1 activity in SHIN-3 cells appeared to have plateaued between days 4 and 6 before apparently declining at day 7. The increased NQO1 activity observed between days 3 and 5 was thought to be the result of the cells reaching 100% confluence, thus leading to them consuming nutrients at a faster rate, which could result in hypoxia. Increased hypoxia would lead to increased production of Hif-α protein, which can then be used to initiate both the production and enhanced activity of cytoprotective proteins, such as NQO1.[30-31]

However, because the studied cells were grown in monolayers with a finite growth area, rapid consumption of nutrients from culture media was believed to have resulted in a NQO1 activity plateauing due to a possible increase in cell senescence. This conclusion was supported by the rationale that senescence, or decline in proliferative ability, will likely lead to metabolic processes (i.e., enzymatic activity) plateauing in to maintain homeostasis.[32-33] However, an analysis to determine exact phase of the cell cycle at which confluent cell populations are in will have to be conducted to pinpoint whether cellular senescence is taking place. Specifically, determining the expression of the bmi-1 gene, which regulates both senescence and proliferation would be advantageous.[32] An alternative direction would be to determine the expression and activity levels of senescence-associated biomarkers (e.g., β-galactosidase) will have to be conducted to determine if senescence is taking place once cell populations have become confluent. [34]

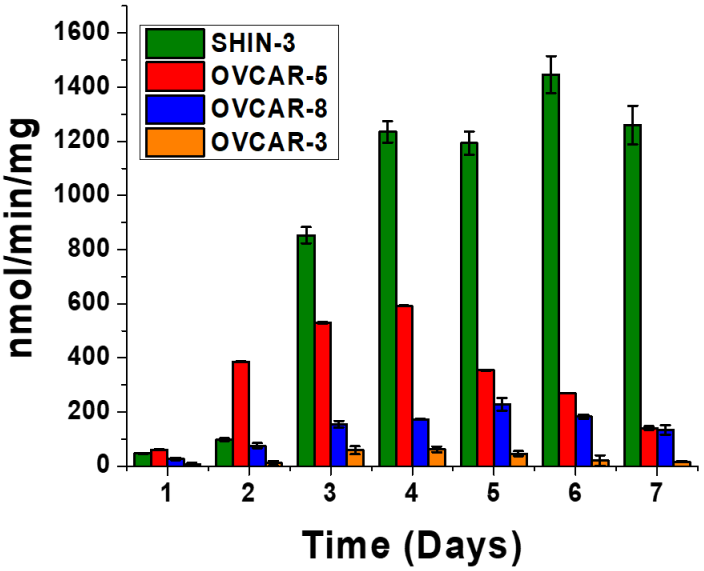

Figure 2.3. NQO1 activity for ovarian cancer cell lines after 7 days of culture obtained from enzymatic assay. 5 μg/mL of protein was used for each sample.

2.3.3 Visualization of NQO1 Activity via Fluorescent Probe Q_3NTCy

Expression and activity were assessed to differentiate between the presence of active NQO1 and inactive NQO1 due to both forms of the enzyme being detected by immunochemical methods. Looking closely at the specific activity of NQO1 at day 4 (Figure 2.3), it was noted that the enzyme activity corroborated NQO1 presence in the western blot and RT-qPCR data shown earlier. Therefore, the increased enzyme activity observed in SHIN-3 and OVCAR-5 cells is strongly associated with of NQO1's enhanced expression in those cell lines relative to OVCAR-8 and OVCAR-3. Furthermore, the moderate to low NQO1 activity observed in OVCAR-8 and OVCAR-3, was also found to be correlated with lower expression of the enzyme. As a result, it was posited that upon incubation with NQO1-activatable fluorescent probe **Q_3NTCy**, an accurate visualization of enzyme activity within cells could be achieved.

Q_3NTCy is a fluorescent probe that can be used in either a turn-on or always-on imaging mode due to a lack of overlap between the emission of the probe (λ_{em} = 765-855 nm) and that of the reporter (λ_{em} = 650-750 nm). Briefly, upon introduction of **Q_3NTCy** to NQO1-active cells, the quinone substrate (Q_3) is selectively reduced and cleaved off, with autonomous removal of the linker following, thereby resulting in the release of the highly fluorescent TCy reporter.[21, 24] Following fixation and subsequent staining of the nucleus, cells are mounted onto glass slides and imaged using confocal microscopy. To visually determine enzyme activity, the NQO1-activable probe **Q_3NTCy** was introduced to cells grown on coverslips 24 hours post culture. For comparative purposes, the NQO1-specific activity measured one day after culture for bulk lysates of each cell line is shown in Figure 2.4. A. below (DCPIP reduction assay). Image analysis revealed there was significantly

higher enzyme activity observed in OVCAR-5 and SHIN-3 cells, while little to no active enzyme was found in OVCAR-8 and OVCAR-3 (Figure 2.4. B). The background corrected mean fluorescence intensity was 22 ±2.8, 21 ±3.5, 5.4 ±0.7, and 2.3 ±0.4 for SHIN-3, OVCAR-5, OVCAR-8, and OVCAR-3, respectively. These findings mimicked that of the spectrometric analysis of cell lysates obtained after one day of culture. Thus, validating my hypothesis that enzyme activity could be effectively measured using the NQO1-activated fluorescent probe **Q_3NTCy**.

A.

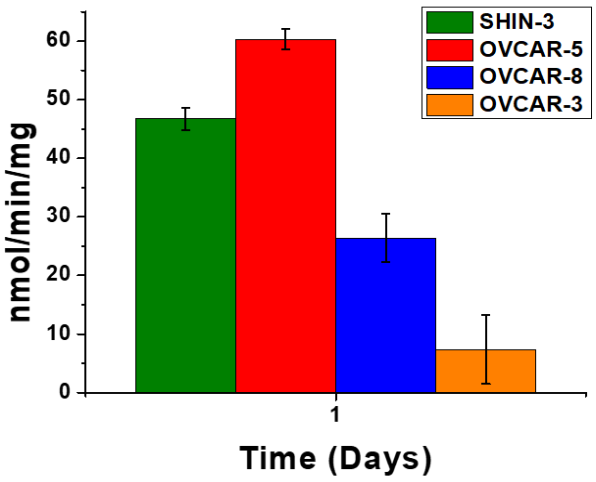

B.

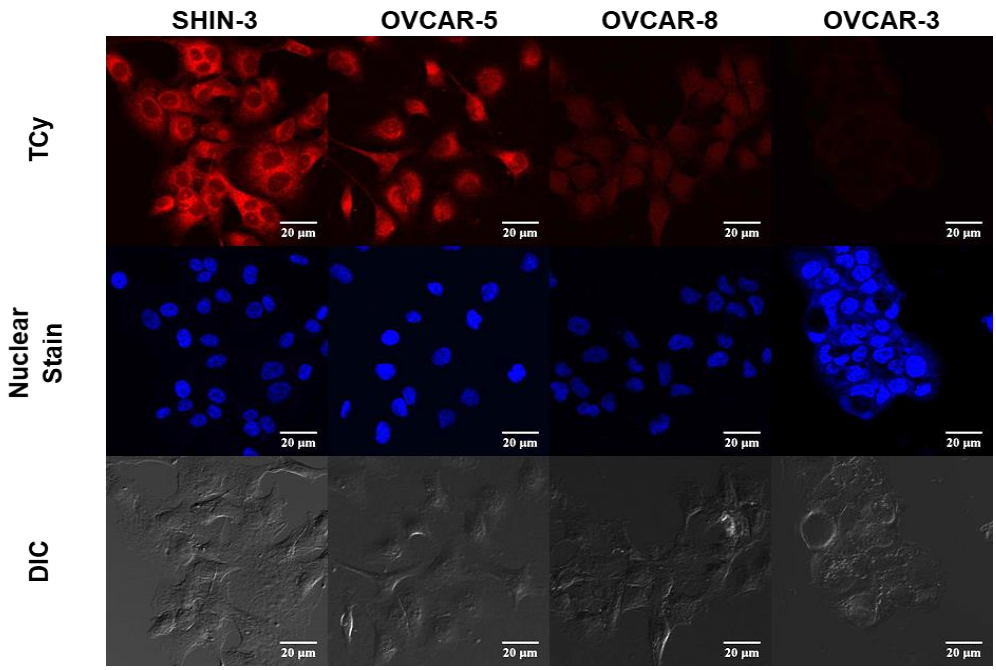

Figure 2.4. (**A**) NQO1 activity for ovarian cancer cell lines after 1 day of culture obtained from enzymatic assay. 5 μg/mL of protein was used for each sample. (**B**) Ovarian cancer cells after treatment with 5 μM **Q_3NTCy** at 37 °C for 20 minutes. Nuclear colocalization was achieved with DAPI nuclear stain.

2.3.4 Proliferation of OC Cell Monolayers

Cellular proliferation was monitored in each cell line using an automated cell counter, and the number of viable cells detected after growth in 2 mL of growth media (viable cells/cm^3) was recorded for each cell line every day for seven days (Figure 2.5). SHIN-3, OVCAR-5, and OVCAR-8 all had doubling times, or the amount of time required for a culture to reach twice the number cells, of less than 48 hours. On the other hand, OVCAR-3 cells proliferated slowly with its doubling time being roughly 72 hours or more. Earlier, it was noted that SHIN-3, OVCAR-5, and OVCAR-8 also had enhanced NQO1 activity when compared to OVCAR-3; thus, it was posited that proliferation may be influenced by NQO1 activity. However, this assumption was challenged, due to the proliferative ability of OVCAR-8 being similar to that of SHIN-3, with both surpassing that of OVCAR-5. However, the NQO1 activity of SHIN-3 and OVCAR-5 was higher than that of OVCAR-8. The apparent contradiction between these findings led to it being concluded that NQO1 activity alone was not solely responsible for proliferation rates.

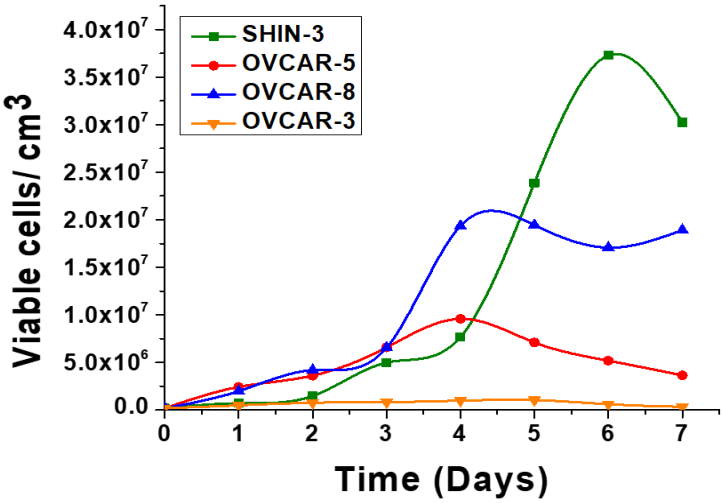

Figure 2.5. Monitoring proliferation of OVCAR cells over 7-days. The smooth curves are merely provided as a guide to the eye for each cell line.

2.4 Conclusions

In sum, NQO1 expression and activity in several ovarian cancer cell lines were evaluated. Analysis of NQO1 expression prior to (i.e., RNA) and after (i.e., NQO1 enzyme) translation of the gene, revealed that SHIN-3 cells displayed the highest expression and activity of NQO1, while OVCAR-3 was found to have the lowest levels/values. Additionally, **Q_3NTCy** activation by the enzyme shows that it is capable of discriminating between cells derived from the same tissue as function of their respective NQO1 activities. In addition, NQO1 activity was closely related to its expression in each cell line, as evidenced by cells having more enzyme expressed having higher activity levels, while those with lower expression having lower NQO1 activity. While a general trend between NQO1 activity and the proliferation rates of SHIN-3, OVCAR-5, and OVCAR-3 was observed, OVCAR-8 cells did not display the same trend. It is postulated that the cancer stage, phenotype, and resistance to chemotherapy of OVCAR-8 may be contributing to its enhanced proliferative abilities. Thus, one or more of these additional factors could be influencing NQO1 activity in each cell line. The coming chapters will further evaluate several of these factors.

2.5 References

1. Konstantinopoulos, P. A.; Spentzos, D.; Fountzilas, E.; Francoeur, N.; Sanisetty, S.; Grammatikos, A. P.; Hecht, J. L.; Cannistra, S. A., Keap1 mutations and Nrf2 pathway activation in epithelial ovarian cancer. *Cancer Research* **2011**.

2. Singh, A.; Misra, V.; Thimmulappa, R. K.; Lee, H.; Ames, S.; Hoque, M. O.; Herman, J. G.; Baylin, S. B.; Sidransky, D.; Gabrielson, E.; Brock, M. V.; Biswal, S., Dysfunctional KEAP1–NRF2 Interaction in Non-Small-Cell Lung Cancer. *PLOS Medicine* **2006,** *3* (10), e420.

3. van der Wijst, M. G.; Huisman, C.; Mposhi, A.; Roelfes, G.; Rots, M. G., Targeting Nrf2 in healthy and malignant ovarian epithelial cells: Protection versus promotion. *Molecular Oncology* **2015,** *9* (7), 1259-1273.

4. Walker, A.; Singh, A.; Tully, E.; Woo, J.; Le, A.; Nguyen, T.; Biswal, S.; Sharma, D.; Gabrielson, E., Nrf2 signaling and autophagy are complementary in protecting breast cancer cells during glucose deprivation. *Free Radical Biology and Medicine* **2018,** *120*, 407-413.

5. Cho, J.-M.; Manandhar, S.; Lee, H.-R.; Park, H.-M.; Kwak, M.-K., Role of the Nrf2-antioxidant system in cytotoxicity mediated by anticancer cisplatin: implication to cancer cell resistance. *Cancer Letters* **2008,** *260* (1-2), 96-108.

6. Dinkova-Kostova, A. T.; Talalay, P., NAD (P) H: quinone acceptor oxidoreductase 1 (NQO1), a multifunctional antioxidant enzyme and exceptionally versatile cytoprotector. *Archives of Biochemistry and Biophysics* **2010,** *501* (1), 116-123.

7. Winski, S. L.; Koutalos, Y.; Bentley, D. L.; Ross, D., Subcellular Localization of NAD(P)H:quinone Oxidoreductase 1 in Human Cancer Cells. *Cancer Research* **2002,** *62* (5), 1420.

8. Siegel, D.; Ross, D., Immunodetection of NAD (P) H: quinone oxidoreductase 1 (NQO1) in human tissues1. *Free Radical Biology and Medicine* **2000,** *29* (3-4), 246-253.

9. Cui, X.; Li, L.; Yan, G.; Meng, K.; Lin, Z.; Nan, Y.; Jin, G.; Li, C., High expression of NQO1 is associated with poor prognosis in serous ovarian carcinoma. *BMC Cancer* **2015,** *15* (1), 244.

10. Lin, L.; Qin, Y.; Jin, T.; Liu, S.; Zhang, S.; Shen, X.; Lin, Z., Significance of NQO1 overexpression for prognostic evaluation of gastric adenocarcinoma. *Experimental and Molecular Pathology* **2014,** *96* (2), 200-205.

11. Yang, Y.; Zhang, Y.; Wu, Q.; Cui, X.; Lin, Z.; Liu, S.; Chen, L., Clinical implications of high NQO1 expression in breast cancers. *Journal of Experimental & Clinical Cancer Research* **2014,** *33* (1), 14.

12. Lewis Anne, M.; Ough, M.; Hinkhouse Marilyn, M.; Tsao, M.-S.; Oberley Larry, W.; Cullen Joseph, J., Targeting NAD(P)H:quinone oxidoreductase (NQO1) in pancreatic cancer. *Molecular Carcinogenesis* **2005,** *43* (4), 215-224.

13. Li, C. J.; Li, Y.-Z.; Pinto, A. V.; Pardee, A. B., Potent inhibition of tumor survival in vivo by β-lapachone plus taxol: Combining drugs imposes different artificial checkpoints. *Proceedings of the National Academy of Sciences* **1999,** *96* (23), 13369.

14. Cabello, C. M.; Bair, W. B.; Bause, A. S.; Wondrak, G. T., Antimelanoma activity of the redox dye DCPIP (2,6-dichlorophenolindophenol) is antagonized by NQO1. *Biochemical Pharmacology* **2009,** *78* (4), 344-354.

15. Siegel, D.; Yan, C.; Ross, D., NAD(P)H:quinone oxidoreductase 1 (NQO1) in the sensitivity and resistance to antitumor quinones. *Biochemical Pharmacology* **2012,** *83* (8), 1033-1040.

16. Best, Q. A.; Johnson, A. E.; Prasai, B.; Rouillere, A.; McCarley, R. L., Environmentally robust rhodamine reporters for probe-based cellular detection of the cancer-linked oxidoreductase hNQO1. *ACS Chemical Biology* **2015,** *11* (1), 231-240.

17. Best, Q. A.; Prasai, B.; Rouillere, A.; Johnson, A. E.; McCarley, R. L., Efficacious fluorescence turn-on probe for high-contrast imaging of human cells overexpressing quinone reductase activity. *Chemical Communications* **2017,** *53* (4), 783-786.

18. Hettiarachchi, S. U.; Prasai, B.; McCarley, R. L., Detection and Cellular Imaging of Human Cancer Enzyme Using a Turn-On, Wavelength-Shiftable, Self-Immolative Profluorophore. *Journal of the American Chemical Society* **2014,** *136* (21), 7575-7578.

19. Nawimanage, R. R.; Prasai, B.; Hettiarachchi, S. U.; McCarley, R. L., Rapid, Photoinduced Electron Transfer-Modulated, Turn-on Fluorescent Probe for Detection and Cellular Imaging of Biologically Significant Thiols. *Analytical Chemistry* **2014,** *86* (24), 12266-12271.

20. Prasai, B.; Silvers, W. C.; McCarley, R. L., Oxidoreductase-Facilitated Visualization and Detection of Human Cancer Cells. *Analytical Chemistry* **2015,** *87* (12), 6411-6418.

21. Shen, Z.; Prasai, B.; Nakamura, Y.; Kobayashi, H.; Jackson, M. S.; McCarley, R. L., A Near-Infrared, Wavelength-Shiftable, Turn-on Fluorescent Probe for the Detection and Imaging of Cancer Tumor Cells. *ACS Chemical Biology* **2017,** *12* (4), 1121-1132.

22. Silvers, W. C.; Payne, A. S.; McCarley, R. L., Shedding light by cancer redox—human NAD (P) H: quinone oxidoreductase 1 activation of a cloaked fluorescent dye. *Chemical Communications* **2011,** *47* (40), 11264-11266.

23. Silvers, W. C.; Prasai, B.; Burk, D. H.; Brown, M. L.; McCarley, R. L., Profluorogenic Reductase Substrate for Rapid, Selective, and Sensitive Visualization and Detection of Human Cancer Cells that Overexpress NQO1. *Journal of the American Chemical Society* **2013,** *135* (1), 309-314.

24. Shen, Z., Visualization and Quantification of Cancer-associated Enzymes with Fluorescent Small-molecule Substrate Probes. In *LSU Doctoral Dissertations*, Louisiana State University: Baton Rouge, LA, 2018.

25. Domcke, S.; Sinha, R.; Levine, D. A.; Sander, C.; Schultz, N., Evaluating cell lines as tumour models by comparison of genomic profiles. *Nature Communications* **2013,** *4*, 2126.

26. Imai, S.; Kiyozuka, Y.; Maeda, H.; Noda, T.; Hosick, H. L., Establishment and Characterization of a Human Ovarian Serous Cystadenocarcinoma Cell Line That Produces the Tumor Markers CA-125 and Tissue Polypeptide Antigen. *Oncology* **1990,** *47* (2), 177-184.

27. Hamilton, T. C.; Young, R. C.; McKoy, W. M.; Grotzinger, K. R.; Green, J. A.; Chu, E. W.; Whang-Peng, J.; Rogan, A. M.; Green, W. R.; Ozols, R. F., Characterization of a human ovarian carcinoma cell line (NIH: OVCAR-3) with androgen and estrogen receptors. *Cancer Research* **1983,** *43* (11), 5379-5389.

28. Hsieh, T.-C.; Wu, J. M., Suppression of proliferation and oxidative stress by extracts of Ganoderma lucidum in the ovarian cancer cell line OVCAR-3. *International Journal of Molecular Medicine* **2011,** *28* (6), 1065-1069.

29. Hamilton, T. C.; Young, R. C.; Ozols, R. F. In *Experimental model systems of ovarian cancer: applications to the design and evaluation of new treatment approaches*, Seminars in Oncology, 1984; p 285.

30. Kim, J.-w.; Tchernyshyov, I.; Semenza, G. L.; Dang, C. V., HIF-1-mediated expression of pyruvate dehydrogenase kinase: A metabolic switch required for cellular adaptation to hypoxia. *Cell Metabolism* **2006,** *3* (3), 177-185.

31. Sullivan, L. B.; Chandel, N. S., Mitochondrial reactive oxygen species and cancer. *Cancer & Metabolism* **2014,** *2* (1), 17.

32. Jacobs, J. J.; Kieboom, K.; Marino, S.; DePinho, R. A.; van Lohuizen, M., The oncogene and Polycomb-group gene bmi-1 regulates cell proliferation and senescence through the ink4a locus. *Nature* **1999,** *397* (6715), 164.

33. Shay, J. W.; Wright, W. E., Senescence and immortalization: role of telomeres and telomerase. *Carcinogenesis* **2005,** *26* (5), 867-874.

34. Debacq-Chainiaux, F.; Erusalimsky, J. D.; Campisi, J.; Toussaint, O., Protocols to detect senescence-associated beta-galactosidase (SA-βgal) activity, a biomarker of senescent cells in culture and in vivo. *Nature Protocols* **2009,** *4* (12), 1798.

CHAPTER 3
EVALUATION OF TUMOR FORMATION FROM HUMAN OVARIAN CANCER CELLS AS A FUNCTION OF NQO1 USING AN IN VITRO SPHEROID MODEL

3.1 Introduction

While still a highly regarded form of in vitro cellular study, monolayer cultures do not accurately reflect gene expression profiles that are found in clinical samples.[1] This is primarily due to cells grown in monolayers lacking the functional and morphological features of the tissues from which they were derived. In addition, monolayer cell cultures are comprised of a homogeneous population of highly proliferative cells, with a flat, stretched morphology. Therefore, studying cellular processes such as the cell cycle, apoptosis, interactions with adjacent cells, and the extracellular matrix (ECM) in monolayers is problematic, as monolayers do not exhibit the behavior and characteristics of cells in vivo. The disadvantages of traditional two-dimensional, monolayer cell culture are heightened when studying therapeutic response and efficacy.[1-2] To overcome the these drawbacks, the use of multicellular tumor spheroid mimics, otherwise known as spheroids, has emerged as an alternative in vitro method to study cellular behaviors, response to therapeutics, and most notably, cancer.[1, 3]

Spheroids are three-dimensional cellular structures that share physical attributes and functionalities that closely resemble those of their parent tissues.[4-6] Their structure results in creation of metabolic and proliferative gradients that give rise to microregions of cells with distinct gene expression profiles. These microregions, as depicted in Figure 3.1, are composed of cells that are either proliferative, quiescent, hypoxic, or necrotic, with the regions greatly impacted by their microenvironment.[3, 6-7] The outermost region of cells, or

the proliferative layer, has the highest exposure to nutrients and is in direct contact with the ECM. The quiescent layer is composed of cells that have entered an inactive, or resting state, because environmental conditions are not favorable for proliferation. Quiescent cells are often viewed as the most problematic, because most anti-tumor drugs target actively dividing cells; thus, this population of cells can go unscathed upon chemotherapeutic agent exposure.[8-9] Hypoxic conditions dominate the third microregion, due to little to no oxygen or other needed nutrients for survival reaching the cells in this layer. Research has shown that hypoxic cells, like those that are quiescent, are linked to increased drug resistance, due to their ability to withstand harsh environmental conditions.[8, 10-11] The innermost layer is dubbed as necrotic, as it is composed of mostly dead cells, due to little to no oxygen or other nutrients essential for growth being present.

Due to the differences in environment associated with each microregion, proteins needed to promote not only continued proliferation, but also survival, are either upregulated or downregulated. For example, several groups have found that NQO1 overexpression has been linked to poor prognosis in gastrointestinal, breast, prostate, and pancreatic cancers.[12-15] These findings have led the McCarley group to question the role of NQO1 in tumor development, particularly in ovarian cancer. Cui and colleagues have shown that NQO1 expression in serous ovarian carcinoma tissues is indicative of poor prognosis.[16] These findings were based on immunohistochemical staining of tissue samples taken from patients with serous ovarian carcinoma, as well as borderline and benign ovarian tumors. While previous reports have enhanced our overall understanding of NQO1 expression in tumors, it has not been determined whether increased NQO1 expression in tumor tissues will result in increased enzymatic activity; that is, NQO1

expression may not correlate with NQO1 activity levels. Moreover, the tumorigenic ability of ovarian cancer cell lines has been evaluated in vivo and in vitro; however, the role of NQO1 in tumor spheroid formation has yet to be determined.[17-18]

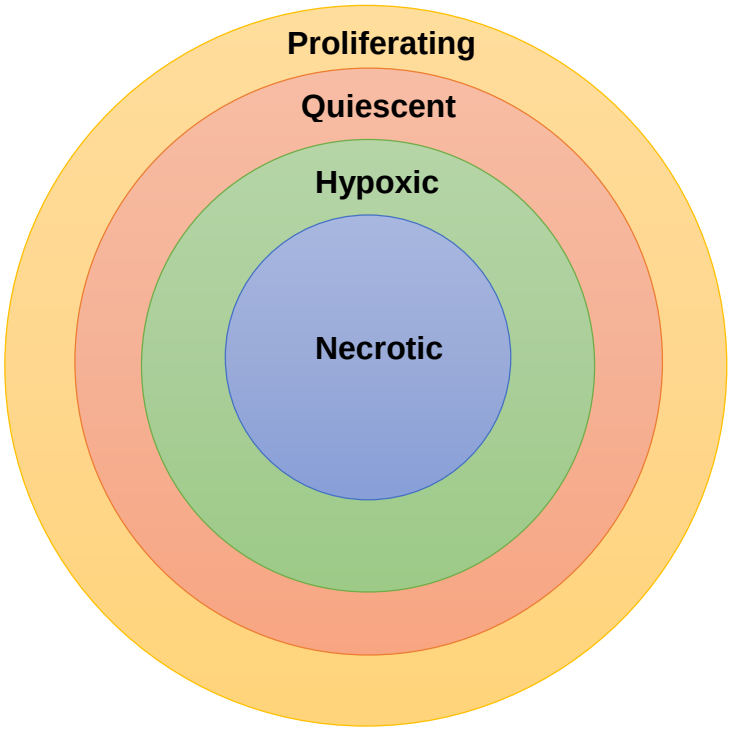

Figure 3.1. Schematic of tumor microregions.

Based on literature regarding NQO1 overexpression in tumor tissues and the findings presented in Chapter 2, it has been postulated that spheroid formation is more likely to occur in those cell lines exhibiting high expression and activity of the enzyme in cell monolayers.[13-14, 16, 19] Therefore, to evaluate the influence of NQO1 on tumor growth and development in ovarian cancer, I will employ an in vitro spheroid model. Specifically, I will examine the propensity of the cell lines under investigation to form spheroids under nonadherent conditions, due to such a transformation in cell growth/assembly capability

being linked to metastatic disease. In addition, I will probe the influence of tumor suppressor protein p53 on this process. Upon successful spheroid formation, I will then examine NQO1 expression and activity levels using immunochemical techniques, in addition to probe studies with the NQO1-activated Q_3NTCy fluorescent probe.[20]

3.2 Experimental

3.2.1 Cell Culture

Human ovarian carcinoma cell lines OVCAR-5, OVCAR-8, and SHIN-3, gifts from Dr. Hisataka Kobayashi at the United States National Institutes of Health, National Cancer Institute, Center for Cancer Research, were used for the studies presented in this chapter. Human ovarian carcinoma cell line OVCAR-3, purchased from American Type Culture Collection (ATCC), was also used. Cells were cultured in RPMI-1640 medium purchased from the ATCC that was supplemented with 10% fetal bovine serum (FBS; ATCC), 10 IU/mL penicillin and 10 μg/mL streptomycin (Life Technologies). Bovine insulin (1 μg/mL) was an additional supplement for OVCAR-3 cells. Cells were cultured in 75 cm^2 treated tissue culture flasks at 37°C under 5% CO_2 in a humidified incubator.

3.2.2 Multicellular Tumor Spheroid Culture

Spheroids were cultured in ultra-low attachment 96-well plates (Corning), as previously described.[7, 21] Briefly, cells were seeded at a density of 1×10^4 cells in each well followed by the addition of growth medium supplemented with 10% FBS, 10 IU/mL penicillin and 10 μg/mL streptomycin. Medium was changed every 2 to 4 days, depending on the cell line. In addition, to observe the ability of cells to form secondary and primary

spheroids, primary spheroids were dissociated with 0.25% trypsin-EDTA solution, counted, and cultured again under the same conditions as primary spheroids.

3.2.3 Stable NQO1 Protein Knockdown Assays

A custom shRNA clone set that targets all four reference sequence variants for NQO1 in psi-LVRU6GP composed of an U6 promoter, eGFP, and puromycin-resistant tags and its respective shRNA scramble control clone was purchased from GeneCopoeia. Stable knockdown of NQO1 was generated by infecting OVCAR-5 cells with polybrene-supplemented culture medium containing the lentiviral shRNA particles targeting NQO1 or the scramble control vector per the manufacturer's instruction. Briefly, 48-hours after culture, OVCAR-5 cells were transfected for 14–16 hours with polybrene-supplemented (5 μg/mL) medium containing either 10 μg lentiviral shRNA particles or 10 μg lentiviral shRNA control particles. Medium was changed 16-hours post transfection, and cells were cultured for an additional 48 hours before shRNA-NQO1 cells were isolated via puromycin selection (2 μg/mL).

3.2.4 Protein Quantification

To determine the total protein concentration, bulk protein was extracted from either monolayers or from intact spheroids (n = 96). Following centrifugation at 900 rpm for 7 minutes at 4 °C to remove any excess cell media, 250-300 μL of radioimmunoprecipitation assay (RIPA, ThermoFisher) buffer with 1 mM phenylmethylsulfonyl fluoride (Sigma) and protease inhibitor cocktail (Sigma) was added to monolayers and spheroids, and they were placed on ice for 15 minutes and 30-45 minutes, respectively. Mechanical pipetting was employed at 10-minute intervals to ensure homogeneity within the sample. Samples

were then centrifuged at 18,000 ×*g* for 20 minutes at 4 °C. The supernatant was obtained and aliquoted into sterile Eppendorf tubes and stored at −80°C until used. Total protein content was quantified using the well-established BCA assay.

3.2.5 Western Blot

NQO1 and p53 expression in the studied cell lines was measured in 25 μg protein samples. Samples were measured using sodium dodecyl sulphate-polyacrylamide gel electrophoresis (SDS-PAGE) using 4–20% polyacrylamide gels (Bio-Rad). 10 μL of Kaleidoscope Pre-Stained Standard marker was used to track proteins. Samples were diluted in 2X Laemmli sample buffer containing 2-mercaptoethanol at a 1:1 ratio. Protein separation was conducted at 100 V for 65 minutes in running buffer (Tris/Glycine/SDS), followed by protein transfer onto nitrocellulose membranes in transfer buffer (Tris-Glycine and 20% methanol). Following transfer, the membrane was blocked with 5% non-fat dry milk for one hour before being washed with tris-buffered saline containing 0.1% Tween-20 (TBST). Simultaneously, working concentrations of the primary mouse anti-NQO1 or anti-p53 were prepared in 1% BSA in TBST. An anti-β-actin rabbit monoclonal antibody was also introduced to the membranes as a loading control.

The membranes were kept overnight at 4 °C with gentle shaking on a microplate shaker. After overnight incubation with the antibodies, the membrane was washed with TBST 3X in 10-minute intervals. Next, both anti-mouse IgG and anti-rabbit IgG, HRP-linked secondary antibodies (Cell Signaling Technologies) were added to the membranes for 1 hour at room temperature with gentle shaking. SuperSignal West Pico chemiluminescent substrate was prepared based on the manufacturer's protocol, and

slowly pipetted onto the membranes several times over a time period of roughly 2 minutes. Membranes were imaged using a Bio-Rad ChemiDoc MP system with an exposure time of 300 seconds at 60 second intervals. Raw images were saved in tagged image file format (TIFF), and band analysis was performed using Fiji/ImageJ software.

3.3.6 RNA Purification and Real-Time Quantitative PCR (RT-qPCR)

Total RNA from cell lines was extracted and purified for analysis using Direct-zol RNA MicroPrep kit (Zymo Research) according to the manufacturer's instructions. RNA was quantified spectrometrically using an Epoch microplate reader (BioTek). Total RNA was reversed transcribed to cDNA using TaqMan Reverse Transcriptase reaction mix provided in the High Capacity RNA-to-cDNA Kit (Applied Biosystems) according to the supplier's instructions. The cDNA was diluted 1:10 in nuclease-free water and 2 μL was used as a template to perform RT-PCR in a 25 μL reaction. B-actin was used as an endogenous control (Applied Biosystems, UK) in single-plexed PCR reactions on an ABI ViiA-7 (qPCR) Detection System (Applied Biosystems) with fast thermocycling conditions (50 °C for 2 minutes, 95 °C for 2 minutes, then 40 cycles at 95 °C for 1 second and 60 °C for 20 seconds), using Taqman Fast Advanced PCR Master Mix (Applied Biosystems). To confirm the modulated expression of the selected target gene and endogenous control, TaqMan 20x gene expression primers and probes (Applied Biosystems) for TP53-Hs01034249_m1 and ACTB-Hs99999903_m1 were used. All PCR reactions were performed in triplicate.

3.3.7 NQO1 Activity via Spectrometric Analysis/Enzyme Kinetics

NQO1 activity was assayed spectrometrically by the dicoumarol-sensitive reduction of the quinone substrate 2,6-dichlorophenolindophenol (DCPIP) at 600 nm, as previously described.[22] The assay buffer consisted of 200 μM NADH and 0.014% BSA in 25 mM of Tris-HCl at pH 7.4 with or without 20 μM dicoumarol, a known hNQO1 inhibitor. A fraction of lysate was added to 0.75 mL of assay buffer to give a final protein concentration of 5 μg in a 2 mL plastic cuvette. To start the reaction, 0.75 mL of 80 μM DCPIP in assay buffer was added, bringing the final volume to 1.5 mL. Enzymatic activity was determined based on NQO1 ability to reduce the DCPIP substrate at 600 nm in the presence and absence of the dicoumarol inhibitor. Each measurement was carried out using a Cary 50 UV/Vis spectrometer over a 2 to 10-minute timeframe, depending on the activity level of cell line being assayed. Dicoumarol-sensitive NQO1 activity was then calculated by subtracting the activity of a sample with dicoumarol from the corresponding activity without dicoumarol. Finally, activity was recorded in units of *nmol DCPIP reduced/mg/min*.

3.2.8 Visualization of NQO1 Activity via Fluorescent Probe Q_3NTCy

OVCAR cell monolayers were cultured overnight on 22 × 22 mm coverslips to allow for attachment. Spheroids were cultured over a 5-day period in sterile ultralow attachment plates (Corning) containing either RPMI-1640 or DMEM growth medium supplemented with 10 % FBS and 10 IU/mL penicillin and 10 μg/mL streptomycin. On the following day (monolayers) and fifth day of culture (spheroids), cells were washed with PBS before warmed RPMI-1640 medium (without phenol red) was added to each well. Q_3NTCy probe was added to each well to yield a final concentration of 5 μM, which was then incubated at 37 °C for 20 minutes for adherent cells and at intervals ranging from 30 minutes to 3

hours for spheroids. Following probe exposure, the culture medium was removed, and cells or spheroids were washed with PBS 3X before 4% PFA was added. A 1-hour fixation period with PFA was implemented in spheroids to ensure fixation occurred, after which cells and spheroids were washed with PBS for an additional hour to ensure unreacted probe was removed. Monolayer cells were then mounted on a glass slide using Prolong Gold with DAPI (ThermoFisher), and subsequently cured overnight. Spheroids were placed into delta T dishes containing RMPI-1640 media without FBS, and then imaged.

Confocal images were collected using a Leica TCS SP8 laser-scanning confocal microscope. The TCy reporter that was released from the Q_3NTCy probe upon exposure to NQO1 was imaged using a white light laser. The TCy reporter was excited at 633 nm with spectral emission was collected between 650–750 nm using hybrid detectors. The pinhole was set at 1 Airy Unit (53.1 μm). The DAPI nuclear stain was excited at 405 nm by an argon laser with spectral emission collected between 410-483 nm. Each image was frame and line averaged 4 and 2 times, respectively, at a scan speed of 8000 Hz. An Apo plan 20X 0.3 NA objective was used. Image analysis was performed using LAS X and Fiji/Image J software.

3.3 Results and Discussion

3.3.1 Anchorage-Independent Spheroid Formation in OC cells

Successful in vitro formation of spheroids without the use of support matrices, like Matrigel or collagen, using ovarian cancer cells has been reported for HEY, OVCA429, and ES-2 cells.[23] OVCAR-3 cells were found to only have increased contractile behavior upon the introduction of malignant ascites fluid to growth media; however, compact

spheroid formation was not observed.[24] Moreover, while the use of ascites fluid or collagen may enhance cell line ability to contract, intrinsic factors play a major role in the process. Thus, for my analysis, I studied the inherit ability of ovarian cancer cell lines to form spheroids. SHIN-3, OVCAR-5, OVCAR-8, and OVCAR-3 cells were grown under conditions that did not promote cell adhesion and were monitored over 5 days (Figure 3.2).

Sphere-forming capacity was evaluated using a modified version of a spheroid ranking system based on the degree of compaction in ovarian cancer cells described by Sodek and colleagues.[23] In this modified scale, compact spheroids were defined as densely packed spherical structures that remained intact upon mechanical pipetting. Semi-compact spheroids were defined as densely packed structures that would partially dissociate upon mechanical pipetting. Finally, spheroid aggregates were classified as cells that readily aggregated, but were easily dissociated upon mechanical pipetting. Applying this modified scale to my studies revealed that only OVCAR-8 cells were capable of forming compact spheroids under the anchorage-independent conditions. Moreover, while SHIN-3 cells produced spheroids, they were not as dense/compact as were those of OVCAR-8. OVCAR-3 cells were used as a negative control, due to their in vitro tumor-forming ability having been determined previously.[23-24]

In addition, upon mechanical agitation by pipetting, SHIN-3 spheroids began to break apart; however, their complete dissociation was not observed. Unlike OVCAR-8 and SHIN-3, OVCAR-5 produced aggregates that were easily dissociated upon mechanical pipetting. The extent of spheroid formation in OVCAR-5 was intriguing, because of its proliferative similarities to OVCAR-8 and SHIN-3 when cultured in monolayers. Aside

from proliferative similarities, OVCAR-5 and SHIN-3 were found to exhibit increased NQO1 expression and activity when compared to OVCAR-8 and OVCAR-3 cells, as described in Chapter 2. Moreover, while the expression of NQO1 was similar in OVCAR-8 and OVCAR-3, OVCAR-8 cells had higher enzyme activity. Based on these observations, it was hypothesized that cells with exhibiting NQO1 activity greater than or equal to that of OVCAR-8 have an increased propensity for spheroid formation.

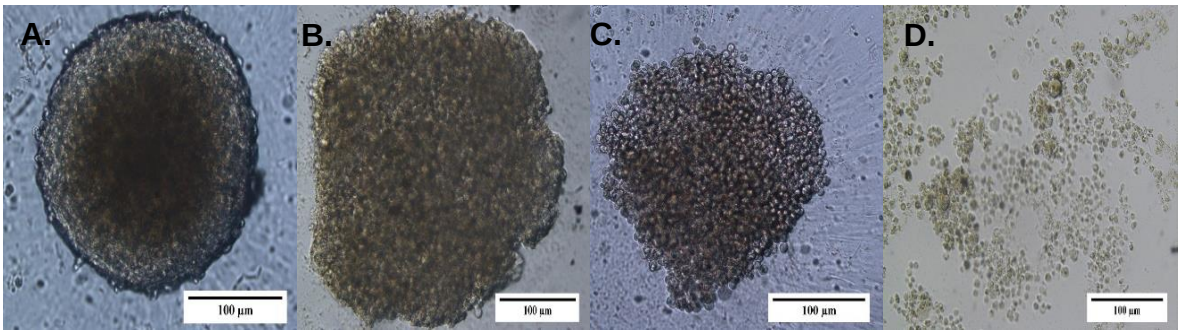

Figure 3.2. Multicellular tumor spheroids after 5-days of culture. **A.** OVCAR-8, **B.** SHIN-3, **C.** OVCAR-5, and **D.** OVCAR-3 cells were imaged using an inverted microscope at 10X magnification. Image analysis was achieved using ImageJ/Fiji software.

Sodek and colleagues observed compact spheroid formation with ovarian cancer cells possessing an invasive, motile phenotype.[23] Based on their work, I decided that it was important to research the origin of the cell lines in this study, because the stage at which cells were retrieved from patients will shed light on their level of invasiveness. OVCAR-8 cells were derived from a carboplatin refractory patient with advanced diseased, which is perhaps why OVCAR-8 cells were able to form compact spheroids in an environment lacking a support matrix.[25-26] Unlike OVCAR-8, SHIN-3 cells were derived from a patient with stage IIc disease, meaning the patient was close to, but had not yet acquired,

metastatic disease.[27] Therefore, it is likely that compact tumor formation in non-adherent conditions would not occur due to the disease not reaching the level of invasiveness observed in OVCAR-8. Further investigation into the origin of OVCAR-5 cells revealed that like OVCAR-8, it was obtained from a tumor from a patient with advance disease.[18] However, it should be noted that both OVCAR-5 and SHIN-3 cells were retrieved from patients who had not yet been treated. Moreover, while OVCAR-3 cells were derived from a cisplatin-resistant patient, they were retrieved from malignant ascites; this is in contrast to the other cell lines in this study, because they were derived from solid tumors. This distinction may be related to the observation that OVCAR-3 cells did not form spheroids or aggregates (Figure 3.2. D.), while also pinpointing to the rationale for increased compaction and aggregation being observed in OVCAR-8, SHIN-3, and OVCAR-5 cells.

3.3.2 Manipulation of NQO1 gene expression in OVCAR-5 cells

In the previous section, it was observed cell lines displaying NQO1 activity greater than or equal to that of OVCAR-8 had increased ability to form spheroids/aggregates (Figure 3.2.). Therefore, it was hypothesized that NQO1 is necessary for spheroid/aggregate formation under anchorage-independent conditions. To test this new hypothesis, I performed gene expression experiments aimed at depleting NQO1 in OVCAR-5 cells. OVCAR-5 cells were chosen for this study because their origin, in regard to the cancer stage at which it was retrieved, and proliferative ability was similar to that of OVCAR-8. To ensure stable knockdown of the NQO1 gene, lentiviral particles against NQO1 expressing a puromycin-resistant gene was introduced to OVCAR-5 cells. After transfection of OVCAR-5 cells with lentiviral particles, puromycin, an antibiotic that will selectively eliminate cells that do not express the puromycin-resistant gene, was added

and NQO1-depleted cells were isolated. I performed western blotting, enzyme kinetics, and treatment of the cells with NQO1-activated probe Q_3NTCy to further validate that the transfection was a success.

As shown in Figure 3.3. A., NQO1 expression was diminished in OVCAR-5 with depleted NQO1 (NQO1(-)) when compared to OVCAR-5 wildtype (WT) cells. The catalytic ability of NQO1(-) after 4-days of culture (Figure 3.3 B) was determined to be 21.4 nmol/min/mg; thus, the enzyme's activity was observed to be 7 times lower than when compared to WT cells cultured under the same conditions. Incubation with Q_3NTCy allowed NQO1 activity to be evaluated visually. Image analysis revealed that the fluorescence intensity resulting from NQO1-activated release of the TCy reporter was considerably higher in OVCAR-5 WT cells with a mean integrated fluorescence intensity of 14 ± 6 compared to 2.0 ± 0.4 in NQO1(-) OVCAR-5 cells (Figure 3.3. C). Here again, the NQO1-depleted OVCAR-5 cells exhibited 7 times lower NQO1 activity in comparison to that of the wildtype OVCAR-5 cells.

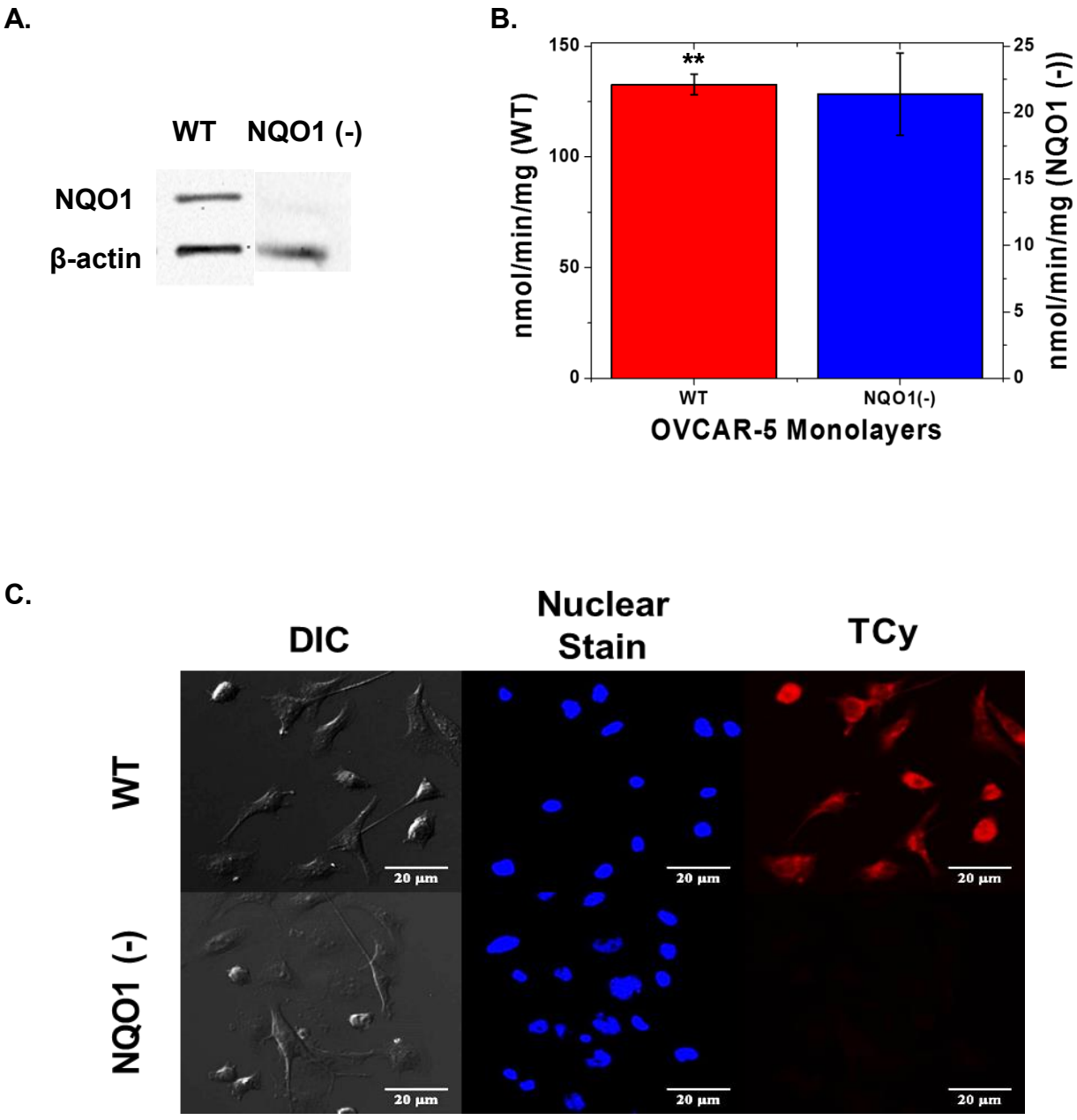

Figure 3.3. (A) Protein bands representative of NQO1 expression using 25 μg of protein extracted from wildtype and NQO1(-) OVCAR-5 cells. β-actin was used as an internal standard. (**B)** NQO1 activity for ovarian cancer cell lines after 1-day of culture obtained from enzymatic assay. 2.5 μg/mL and 5 μg/mL protein used in WT and NQO1(-) OVCAR-5 cells, respectively. (*** denotes a *p*-value <0.001). (**C)** OVCAR-5 wildtype and NQO1(-) cells after treatment with 5 μM **Q_3NTCy** at 37°C for 20 minutes. Nuclear colocalization was achieved with a DAPI nuclear stain.

The newly created NQO1-negative OVCAR-5 cells were then plated under anchorage-independent conditions for 5-days to determine if spheroid formation would occur. At day 5, the spheroids were imaged with an inverted microscope (Figure 3.4.). Neither aggregation nor compact spheroid formation was observed in the OVCAR-5 cells depleted of NQO1. The lack of spheroid formation confirmed my hypothesis was correct regarding NQO1 expression/activity being necessary for successful spheroid and/or aggregate formation. In fact, these findings are similar in many ways to those observed by Madajewski in non-small cell lung cancer cells, which were found to have diminished colony forming potential upon NQO1 depletion.[28] Based on these findings, it was posited that highly invasive ovarian cancer cells with moderate to high expression of NQO1 may be necessary to observe spheroid and/or aggregate formation in vitro.

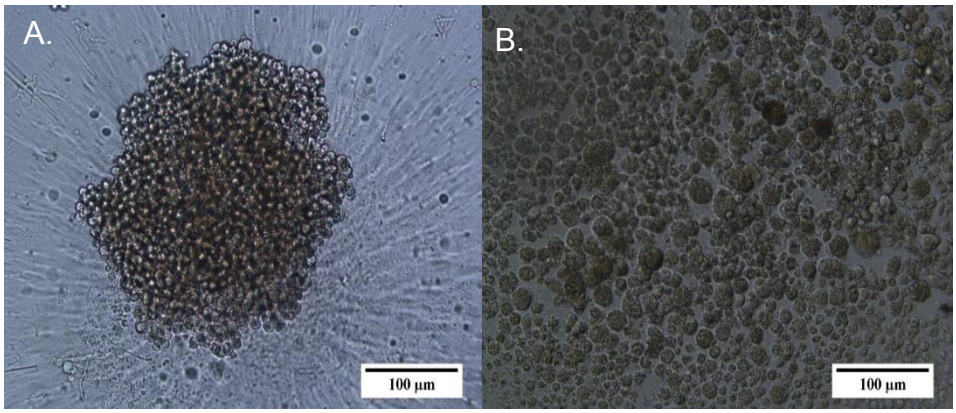

Figure 3.4. OVCAR-5 (**A**) WT and (**B**) NQO1 (-) cells after 5-days of culture in non-adherent conditions. Images were obtained with an Olympus IX81 brightfield fluorescence microscope at 10X magnification.

3.3.3 Expression of p53 in OC cells

While the ability of the studied cell lines to produce spheroids as a function of NQO1 was intriguing, it added a layer of depth to this research. Literature studies indicate that

tumor suppressor protein p53 is stabilized by NQO1; thus, increased NQO1 presence and/or activeness should make tumor formation less likely.[29-30] Based on my findings, this rationale holds true to some extent, due to OVCAR-8 cells, which exhibited low activity and undetectable expression of NQO1 in bulk samples, being capable of compact spheroid formation. However, the appearance of spheroids/aggregates in the SHIN-3 and OVCAR-5 WT cells, both of which displayed high expression and activity of NQO1, contradicts the notion that increased presence and/or activeness of the enzyme will negatively impact tumor formation. Furthermore, evaluation of OVCAR-5 NQO1 (-) cells revealed that they were unable to form spheroids/aggregates, which should have resulted in spheroid/aggregate formation due to p53 being unstable.

To explore these findings, western blot analysis was used to probe p53 expression in OVCAR-5, OVCAR-8, SHIN-3, and OVCAR-3. Figure 3.5 depicts the results of western blot analysis of bulk protein extracted from ovarian cancer cell monolayers. Dense bands corresponding to p53 protein expression were observed for OVCAR-8 and SHIN-3 cells. It was concluded that the enhanced p53 protein expression in OVCAR-8 may have been due to the cells attempting to inhibit tumor formation. However, one of NQO1's functions is to stabilize p53 so that it does not undergo proteasomal degradation, and OVCAR-8 has low NQO1 expression, so it was surprising that p53 expression was so pronounced.[30-31] Similarly, SHIN-3 was found to express p53 protein, but because of its high expression and activity of NQO1, it was proposed that semi-compact spheroid formation was likely the result of partial tumor suppression by p53. Unlike OVCAR-8 and SHIN-3, p53 protein expression was low and undetectable in OVCAR-3 and OVCAR-5, respectively. Theoretically low and/or no expression of p53 gene and/or protein should result in

increased tumor-forming ability, which to an extent holds true for OVCAR-5 WT cells, as aggregation with them was observed, but neither spheroid formation nor aggregation was observed in OVCAR-3 cells.

To determine whether the expression of p53 in protein form was indicative of its expression at the genomic level, the relative gene expression of p53 in each cell line is shown in Figure 3.5. B. Surprisingly, OVCAR-3 cells had the highest relative gene expression of p53 followed by SHIN-3 andOVCAR-8 cells, while gene expression in OVCAR-5 cells was lowest. Also, the difference in p53 gene expression between OVCAR-8 and SHIN-3 was statistically insignificant (p = 0.07). However, the most profound observation of this study was that it contradicted the western blot results shown in Figure 3.5. A. Specifically, OVCAR-3 was found to highest expression of the p53 gene, but its expression of the translated protein form was noticeably lower than that of OVCAR-8 and SHIN-3. Similarly, both SHIN-3 and OVCAR-8 displayed enhanced expression of the p53 protein, while the gene expression was low relative to OVCAR-3. Also, although OVCAR-5 cells did not appear to express the p53 protein, the gene was present, though it was expressed at a much lower degree compared to the other cell lines.

Moreover, the findings presented in this section suggest that modifications in either the p53 gene sequence or the translated protein may have occurred in the studied cell lines. Literature suggests that the expression of a gene is not always reflective of the presence of the translated protein.[32-34] In addition, it has been found that posttranslational accumulation of p53 may inhibit its proteasomal degradation.[35] Previous research has reported mutations in the p53 gene in 73% of ovarian cancer cells.[36] Moreover, it was found that the p53 gene in OVCAR-8 and OVCAR-3 cells has mutations within its

nucleotide sequence resulting from guanine being replaced by adenine within their DNA sequences.[36-37] Such mutations may be responsible for spheroid formation or lack thereof in OVCAR-8 and OVCAR-3 cells, respectively. To my knowledge, p53 expression in SHIN-3 cells has not been evaluated prior to my studies; therefore, mutations, if any, in the gene sequence of p53 have not been identified. Additionally, the status of p53 in OVCAR-5 cells has led to conflicting narratives of regarding its expression. While the catalogue of somatic mutations in cancer (COSMIC) identified wildtype p53 in OVCAR-5 cells, other researchers have found that the cell line is p53 null.[36-39] However, it was unclear whether the latter were based their findings on the expression of the p53 gene or protein. Based on my findings, it was posited that low expression of the p53 gene in OVCAR-5 WT cells results in little to no p53 protein being expressed.

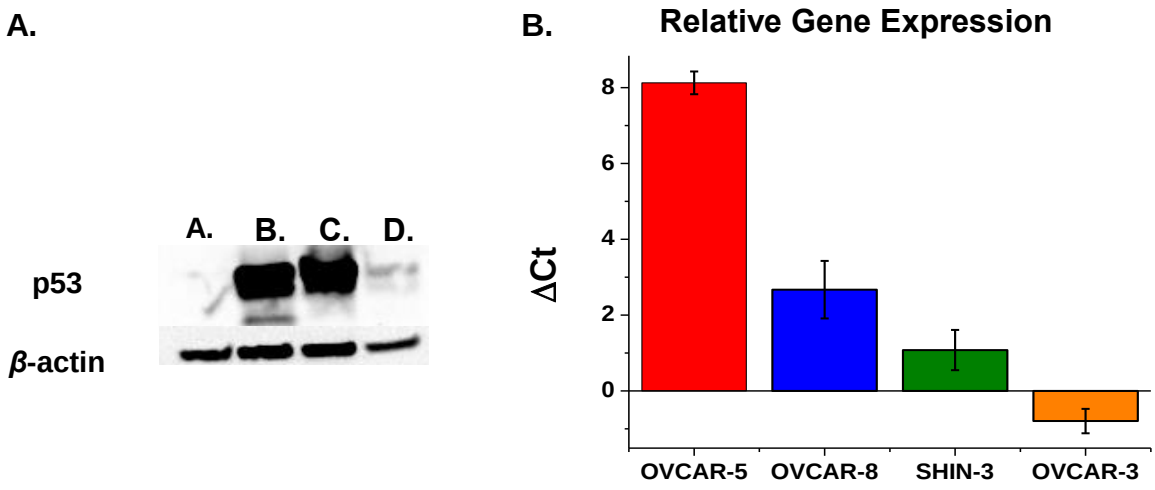

Figure 3.5. (**A**) Protein bands representative of p53 expression in 25 μg samples of (A) OVCAR-5 WT, (B) OVCAR-8, (C) SHIN-3, and (D) OVCAR-3. β-actin was used as an internal standard. (**B**) Relative gene expression of p53 (ΔCt_{mean}) in OC cell monolayers.

3.3.4 NQO1 Expression and Activity in OVCAR-8 and SHIN-3 Spheroids

At the beginning of this chapter, it was stated that there are observable differences in gene expression between monolayer and spheroid models of disease. Thus, to evaluate whether differences in the expression and activity of NQO1 was altered in spheroids, OVCAR-8 and SHIN-3 cells were grown under anchorage-independent conditions and harvested on the 5th and 12th days of culture. NQO1 expression level was found to be invariant in OVCAR-8 and SHIN-3 spheroids regardless of culture time. Interestingly, NQO1 presence was detectable in OVCAR-8 spheroids via western blot (Figure 3.6.), but not in OVCAR-8 cells grown in traditional monolayer culture (Chapter 2, Figure 2.2 A). Moreover, the expression of NQO1 in SHIN-3 spheroids was found to be increased, as the band density corresponding to the enzyme in spheroids is much higher than that for monolayers. This outcome is attributed to less oxygen and nutrients reaching cells housed in the innermost microregions of spheroids, thereby yielding increased expression of cytoprotective proteins, such as NQO1. In addition, these findings support studies of high NQO1 expression in tumor samples.[13-14, 16, 19, 40]

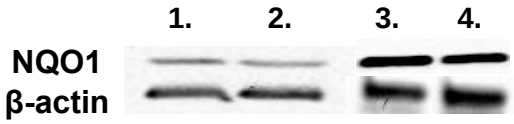

Figure 3.6. Protein bands representing levels of NQO1 activity in 5-day-old (**1**) OVCAR-8 and (**3**) SHIN-3, and 12-day old (**2**) OVCAR-8 and (**4**) SHIN-3 spheroids, using 25 μg of protein. β-actin was used as an internal standard.

Upon examining whether enhanced expression of the enzyme yields increased activity in OVCAR-8 spheroids, it was determined that NQO1 activity was comparable to that of OVCAR-8 monolayers after 1-2 days of culture. Therefore, it was surmised that culture time did not greatly impact NQO1 activity levels in spheroids. This finding was supported when two-tailed statistical analysis led to the conclusion that there is no significant difference in NQO1 activity for 5-day-old and 12-day old OVCAR-8 spheroids ($p = 0.11$). Similarly, SHIN-3 spheroids exhibited lower NQO1 activity than SHIN-3 cell monolayers of the same growth age. Specifically, 5-day old SHIN-3 monolayers had an NQO1 activity value of 1193 ± 42 nmol/min/mg, while 5-day old spheroids had one of 82 ± 2 nmol/min/mg. Despite the observed decrease in NQO1 activity in SHIN-3 spheroids relative to monolayers, there was a statistical difference ($p = 0.02$) in NQO1 activity between day-5 and day-12 SHIN-3 spheroids. Thus, suggesting that NQO1 activity increases with time in SHIN-3 spheroids. Also, no statistical difference in NQO1 activity ($p = 0.33$ and $p = 0.69$) was found when comparing 5-day-old and 12-day-old OVCAR-8 and SHIN-3 spheroids, respectively. Therefore, these findings are in contrast to those observed in cell monolayers, where it was determined that a difference in activity existed between the two cell lines. In addition, these findings further support the notion that gene expression and the behavior of cells in monolayer culture is not entirely reflective of how those same cells will behave in three-dimensional culture.

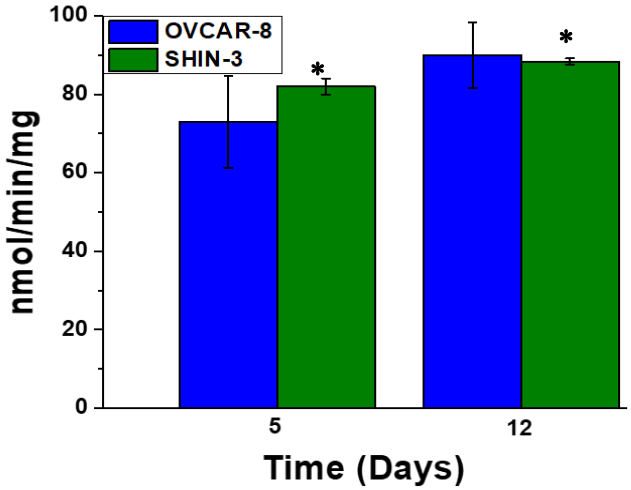

Figure 3.7. Specific activity of NQO1 from bulk protein lysates collected from OVCAR-8 and SHIN-3 spheroids where the asterisk denotes a statistical difference in activity ($p < 0.05$) within a 95% confidence interval.

These findings, specifically, the differences in NQO1 expression and activity between 2-dimensional and 3-dimensional culture, support literature on behavior of cells in monolayers not accurately depicting how cells will behave in tissues. Therefore, in analyzing the data based solely on my findings in spheroid culture, it was posited that lower NQO1 activity could be due to the different nutrient gradients in spheroids, leading to more active enzyme being present in the layer of cells in direct contact with nutrients and oxygen. Moreover, cells that are in a state of quiescence or hypoxia in the inner layers of the spheroids, which are considered to be in a state of rest, have the potential to contribute to NQO1 activity if environmental conditions change. For instance, if a patient is treated with radiation therapy, which targets actively dividing cells, it will likely only have an effect on the outer proliferating layer of cells within a tumor. Thus, cells present within the quiescent level are left unharmed. Due to their newfound exposure to the ECM and

its nutrients, quiescent cells within a tumor can begin actively dividing again, which could lead to increased activity in cytoprotective proteins, like NQO1.

3.3.5 Visualization of NQO1 Activity in OVCAR-8 and SHIN-3 Spheroids via Q_3NTCy

To determine the applicability of NQO1-activated fluorescent probe **Q_3NTCy** in three-dimensional models of cancer, it was introduced to OVCAR-8 and SHIN-3 spheroids a concentration of 5 μM (Figures 3.8. and 3.9.). Probe activation was evaluated by varying the probe incubation time—30 minutes, 1 hour, 1.5 hours, 2 hours, 2.5 hours, and 3 hours. Following three successive 20-minute washes and a 1-hour fixation period, samples were imaged with confocal fluorescence microscopy. Confocal microscopy was useful for obtaining high-resolution images of spheroids using **Q_3NTCy** in an OFF-ON mode, which would only allow for fluorescence light emitted from the TCy reporter to be detected. At first glance, it can be assumed that NQO1 activity is higher at the periphery of the OVCAR-8 and SHIN-3 spheroids. This suggests that probe penetration through the spheroids is occurring, but little to no active NQO1 is present in the inner levels of spheroids. However, previously published findings with **Q_3STCy** probe in spheroids derived from colorectal cancer cell line, HT-29, contradict this notion.[41] Specifically, it was found that increased NQO1 activity was localized that the periphery of aged spheroids whose necrotic region was enlarged.[41] Considering the age of the spheroids from previous studies (i.e., 23 days old) and those presented in this study (5 days old), it is plausible that active NQO1 distributed throughout younger spheroids. This assumption is supported by unpublished findings in the McCarley lab in live 5-day-old HT-29 spheroids. In this study, spheroids were sectioned (i.e., sliced) and exposed to **Q_3NTCy** for 10-minutes and upon imaging, an even fluorescence signal was observed across the

spheroid.[20] Thus, it was concluded that not only was active enzyme was present in the interior of spheroids, but limited penetration of light through intact spheroids rendered it impossible to detect emitted light beyond 100 μm.

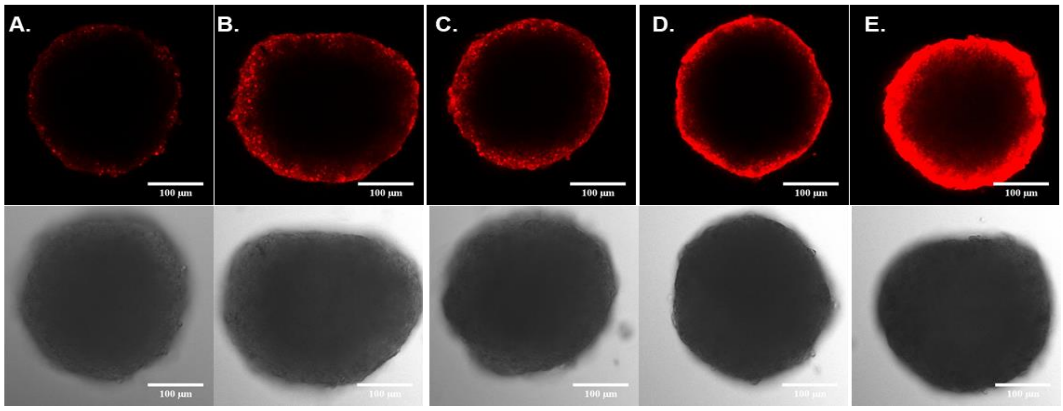

Figure 3.8. 5-day-old OVCAR-8 spheroids after incubation at 37 °C and 5% CO_2 with 5 μM **Q_3NTCy** in RPMI-1640 without phenol red for **A.)** 30 minutes, **B.)** 1 hour, **C.)** 2 hours, **D.)** 2.5 hours, **E.)** 3 hours. Images were acquired using confocal fluorescence microscopy using 20X magnification. Differential interference contrast (DIC) images were taken at each time point.

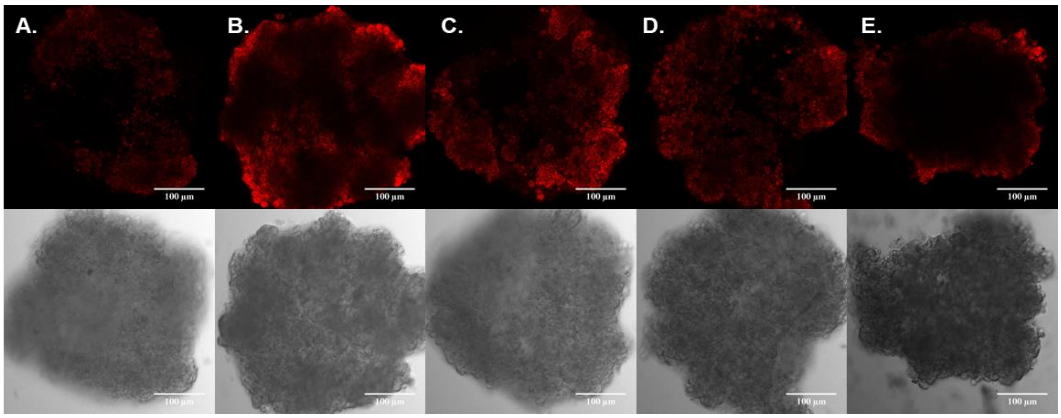

Figure 3.9. 5-day-old SHIN-3 aggregates after incubation at 37 °C and 5% CO_2 with 5 μM **Q3NTCy** without phenol red for **A.)** 30 minutes, **B.)** 1 hour, **C.)** 2 hours, **D.)** 2.5 hours, **E.)** 3 hours. Images were acquired using confocal fluorescence microscopy using 20X magnification. Differential interference contrast (DIC) images were taken at each time point.

3.4 Conclusion

In summary, the tumorigenic potential of several ovarian cancer cell lines was evaluated under anchorage-independent conditions. Initially, it was hypothesized that spheroid formation is correlated with increased expression and activity of NQO1. It was found that three of the four cell lines formed spheroid and/or aggregates. One of which was OVCAR-8, whose NQO1 expression and activity was low, thus rejecting my initial hypothesis. In addition, by employing the modified scale to define spheroid/aggregates it was observed that OVCAR-8, SHIN-3, and OVCAR-5 WT cells produced a compact spheroid, semi-compact spheroids, and loose aggregates, respectively. Due to OVCAR-8's spheroid forming ability and its associated low expression/activity of NQO1, I opted to perform a NQO1 knockdown in OVCAR-5 cells to determine whether depleting NQO1 would still result in the formation of an aggregate. Interestingly, depleting NQO1 in OVCAR-5 cells had the opposite effect, with aggregation being inhibited. Therefore, I concluded that NQO1 expression and activity that was greater than or equal to that observed in OVCAR-8 cells was necessary to induce spheroid/aggregate formation.

However, I decided to examine the expression of tumor suppressor gene p53, which is stabilized by NQO1.[30] It was found that an indirect relationship between p53 gene and protein expression was observed in three of the four cell lines presented in this study. While OVCAR-3 cells highly expressed the p53 gene, they exhibited low expression of the p53 protein. On the contrary, SHIN-3 and OVCAR-8 highly expressed the p53 protein, while their p53 gene expression was low compared to that observed in OVCAR-3. Unlike the other cell lines in this study, p53 gene and protein expression in OVCAR-5 WT cells were directly related (i.e., low and undetectable expression of the gene and protein,

respectively). Expanding these new findings to include those of the spheroid formation studies, it was determined that cell lines with enhanced expression of the p53 protein formed compact or semi-compact spheroids (i.e., OVCAR-8 and SHIN-3, respectively), while OVCAR-5 cells, whose p53 gene and protein expression levels were low, were capable of aggregate formation. Moreover, OVCAR-3 cells with high p53 gene and low p53 protein expression compared to OVCAR-8 and SHIN-3 cells, were not capable of spheroid or aggregate formation. Therefore, it was concluded that p53 protein expression greater than or equal to that of OVCAR-5 was likely to be involved in spheroid and/or aggregate formation in the studied cell lines. Furthermore, these findings support the observation that cell lines exhibiting NQO1 activity greater than or equal to that of OVCAR-8 are more likely to form spheroids or aggregates under the anchorage-independent conditions. Despite this, further assessment of additional factors that may be aiding in this process will be detailed in the next chapter.

Aside from probing the role of NQO1 in spheroid formation, I also worked to determine the level of expression and activity of enzyme in the cell lines that displayed enhanced ability to form compact spheroids. NQO1's presence was found upregulated in OVCAR-8 spheroids when compared to monolayer culture, whereas its expression was constant in 2-dimensional and 3-dimensional culture of SHIN-3. However, enzyme activity in spheroids of either cell line was found to be comparable to that in monolayer culture of OVCAR-8 after 2 days. Despite the decrease in activity of spheroids when compared to monolayers cultured for the same amount of time, the NQO1-activated probe Q_3NTCy was activated by the enzyme in as little as 30 minutes with an increase in reporter release

after prolonged exposure (≥1-hour). However, due to the lack of light penetration through spheroids, the applicability of Q_3NTCy for imaging of thick tissue samples is limited.

3.5 References

1. LaBarbera, D. V.; Reid, B. G.; Yoo, B. H., The multicellular tumor spheroid model for high-throughput cancer drug discovery. *Expert Opinion on Drug Discovery* **2012,** *7* (9), 819-830.

2. Kunz-Schughart, L., Multicellular tumor spheroids: intermediates between monolayer culture and in vivo tumor. *Cell Biology International* **1999,** *23* (3), 157-161.

3. Sutherland, R. M., Cell and environment interactions in tumor microregions: the multicell spheroid model. *Science* **1988,** *240* (4849), 177.

4. Mueller-Klieser, W., Multicellular spheroids. *Journal of Cancer Research and Clinical Oncology* **1987,** *113* (2), 101-122.

5. Santini, M. T.; Rainaldi, G., Three-dimensional spheroid model in tumor biology. *Pathobiology* **1999,** *67* (3), 148-157.

6. Hirschhaeuser, F.; Menne, H.; Dittfeld, C.; West, J.; Mueller-Klieser, W.; Kunz-Schughart, L. A., Multicellular tumor spheroids: an underestimated tool is catching up again. *Journal of Biotechnology* **2010,** *148* (1), 3-15.

7. Acker, H., Microenvironmental Conditions in Multicellular Spheroids Grown Under Liquid-Overlay Tissue Culture Conditions. In *Spheroids in Cancer Research: Methods and Perspectives*, Acker, H.; Carlsson, J.; Durand, R.; Sutherland, R. M., Eds. Springer Berlin Heidelberg: Berlin, Heidelberg, 1984; pp 116-133.

8. Jackson, R. C., The problem of the quiescent cancer cell. *Advances in Enzyme Regulation* **1989,** *29*, 27-46.

9. Bauer, K. D.; Keng, P. C.; Sutherland, R. M., Isolation of Quiescent Cells from Multicellular Tumor Spheroids Using Centrifugal Elutriation. *Cancer Research* **1982,** *42* (1), 72-78.

10. Hashimoto, O.; Shimizu, K.; Semba, S.; Chiba, S.; Ku, Y.; Yokozaki, H.; Hori, Y., Hypoxia Induces Tumor Aggressiveness and the Expansion of CD133-Positive Cells in a

Hypoxia-Inducible Factor-1α-Dependent Manner in Pancreatic Cancer Cells. *Pathobiology* **2011,** *78* (4), 181-192.

11. Sartorelli, A. C., Therapeutic attack of hypoxic cells of solid tumors: presidential address. *Cancer Research* **1988,** *48* (4), 775-778.

12. Yang, Y.; Zhou, X.; Xu, M.; Piao, J.; Zhang, Y.; Lin, Z.; Chen, L., β-lapachone suppresses tumour progression by inhibiting epithelial-to-mesenchymal transition in NQO1-positive breast cancers. *Scientific Reports* **2017,** *7* (1), 2681.

13. Lin, L.; Qin, Y.; Jin, T.; Liu, S.; Zhang, S.; Shen, X.; Lin, Z., Significance of NQO1 overexpression for prognostic evaluation of gastric adenocarcinoma. *Experimental and Molecular Pathology* **2014,** *96* (2), 200-205.

14. Yang, Y.; Zhang, Y.; Wu, Q.; Cui, X.; Lin, Z.; Liu, S.; Chen, L., Clinical implications of high NQO1 expression in breast cancers. *Journal of Experimental & Clinical Cancer Research* **2014,** *33* (1), 14.

15. Lewis Anne, M.; Ough, M.; Hinkhouse Marilyn, M.; Tsao, M.-S.; Oberley Larry, W.; Cullen Joseph, J., Targeting NAD(P)H:quinone oxidoreductase (NQO1) in pancreatic cancer. *Molecular Carcinogenesis* **2005,** *43* (4), 215-224.

16. Cui, X.; Li, L.; Yan, G.; Meng, K.; Lin, Z.; Nan, Y.; Jin, G.; Li, C., High expression of NQO1 is associated with poor prognosis in serous ovarian carcinoma. *BMC Cancer* **2015,** *15* (1), 244.

17. Haley, J.; Tomar, S.; Pulliam, N.; Xiong, S.; Perkins, S. M.; Karpf, A. R.; Mitra, S.; Nephew, K. P.; Mitra, A. K., Functional characterization of a panel of high-grade serous ovarian cancer cell lines as representative experimental models of the disease. *Oncotarget* **2016,** *7* (22), 32810-32820.

18. Hamilton, T. C.; Young, R. C.; Ozols, R. F. In *Experimental model systems of ovarian cancer: applications to the design and evaluation of new treatment approaches*, Seminars in Oncology, 1984; p 285.

19. Ma, Y.; Kong, J.; Yan, G.; Ren, X.; Jin, D.; Jin, T.; Lin, L.; Lin, Z., NQO1 overexpression is associated with poor prognosis in squamous cell carcinoma of the uterine cervix. *BMC Cancer* **2014,** *14* (1), 414.

20. Shen, Z., Visualization and Quantification of Cancer-associated Enzymes with Fluorescent Small-molecule Substrate Probes. In *LSU Doctoral Dissertations*, Louisiana State University: Baton Rouge, LA, 2018.

21. Costa, E. C.; Gaspar, V. M.; Coutinho, P.; Correia, I. J., Optimization of liquid overlay technique to formulate heterogenic 3D co-cultures models. *Biotechnology and Bioengineering* **2014,** *111* (8), 1672-1685.

22. Cabello, C. M.; Bair, W. B.; Bause, A. S.; Wondrak, G. T., Antimelanoma activity of the redox dye DCPIP (2,6-dichlorophenolindophenol) is antagonized by NQO1. *Biochemical Pharmacology* **2009,** *78* (4), 344-354.

23. Sodek, K. L.; Ringuette, M. J.; Brown, T. J., Compact spheroid formation by ovarian cancer cells is associated with contractile behavior and an invasive phenotype. *International Journal of Cancer* **2009,** *124* (9), 2060-2070.

24. Sodek, K. L.; Murphy, K. J.; Brown, T. J.; Ringuette, M. J., Cell–cell and cell–matrix dynamics in intraperitoneal cancer metastasis. *Cancer and Metastasis Reviews* **2012,** *31* (1), 397-414.

25. Godwin, A. K.; Meister, A.; Dwyer, P. J.; Huang, C. S.; Hamilton, T. C.; Anderson, M. E., High resistance to cisplatin in human ovarian cancer cell lines is associated with marked increase of glutathione synthesis. *Proceedings of the National Academy of Sciences* **1992,** *89* (7), 3070.

26. Eckstein, N., Platinum resistance in breast and ovarian cancer cell lines. *Journal of Experimental & Clinical Cancer Research* **2011,** *30* (1), 91.

27. Imai, S.; Kiyozuka, Y.; Maeda, H.; Noda, T.; Hosick, H. L., Establishment and Characterization of a Human Ovarian Serous Cystadenocarcinoma Cell Line That Produces the Tumor Markers CA-125 and Tissue Polypeptide Antigen. *Oncology* **1990,** *47* (2), 177-184.

28. Madajewski, B.; Boatman, M. A.; Chakrabarti, G.; Boothman, D. A.; Bey, E. A., Depleting Tumor-NQO1 Potentiates Anoikis and Inhibits Growth of NSCLC. *Molecular Cancer Research* **2016,** *14* (1), 14-25.

29. Dinkova-Kostova, A. T.; Talalay, P., NAD (P) H: quinone acceptor oxidoreductase 1 (NQO1), a multifunctional antioxidant enzyme and exceptionally versatile cytoprotector. *Archives of Biochemistry and Biophysics* **2010,** *501* (1), 116-123.

30. Asher, G.; Lotem, J.; Kama, R.; Sachs, L.; Shaul, Y., NQO1 stabilizes p53 through a distinct pathway. *Proceedings of the National Academy of Sciences* **2002,** *99* (5), 3099-3104.

31. Asher, G.; Lotem, J.; Cohen, B.; Sachs, L.; Shaul, Y., Regulation of p53 stability and p53-dependent apoptosis by NADH quinone oxidoreductase 1. *Proceedings of the National Academy of Sciences* **2001,** *98* (3), 1188-1193.

32. Maier, T.; Güell, M.; Serrano, L., Correlation of mRNA and protein in complex biological samples. *FEBS Letters* **2009,** *583* (24), 3966-3973.

33. Greenbaum, D.; Colangelo, C.; Williams, K.; Gerstein, M., Comparing protein abundance and mRNA expression levels on a genomic scale. *Genome Biology* **2003,** *4* (9), 117.

34. Koussounadis, A.; Langdon, S. P.; Um, I. H.; Harrison, D. J.; Smith, V. A., Relationship between differentially expressed mRNA and mRNA-protein correlations in a xenograft model system. *Scientific Reports* **2015,** *5*, 10775.

35. Vogelstein, B.; Lane, D.; Levine, A. J., Surfing the p53 network. *Nature* **2000,** *408* (6810), 307.

36. Harsha, B.; Creatore, C.; Kok, C. Y.; Hathaway, C.; Cole, C. G.; Ramshaw, C. C.; Rye, C. E.; Beare, D. M.; Dawson, E.; Boutselakis, H.; Noble, K.; Ponting, L.; Bindal, N.; Fish, P.; Campbell, P. J.; Stefancsik, R.; Bamford, S.; Thompson, S. L.; Ward, S.; Wang, S.; Forbes, S. A.; Jupe, S. C.; Sondka, Z.; Tate, J. G.; Jubb, H. C.; Speedy, H. E., COSMIC: the Catalogue Of Somatic Mutations In Cancer. *Nucleic Acids Research* **2018,** *47* (D1), D941-D947.

37. Leroy, B.; Girard, L.; Hollestelle, A.; Minna, J. D.; Gazdar, A. F.; Soussi, T., Analysis of TP53 mutation status in human cancer cell lines: a reassessment. *Human Mutation* **2014,** *35* (6), 756-765.

38. Debernardis, D.; Siré, E. G.; De Feudis, P.; Vikhanskaya, F.; Valenti, M.; Russo, P.; Parodi, S.; Incalci, M.; Broggini, M., p53 Status Does Not Affect Sensitivity of Human Ovarian Cancer Cell Lines to Paclitaxel. *Cancer Research* **1997,** *57* (5), 870.

39. Mabuchi, S.; Altomare, D. A.; Cheung, M.; Zhang, L.; Poulikakos, P. I.; Hensley, H. H.; Schilder, R. J.; Ozols, R. F.; Testa, J. R., RAD001 Inhibits Human Ovarian Cancer Cell Proliferation, Enhances Cisplatin-Induced Apoptosis, and Prolongs Survival in an Ovarian Cancer Model. *Clinical Cancer Research* **2007,** *13* (14), 4261.

40. Siegel, D.; Ross, D., Immunodetection of NAD (P) H: quinone oxidoreductase 1 (NQO1) in human tissues1. *Free Radical Biology and Medicine* **2000,** *29* (3-4), 246-253.

41. Shen, Z.; Prasai, B.; Nakamura, Y.; Kobayashi, H.; Jackson, M. S.; McCarley, R. L., A Near-Infrared, Wavelength-Shiftable, Turn-on Fluorescent Probe for the Detection and Imaging of Cancer Tumor Cells. *ACS Chemical Biology* **2017,** *12* (4), 1121-1132.

CHAPTER 4
DETERMINATION OF CANCER STEM CELL PRESENCE AND PHENOTYPIC HETEROGENEITY IN 2-DIMENSIONAL AND 3-DIMENSIONAL MODELS OF OVARIAN CANCER

4.1 Introduction

Oncogenic transformation is speculated to be the result of a small subset of cancer cells that have acquired stem-like functions.[1-2] These cells, dubbed cancer stem cells (CSC), have the ability to self-renew and produce daughter cells capable of shifting into phenotypes that often cross lineages.[2-3] The stem-like nature of these cells enables them to adapt to environmental changes, such as a diminished nutrient supply and exposure to chemotherapeutics, thus leading to increased survival.[4] Due to its 70% recurrence rate after initial treatment, CSC presence in ovarian cancer has been of great interest to researchers.[5-6] As detailed in Chapter 1 ovarian cancer-associated CSC markers have been identified as having increased tumor-initiating ability, invasiveness, angiogenic ability, and chemoresistance in vivo.[6] Several biomarkers have been found to be associated with ovarian CSCs, four of which will be highlighted in the following section.[6]

CD133, or Prominin-1, is one of the most widely studied ovarian CSC markers to date. Several researchers have shown that CD133-positive cells from both established and primary ovarian cells have increased tumor-initiating capacity.[7-8] Curley and colleagues isolated a CD133-negative population of cells that gave rise to a tumor composed of 10% CD133-positive cells in immunocompromised mice.[7] These findings suggest that either CD133-negative cells transform into CD133-postive ones, or as little as 1% CD133-positive cells have the ability to drive tumor formation.[7] Aside from these findings, Kryczek

and colleagues observed that both in vitro and in vivo spheroid forming ability was increased in cells that co-expressed aldehyde dehydrogenase isozyme-1 (ALDHA1) and CD133.[9] Similarly, Silva et al. observed that co-expression of CD133 and ALDHA1 resulted in increased tumorigenic and angiogenic potential in immunocompromised mice.[10] Additionally, they found that ALDHA1-positive cells isolated from CD133-negative primary and established cell lines could give rise to tumors in mice, while ALDHA1-negative cells could not. This suggests that ALDHA1 expression, like CD133, is correlated with increased tumorigenic potential. It was noted that primary tumor cells and established cell lines have different propensities for tumor formation in vivo related to the expression of CD133 and ALDHA1. Specifically, established cell lines positive for CD133 but lacking ALDHA1 could form tumors in mice, while primary tumor cells could not.[10]

Aside from CD133 and ALDHA1, hyaluronic acid receptor CD44, has been implicated as a CSC marker in breast, prostate, colorectal, and pancreatic cancer, due to populations enriched for it being highly tumorigenic.[11-14] Its expression has been associated with enhanced cell adhesion and binding to extracellular matrix proteins that are highly expressed in solid tumors.[15-16] Alvero and colleagues found that patients with metastatic disease had enhanced CD44 expression.[17] In the same study, isolated primary cells showed increased frequency of tumor formation and resembled the native tissue when harvested in mice. In a follow-up study, it was found that CD44-positive cells were capable of differentiating into human CD34-expressing blood vessels, thus indicating that they are involved in angiogenesis.[6, 18] Like CD133 and CD44, CD117 is a surface protein whose function is to maintain cells in an undifferentiated state and promote self-renewal in embryonic, hematopoietic, and mesenchymal stem cells, and has also been identified

as an ovarian CSC.[19-21] Lu et al. observed that populations of CD117-positive cells were capable of asymmetric division, tumorigenesis, and increased chemo-resistance.[22] In a different study, Zhang and colleagues identified a population of cells co-expressing CD44 and CD117, which were observed to be tumorigenic and chemoresistant in vivo.[6, 23]

Apart from CSC presence, phenotypic heterogeneity within tumors has been linked to increased metastasis, chemoresistance, and recurrence. Cancer cells have been shown to undergo phenotypic transitions in an effort to not only aid their spread to distant tissues, but also in response to environmental stressors. Such changes in phenotype, as detailed in Chapter 1, are the result of an epithelial-to-mesenchymal transition, or EMT. It is speculated that during neoplastic progression, ovarian cancer tumors are composed of cells having an epithelial phenotype, but as the disease advances, they acquire mesenchymal features, thus resulting in metastatic disease. [24] However, there are populations of cells that may exhibit features of one or both phenotypes. In one study, it was found that a side population of ovarian cancer cells, derived from primary ascites and mesenchymal cells, were epithelial; whereas the remaining cells were found to be mesenchymal.[25] In a separate study, Strauss et al. isolated populations of ovarian cancer cells from mouse xenografts and tissue culture that expressed a hybrid epithelial-mesenchymal phenotype.[26] While the two previously mentioned works were representative of cells derived from patient samples, Gardi and colleagues found that established ovarian cancer cell lines underwent phenotypic transitions when cultured in vitro under conditions that either promoted or inhibited attachment to an extracellular matrix (ECM) substrate.[27] Each study indicates that phenotypic heterogeneity is not

limited to cells cultured in vivo, thus suggesting that monitoring these changes in vitro will also not compromise the integrity of information.

In Chapter 3, it was determined that NQO1 could not be implicated as the sole driving force behind spheroid formation, though NQO1 activity in cells and their ability to form spheroids and/or aggregates appeared to be related. These findings mirrored those presented in Chapter 2, where it was observed that NQO1 activity and proliferative ability were connected in three of the four studied cell lines. To pinpoint additional factors that may have an impact on proliferation and tumorigenesis in ovarian cancer, CSC presence and the phenotypic nature of each cell line in two-dimensional and three-dimensional culture will be evaluated. Furthermore, similarities and differences that exist between CSC expression and cell phenotype in two-dimensional and three-dimensional culture will be examined.

4.2 Experimental

4.2.1 Cell Culture

Human ovarian carcinoma cell lines SHIN-3, OVCAR-5, and OVCAR-8 were gifts from Dr. Hisataka Kobayashi at the United States National Institutes of Health, National Cancer Institute, Center for Cancer Research. Human ovarian carcinoma cell line OVCAR-3 was purchased from American Type Culture Collection (ATCC). All cell lines were cultured in either DMEM or RPMI-1640 medium purchased from ATCC supplemented with 10% fetal bovine serum (FBS; ATCC), 10 IU/mL penicillin and 10 μg/mL streptomycin (Life Technologies) unless stated otherwise. Bovine insulin (1 μg/mL) was an additional supplement for OVCAR-3 cells. Cells were cultured in 75 cm^2 treated tissue culture flasks at 37 °C under 5% CO_2 in a humidified incubator.

4.2.2 Multicellular Tumor Spheroid Culture

MCTS were cultured in ultra-low attachment dishes (Corning). Briefly, cells were seeded at 1×10^4 cells in each well of a 96-well plate coated with 1% agarose. Medium was changed every 2 to 4 days, depending on the cell line.

4.2.3 Protein Quantification

Protein quantification was carried out as described in Chapters 2 and 3. Briefly, monolayer cells were dissociated from culture dishes using trypsin-EDTA, while intact spheroids were harvested from 96-well plates. Monolayer cells were centrifuged at 900 rpm for 7 minutes at 4 °C, to remove tryspin-EDTA or media, followed by the introduction of 150-200 μL of radioimmunoprecipitation assay (RIPA, ThermoFisher) buffer with 1 mM phenylmethylsulfonyl fluoride (Sigma) and protease inhibitor cocktail (Sigma). Intact spheroids (n=96) were exposed to 250 μL of RIPA buffer with 1 mM phenylmethylsulfonyl fluoride (Sigma) and protease inhibitor cocktail (Sigma) for 30–45 minutes on ice. Mechanical pipetting was employed at 10-minute intervals to ensure that all cells with each sample were lysed. Monolayer and spheroid samples were then centrifuged at 18,000 ×g for 20 minutes at 4 °C. The supernatant was obtained and aliquoted into sterile Eppendorf tubes at −80 °C until use. Total protein content was quantified using a well-established BCA assay.

4.2.4 Western Blot

CSC and EMT marker expression were measured in 25 μg protein samples. Samples were measured using sodium dodecyl sulphate-polyacrylamide gel electrophoresis (SDS-PAGE) using 4–20% polyacrylamide gels (Bio-Rad). 10 μL of Kaleidoscope Pre-Stained

Standard marker was used to track proteins. Samples were diluted in 2X Laemmli sample buffer containing 2-mercaptoethanol at a 1:1 ratio. Protein separation was conducted at 100 V for 65 minutes in running buffer (Tris/Glycine/SDS), followed by protein transfer onto nitrocellulose membranes in transfer buffer (Tris-Glycine and 20% methanol). Following transfer, the membrane was blocked with 5% non-fat dry milk (NFDM) for one hour before being washed with TBST solution.

To assess stemness, mouse anti-CD44, rabbit anti-CD133, and rabbit anti-ALDHA1 (Cell Signaling Technologies) and a mouse anti-CD117 antibody (Santa Cruz) were used. EMT was evaluated with primary monoclonal antibodies rabbit anti-vimentin, rabbit anti-E-cadherin, rabbit anti-N-Cadherin, and mouse anti-EpCAM antibodies, all of which were purchased from Cell Signaling Technologies. An anti-β-actin monoclonal antibody (Cell Signaling Technologies) was also introduced to the membranes as a loading control. All antibodies were diluted to a 1:1000 concentration in NFDM. The membranes were kept overnight at 4 °C with gentle shaking. After overnight incubation with the antibodies, membranes were washed with TBST 3X in 10-minute intervals. The following day, both mouse anti-IgG and rabbit anti-IgG, HRP-linked secondary antibodies (Cell Signaling Technologies) were added to the membranes for 1 hour at room temperature with gentle shaking. Super Signal West Pico chemiluminescent substrate was prepared based on the manufacturer's protocol, and slowly pipetted onto the membranes several times for roughly two minutes. Membranes were imaged using a Bio-Rad ChemiDoc MP system with an exposure time of 300 seconds at 60 second intervals. Raw images were saved as tagged image file format (TIFF) files, and band analysis was performed using Fiji/ImageJ software.

4.2.5 Immunocytochemistry/Immunofluorescence (ICC/IF)

OVCAR-5, SHIN-3, OVCAR-8, and OVCAR-3 cells were cultured overnight in a 16-well chambered slide (LabTek) at 37 °C. The following day, cells were washed with ice cold PBS for 5 minutes to remove excess media. Samples were then treated with 200 μL of cold 4% paraformaldehyde (PFA) for 20 minutes in the dark at room temperature. Once the fixation step was completed, samples were washed with ice-cold PBS for 5 minutes. Samples were then permeabilized with 3% Tween-20 in PBS (PBST) for 15 minutes at 37 °C. 200 μL 5% BSA in PBST (PBS with 1% Tween-20) was added to the cells for 1-hour to allow for blocking. While the cells were blocked, a working concentration of each primary antibody vimentin, N-cadherin, E-cadherin, EpCAM, CD44, CD133, ALDHA1 and CD117 was prepared in 1% BSA in PBST at 1:200 dilutions. The antibody solutions were added at the volume of 200 μL per well. The slides were then incubated at 4 °C for 1 hour with shaking. Following removal of the primary antibody solutions, samples were washed with PBST 3X for 10 minutes. Goat anti-mouse AlexaFluor 633 and anti-rabbit AlexaFluor 488 conjugated secondary antibodies (ThermoFisher) were prepared at 1:500 dilutions in PBST and added to their respective wells for 1 hour. After this, the cells were washed an additional three times with PBS. Upon removal of the separating chamber and polymer coating, coverslips were mounted onto the slides using Prolong Gold Antifade mountant with DAPI. Images were collected using a Leica TCS SP8 laser-scanning confocal microscope.

Stained cells were imaged using either a 488-nm or a 633-nm white light laser with spectral emission collected between 495–520 nm and 650–750 nm, respectively. The pinhole was set at 1 Airy unit (53.1 μm). The DAPI nuclear stain was imaged using the

AOTF (405) Ar. Each image was frame and line averaged 4 and 2 times, respectively, at a scan speed of 8000 Hz. An Apo plan 20X 0.3 NA objective was used. Image analysis was performed using LAS X and Fiji/Image J software.

4.2.6 Extreme Limited Dilution Assay

An extreme limited dilution assay is a dose-response experiment that allows quantification of biologically active populations.[28] It was employed in this work to determine the stem cell frequency within small populations of cells as previously described.[29] Briefly, OVCAR-8 and SHIN-3 cells were seeded at densities of 50, 100, 250, and 500 cells in ultralow attachment 96-well plates. Spheroid formation was monitored over a period of 21 days. On the 21st day of culture, the number of wells containing a spheroid were counted. Based on initial cell density, along with number of tested and positive samples, a measure of the confidence interval for cancer stem cell frequency was generated using ELDA software provided developed at the Bioinformatics Division of the Walter and Eliza Hall Institute (WEHI) of Medical Research.

4.3 Results and Discussion

4.3.1 CSC in OC Cell Monolayers

Due to its level of recurrence and subsequent chemoresistance, a considerable amount research has been devoted to the study of CSCs in ovarian cancer. Therefore, in this section, the presence of several biomarkers associated with ovarian CSCs, namely, CD117, CD133, CD44, and ALDHA1, were evaluated in SHIN-3, OVCAR-5, OVCAR-8, and OVCAR-3 cells. As mentioned earlier, each marker has been associated with increased self-renewal, tumorigenesis, chemoresistance, and angiogenesis.[1, 6, 15, 30-31]

Through my analysis of OC cell monolayers, it was found that CD117 expression was not observed in either cell line. Expression of both CD133 and CD44 in OVCAR-5 and OVCAR-8 cells was observed, while OVCAR-3 and SHIN-3 expressed CD133 and CD44, respectively (Figure 4.1. A. and B). Both OVCAR-3 and SHIN-3 were found to express ALDHA1; however, ALDHA1 was observed to have nuclear localization in OVCAR-3 as opposed to the cytosol for SHIN-3 cells. Expression of ALDHA1 in OVCAR-3 nuclei will have to be investigated further as it suggests that active enzyme is present. From these findings and those presented in Chapter 3, it is hypothesized that cells expressing either CD44 and CD133, or those expressing CD44 in conjunction with ALDHA1, have increased potential to form spheroids or cell aggregates under conditions that lack a support matrix. This observation is supported by OVCAR-5 and OVCAR-8 cells being positive for CD44 and CD133 and forming loose aggregates and spheroids, respectively. SHIN-3, on the other hand, lacked CD133, but expressed both CD44 and ALDH— both which have been found to initiate tumor growth in the absence of CD133.[10-11, 13-14]

Furthermore, it was noticed that cell lines derived from patients with advanced disease lacked expression of ALDHA1, which would explain why OVCAR-5, OVCAR-8, and OVCAR-3 were found to be ALDHA1-negative. In addition, CD44 was observed in OVCAR-5, OVCAR-8, and SHIN-3, all of which had more aggressive proliferation patterns. Additionally, the findings presented in Chapters 2 and 3 suggested that increased proliferation and sphere-forming ability was associated with cell lines that had increased NQO1 activity. Therefore, CD44 expression may be linked to enhanced NQO1 activity as well. It is plausible that the absence of CD44 and low NQO1 activity may be

affecting both proliferative and sphere-forming ability in OVCAR-3 cells, despite their expression of CD133, which has long been associated with tumorigenesis.[30]

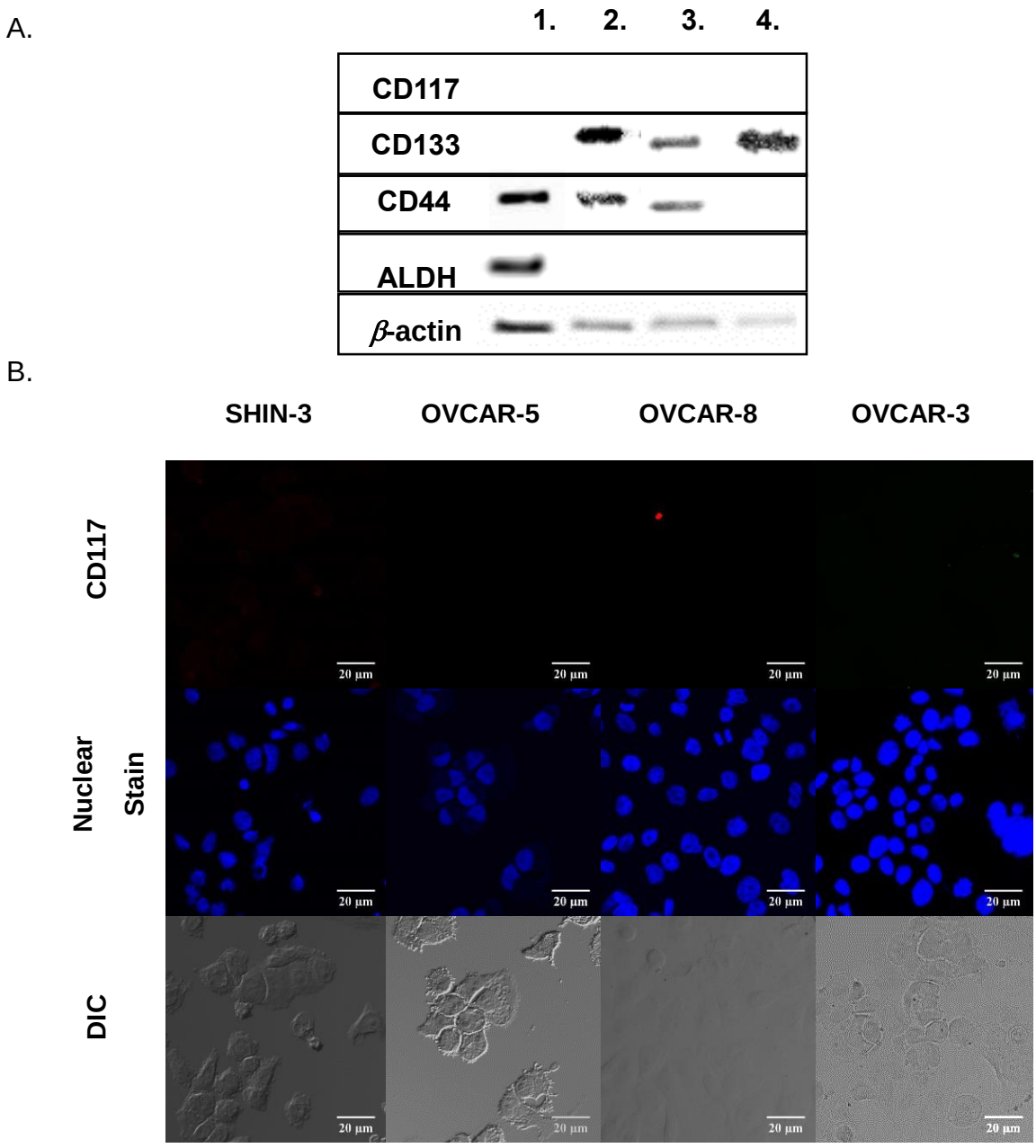

Figure 4.1. (**A**) Western blot analysis of OC cell monolayers against CSC markers in (**1**) SHIN-3, (**2**) OVCAR-5, (**3**) OVCAR-8, and (**4**) OVCAR-3. Bands represent 25 μg of protein. β-actin was used as an internal standard. (**B**) ICC/IF images of staining against CSC biomarkers in OC cell monolayers. Nuclear colocalization was achieved using DAPI stain.

(Fig. cont'd.)

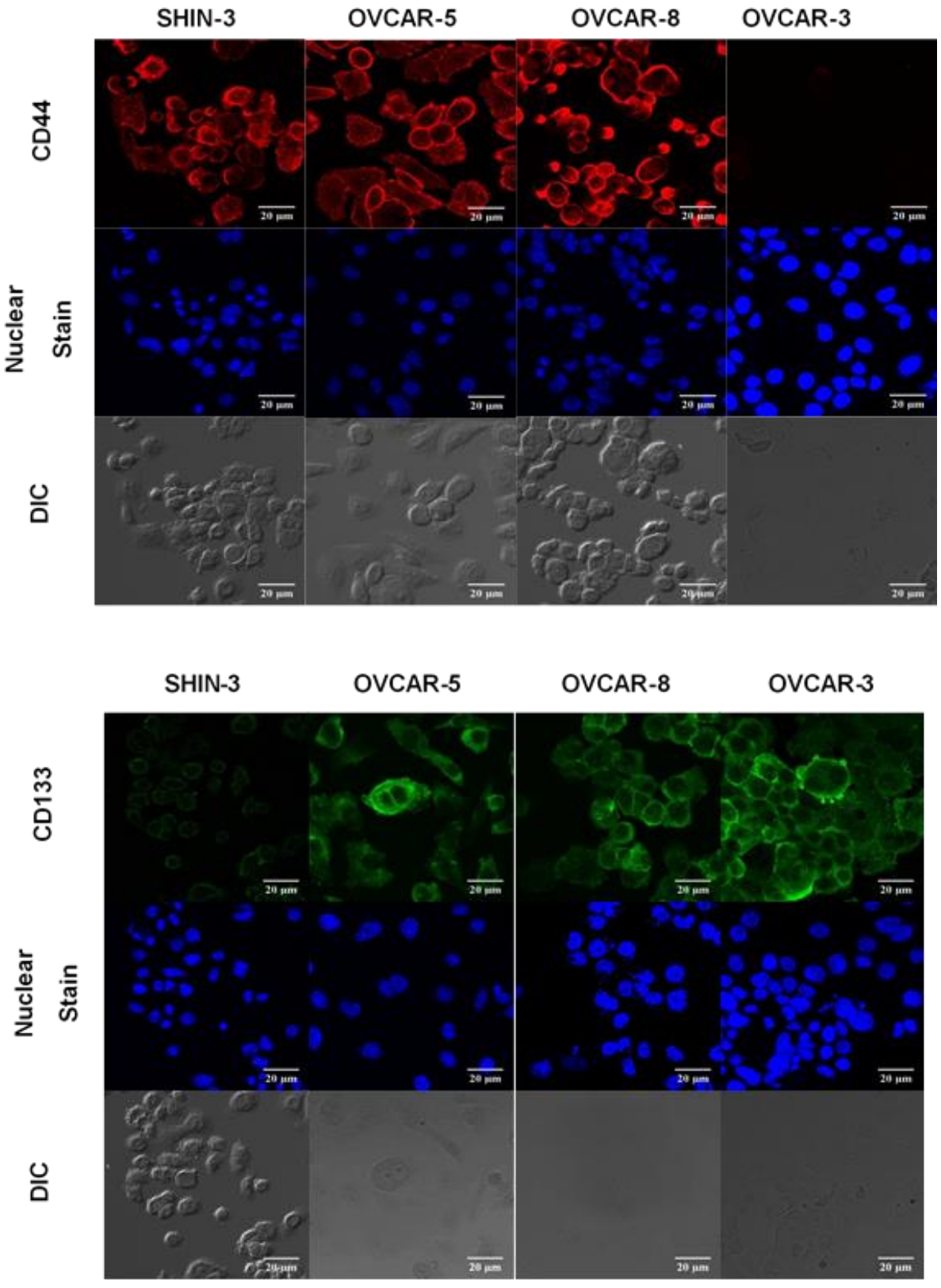
SHIN-3
OVCAR-5
OVCAR-8
OVCAR-3
CD44
Nuclear Stain
DIC
20 μm
SHIN-3
OVCAR-5
OVCAR-8
OVCAR-3
CD133
Nuclear Stain
DIC
20 μm

(Fig. cont'd.)

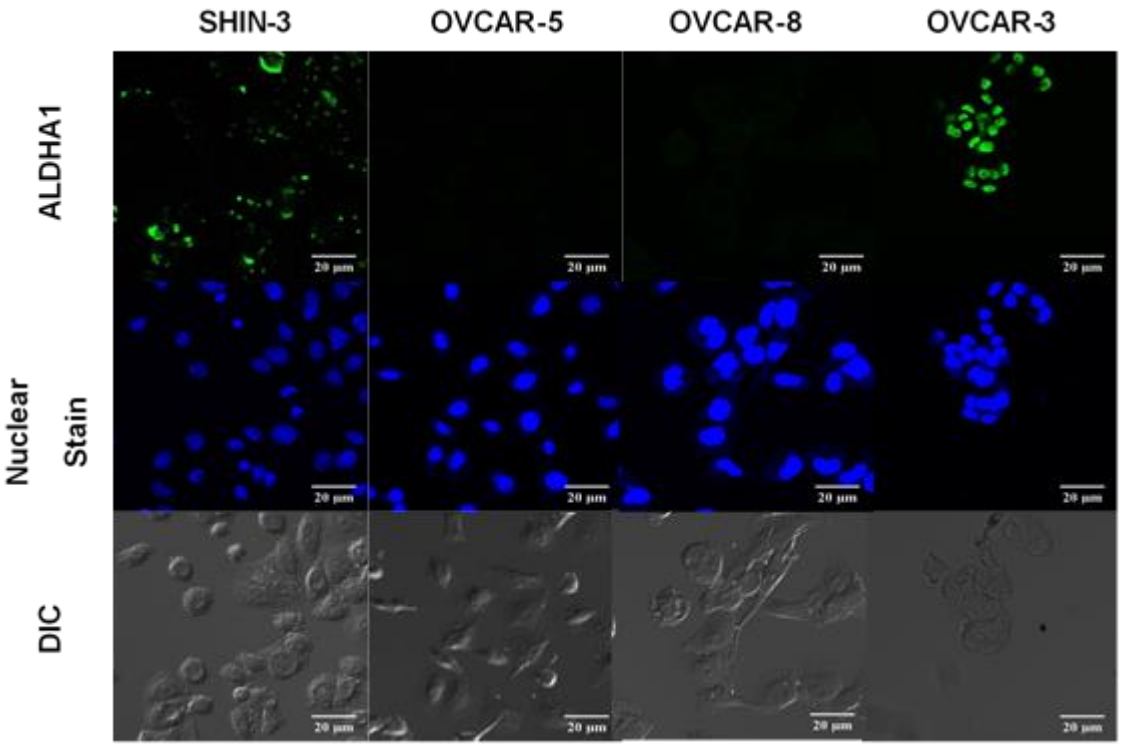

4.3.2 CSC in OVCAR-8 and SHIN-3 Spheroids

Although CSC presence in cell monolayers provided insight into the proliferative and tumorigenic potential of the studied cell lines, determining whether those findings would hold true within spheroids would be advantageous. As noted in Chapter 3, gene expression in monolayers is often questionable due to cells lacking the intra-and extracellular interactions that are often observed in tumors. Thus, CSC presence in OVCAR-8 and SHIN-3 spheroids was evaluated in bulk culture via western blot. Consistent expression of CD44 was noticed in 5-day and 12-day old OVCAR-8 and SHIN-3 spheroids (Figure 4.2). However, based on the observed western blot band densities, OVCAR-8 spheroids appear to have enhanced expression of CD44 when compared to SHIN-3. This increased expression in OVCAR-8 supports findings by Alvero et al., whose

work suggests that patients with metastatic disease have higher expression of CD44 when compared to tissues derived from patients prior to chemotherapy (i.e., SHIN-3).[17] In addition, it was noticed that CD133 was not present in spheroid culture despite being expressed in OVCAR-8 monolayers. It is speculated that CD133 expression is downregulated in OVCAR-8 spheroids; however, the cause of this decrease in expression is unknown. In contrast, the lack of CD133 in SHIN-3 spheroids resembled that for monolayers in that the protein was not found in bulk samples in either study. These observations further suggest that CD133 may be upregulated in OC CSCs isolated from tumor tissues because it assists in tumor formation. However, it may be downregulated once tumors are established. In contrast, ALDHA1 expression was found to remain constant in SHIN-3 cells grown as both monolayers and spheroids; these outcomes indicate that ALDHA1 presence may be necessary for tumor formation and progression. Also, evaluation of CD117 in OVCAR-8 and SHIN-3 spheroids revealed that CD117 was not present, which parallels the findings in monolayer culture.

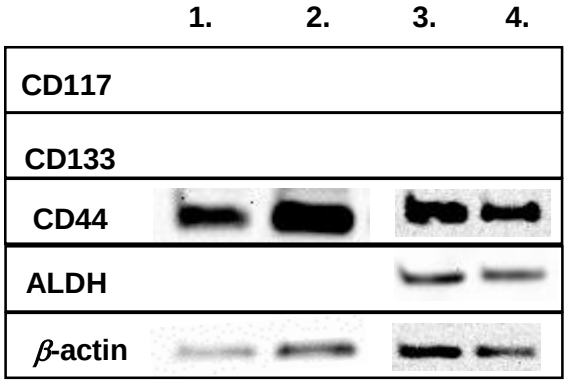

Figure 4.2. Assessment via western blot of cancer stem cell marker presence in (**1**) 5-day-old and (**2**) 12-day-old OVCAR-8 spheroids, and (**3**) 5-day-old and (**4**) 12-day-old SHIN-3 spheroids. Bands are representative of 25 μg of protein. β-actin was used as an internal standard.

4.3.3 CSC Frequency in OVCAR-8 and SHIN-3 Spheroids

Aside from expression of specific CSC-associated biomarkers, the ability of a cell to initiate tumor formation is another hallmark of stemness in cancer. Non-tumorigenic cells are thought to comprise the majority of tumor tissues, so researchers have posited that small populations of tumor-initiating cells within tissues are actually CSCs. In order to evaluate CSC frequency within a large population of cells, an extreme limiting dilution assay (ELDA) was performed with OVCAR-8 and SHIN-3 cells. Cells were plated at low densities (i.e., 50, 100, 250, and 500 cells) in ultralow attachment 96-well plates. After 21 days, the number of wells containing a spheroid were counted, and the frequency of CSC presence was calculated using ELDA software. In Table 4.3 are shown the number of spheroids observed at each of the plated densities in addition to the confidence interval for CSC frequency as determined by the ELDA software. From this data, it was found that in every 96 OVCAR-8 cells there will be at least one CSC, while in every 130 SHIN-3 cells there will be one CSC. Based on the obtained confidence intervals, it was determined that CSC presence in OVCAR-8 is 1.4X more likely to be observed when compared to SHIN-3 cells plated at the same density.

Table 4.1. The confidence interval of frequency of CSC occurrence in OVCAR-8 and SHIN-3 cells relative to spheroid formation under attachment-free conditions.

	50 Cells	100 Cells	250 Cells	500 Cells	CSC Frequency
OVCAR-8	90	80	86	79	1/96
SHIN-3	35	77	74	88	1/130

4.3.4 Phenotypic Evaluation of OC Cell Monolayers

As previously mentioned, CSC are thought to drive EMT in cancer cells**.** To evaluate whether an epithelial, mesenchymal, or a mixture of the two phenotypes exists within the studied cells, western blot (Figure 4.3.A) and ICC/IF (Figure 4.3.B) were conducted. OVCAR-3 cells displayed a purely epithelial phenotype due to its high expression of EpCAM and low expression of E-cadherin, which supports previous literature regarding its phenotypic nature.[32] Analysis of OVCAR-8 cells revealed a dominant mesenchymal phenotype, as evidenced by high expression of vimentin. Additionally, it was the only cell line to express the mesenchymal marker, N-cadherin, though the latter's presence is minimal and only detectable via fluorescence-based techniques. As with OVCAR-3, these findings are consistent with prior research on OVCAR-8 phenotype.[33]

While OVCAR-3 and OVCAR-8 were representative of either a highly epithelial or mesenchymal phenotype, SHIN-3 and OVCAR-5 cells appeared to possess mixed phenotype, as both epithelial and mesenchymal markers were identified. However, it was determined that each possessed dominant and recessive expression profiles associated with each phenotype. SHIN-3 was found to have a dominant epithelial phenotype, as evidenced by a dense band for EpCAM using western blot, while vimentin was observed to a lesser degree. ICC/IF corroborated these findings with staining of both EpCAM and vimentin. On the contrary, OVCAR-5 cells had a dominant mesenchymal phenotype, because dense bands and highly fluorescent staining of vimentin was observed via western blotting and ICC/IF, respectively. Moreover, ICC/IF analysis revealed that OVCAR-5 had low expression of E-cadherin and EpCAM. The presented data supports

previous findings regarding an intermediate mesenchymal phenotype in OVCAR-5 monolayers.[33]

Phenotypic characterization of the studied cell lines also reflects their proliferative abilities detailed in Chapter 2. It can be posited that the increased proliferation rates recorded in OVCAR-5, OVCAR-8, and SHIN-3 cells are a result of their mesenchymal characteristics, thus enabling more aggressive growth patterns. Whereas, the highly epithelial OVCAR-3 cells were less proliferative due to their less invasive phenotype. It was also observed that spheroid and aggregate formation was closely associated with cells exhibiting either a mixed or mesenchymal phenotype. Moreover, the presence of a mesenchymal phenotype or mesenchymal features in OVCAR-8, OVCAR-5, and SHIN-3 further supports the notion that CD44 expression is associated with cells harboring an aggressive phenotype. Also, CD44 expression was observed in both two-dimensional and three-dimensional culture systems. In addition, CD133 expression did not appear to be correlated with epithelial or mesenchymal cells; therefore, it is likely that it is a universal CSC marker.

A.

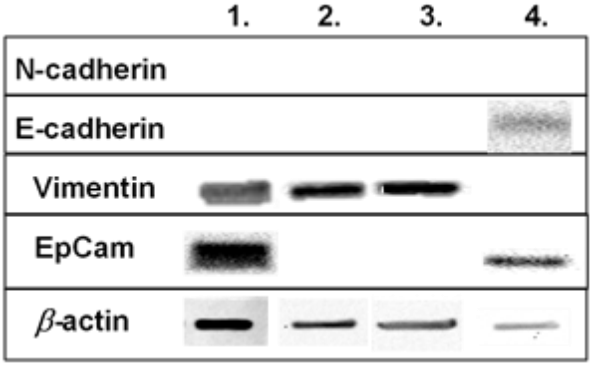

Figure 4.3. (**A**) Western blot analysis of OC cell monolayers against EMT markers in (**1**) SHIN-3, (**2**) OVCAR-5, (**3**) OVCAR-8, and (**4**) OVCAR-3. Bands result from analysis of 25 μg of protein. β-actin was used as an internal standard.

(Fig. cont'd.)

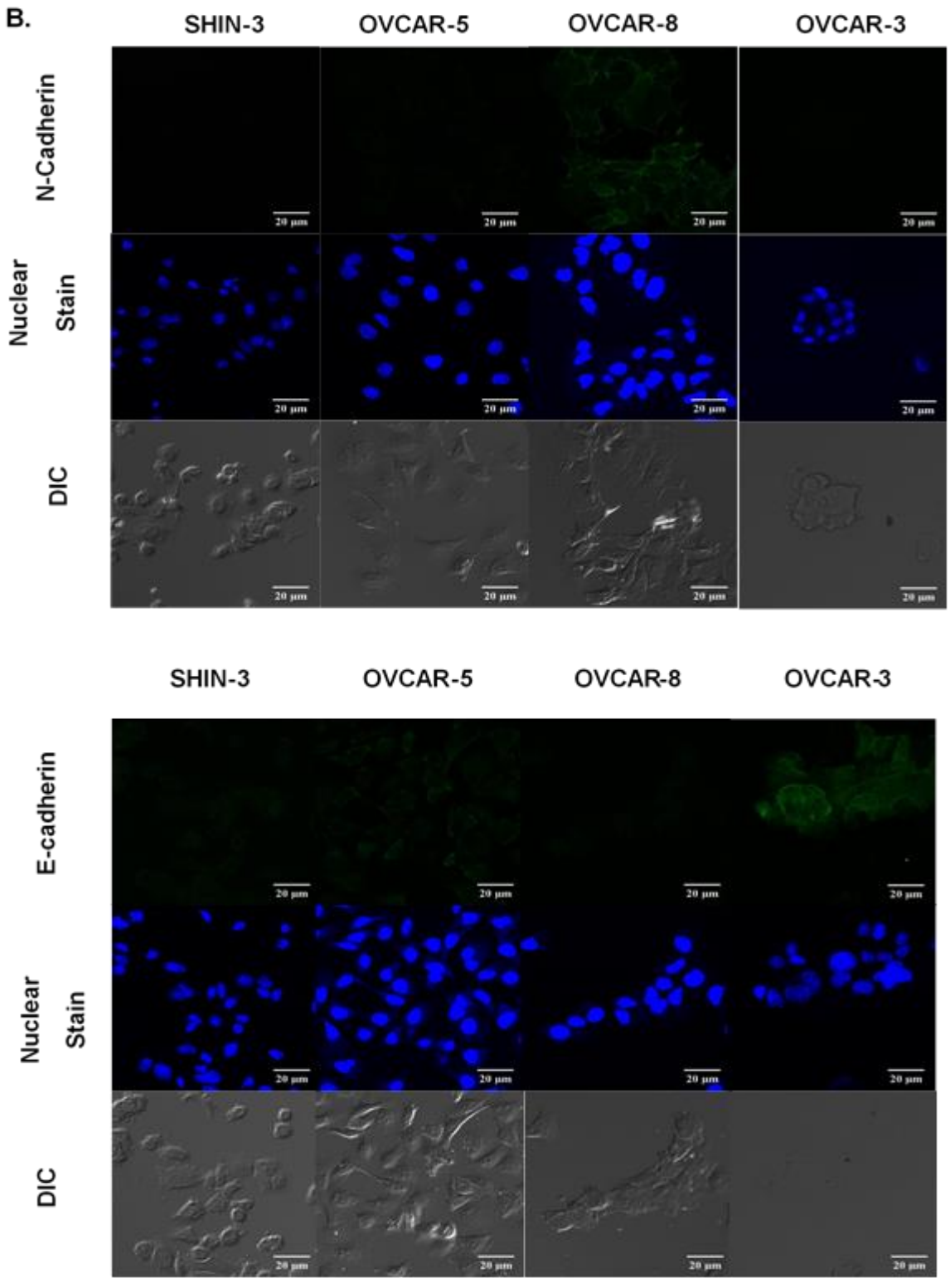
B.
SHIN-3
OVCAR-5
OVCAR-8
OVCAR-3
N-Cadherin
Nuclear Stain
DIC
20 μm
SHIN-3
OVCAR-5
OVCAR-8
OVCAR-3
E-cadherin
Nuclear Stain
DIC
20 μm

(Fig. cont'd.)

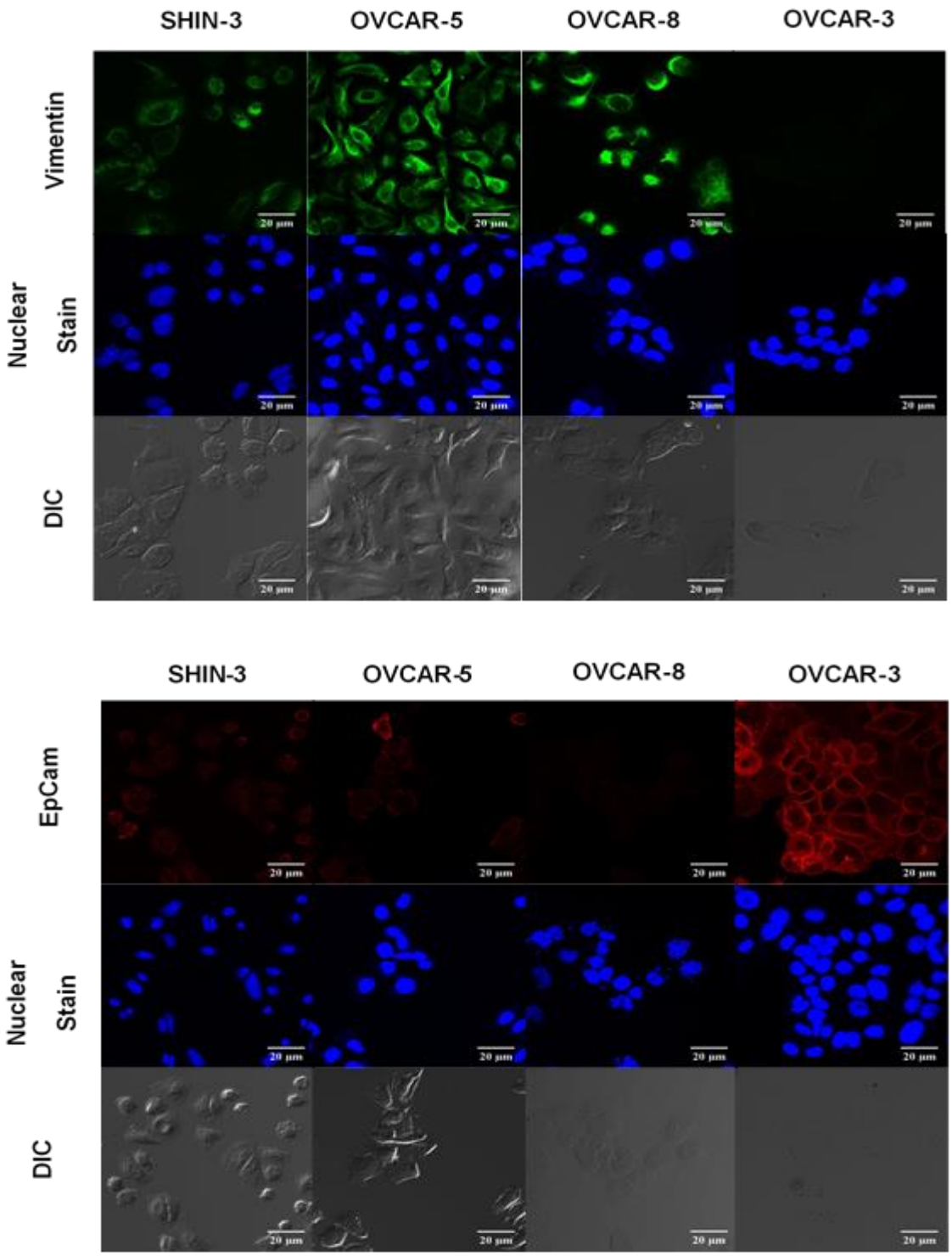

Figure 4.3. (**B**) ICC/IF images of staining against epithelial and mesenchymal biomarkers in OC cell monolayers. Nuclear colocalization was achieved using a DAPI stain.

4.3.5 Phenotypic Heterogeneity in OVCAR-8 and SHIN-3 Spheroids

To examine phenotypic plasticity, bulk protein was extracted from 96 intact spheroids for western blot analysis. The presence of EMT biomarkers E-cadherin, EpCAM, vimentin, and N-cadherin were evaluated in each of the spheroids derived from OVCAR-8 and SHIN-3 (Figure 4.4.). It was found that OVCAR-8 and SHIN-3 spheroids exhibit a mixed phenotype, which supports literature regarding tumor heterogeneity.[26, 34] While both E-cadherin and EpCAM were observed in OVCAR-8 spheroids, only E-cadherin was expressed in SHIN-3. In addition, EpCAM expression appeared to diminish with time as evidenced by the decreased band density in samples extracted from 12-day-old spheroids. Vimentin was also observed in SHIN-3 and OVCAR-8 spheroids regardless of age, suggesting cells with enhanced motility are present. It was also noticed that N-cadherin, whose expression was low in OVCAR-8 monolayers, had increased in spheroid culture. Literature states that upregulation of N-cadherin is often observed in more aggressive tumor tissues, meaning that in spheroid form, OVCAR-8 is likely more aggressive than SHIN-3. Interestingly, EpCAM expression dominated SHIN-3 monolayers, while E-cadherin expression was upregulated in SHIN-3 spheroids. It can be assumed that EpCAM, an adhesion molecule, was highly expressed due to the cells being grown in monolayer culture.[35] While E-cadherin, which is also associated with cell-cell adhesion, is prevalent in tissue samples, thus leading to is upregulation in spheroids.[24, 26, 36]

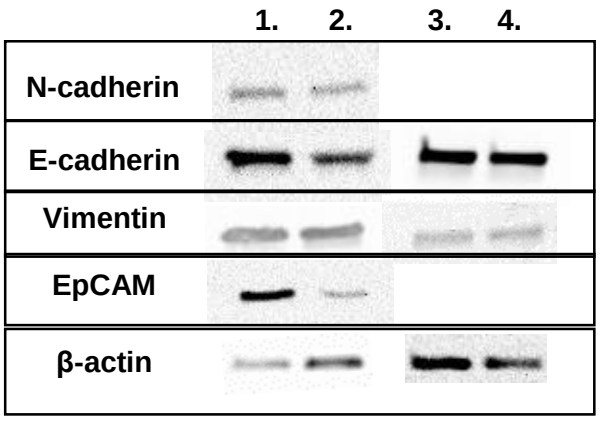

Figure 4.4 Analysis of phenotypic heterogeneity in (**1**) 5-day-old and (**2**) 12-day-old OVCAR-8 spheroids, and (**3**) 5-day-old and (**4**) 12-day-old SHIN-3 spheroids via western blot. Bands are representative of 25 μg of protein. β-actin was used as an internal standard.

4.4 Conclusions

In sum, it was found that while one or more CSC markers were found to be expressed in monolayers of each cell line, the same level of expression may or may not be observed in spheroids. For example, CD133 was present in OVCAR-8 monolayers, but not in spheroids derived from the cell line. It was astounding that CD133 was not observed in bulk culture of spheroids because it is a marker that is closely associated with the formation of tumors.[7-8, 37-39] Therefore, it was concluded CSCs have the ability to upregulate and downregulate CD133 prior to and after formation of spheroids, respectively. This finding further supports the claim that cancer cells exhibit phenotypic plasticity in that under different conditions certain genes are upregulated or downregulated.[24, 26, 40] Additionally, due to high expression of CD133 being associated with tumor formation with and without ALDHA1 being present, it can be concluded that OVCAR-8 cells have a propensity for spheroid formation that supersedes that of SHIN-3. The results of the ELDA further support this conclusion because it was found that as little

as fifty OVCAR-8 cells were capable of producing 2.6X more spheroids than SHIN-3 cells plated at the same density.

Moreover, based on the formation of spheroids and/or aggregates in OVCAR-8, SHIN-3, and OVCAR-5, it was posited that CD44 expression is closely associated with increased propensity to form tumors in vitro. This finding was further supported by the lack of spheroid formation in OVCAR-3 cells, in which CD44 expression was undetectable. Furthermore, both CD44 and ALDHA1 were found to be consistently expressed in two-dimensional and three-dimensional culture of SHIN-3, while only CD44 was expressed in monolayer and spheroid culture of OVCAR-8. Thus, it was implied that when the expression of a CSC marker is unaffected by changes in culture format suggest that it is unique to those cells. Therefore, said CSC marker(s) can be used as a reference when assessing the expression and activity of enzymes and phenotypic changes within different samples.

Aside from CSCs, the phenotypic nature of each cell line was examined. It was found that cells presenting either dominant or partial mesenchymal nature in cell monolayers were more likely to form spheroids or aggregates under adhesion-free conditions. In addition, when relating these observations back to the proliferation rates of each cell line in monolayers the same correlation was found—a mesenchymal phenotype in monolayers resulted in increased proliferation. As with CSC, the shift from monolayer to spheroid culture revealed heterogeneity in OVCAR-8 and SHIN-3, with their spheroids displaying expression of epithelial and mesenchymal markers. The most noticeable shift in phenotype was observed in OVCAR-8 spheroids, which displayed enhanced epithelial nature—which was undetectable in monolayers. On the other hand, SHIN-3 continued to

display a mixed phenotype, but the expression of a different epithelial marker (i.e., E-cadherin) was observed. The degree of phenotypic heterogeneity observed in spheroids speaks to the plastic nature of the disease. It is likely that co-expression of epithelial and mesenchymal markers in spheroids is the result of some cells dedifferentiating so as to reacquire or move toward regaining epithelial functionality, while those harboring only mesenchymal features scurry to find new areas to invade.

4.5 References

1. Mitra, A.; Mishra, L.; Li, S., EMT, CTCs and CSCs in tumor relapse and drug-resistance. *Oncotarget* **2015,** *6* (13), 10697-10711.

2. Marjanovic, N. D.; Weinberg, R. A.; Chaffer, C. L., Cell plasticity and heterogeneity in cancer. *Clinical Chemistry* **2012**, clinchem. 2012.184655.

3. Meacham, C. E.; Morrison, S. J., Tumour heterogeneity and cancer cell plasticity. *Nature* **2013,** *501*, 328.

4. Singh, A.; Settleman, J., EMT, cancer stem cells and drug resistance: an emerging axis of evil in the war on cancer. *Oncogene* **2010,** *29*, 4741.

5. Torre, L. A.; Trabert, B.; DeSantis, C. E.; Miller, K. D.; Samimi, G.; Runowicz, C. D.; Gaudet, M. M.; Jemal, A.; Siegel, R. L., Ovarian cancer statistics, 2018. *CA: A Cancer Journal for Clinicians* **2018,** *68* (4), 284-296.

6. Burgos-Ojeda, D.; Rueda, B. R.; Buckanovich, R. J., Ovarian cancer stem cell markers: Prognostic and therapeutic implications. *Cancer Letters* **2012,** *322* (1), 1-7.

7. Curley, M. D.; Therrien, V. A.; Cummings, C. L.; Sergent, P. A.; Koulouris, C. R.; Friel, A. M.; Roberts, D. J.; Seiden, M. V.; Scadden, D. T.; Rueda, B. R., CD133 expression defines a tumor initiating cell population in primary human ovarian cancer. *Stem Cells* **2009,** *27* (12), 2875-2883.

8. Baba, T.; Convery, P.; Matsumura, N.; Whitaker, R.; Kondoh, E.; Perry, T.; Huang, Z.; Bentley, R.; Mori, S.; Fujii, S., Epigenetic regulation of CD133 and tumorigenicity of CD133+ ovarian cancer cells. *Oncogene* **2009,** *28* (2), 209.

9. Kryczek, I.; Liu, S.; Roh, M.; Vatan, L.; Szeliga, W.; Wei, S.; Banerjee, M.; Mao, Y.; Kotarski, J.; Wicha Max, S.; Liu, R.; Zou, W., Expression of aldehyde dehydrogenase

and CD133 defines ovarian cancer stem cells. *International Journal of Cancer* **2011,** *130* (1), 29-39.

10. Silva, I. A.; Bai, S.; McLean, K.; Yang, K.; Griffith, K.; Thomas, D.; Ginestier, C.; Johnston, C.; Kueck, A.; Reynolds, R. K.; Wicha, M. S.; Buckanovich, R. J., Aldehyde Dehydrogenase in Combination with CD133 Defines Angiogenic Ovarian Cancer Stem Cells That Portend Poor Patient Survival. *Cancer Research* **2011**.

11. Al-Hajj, M.; Wicha, M. S.; Benito-Hernandez, A.; Morrison, S. J.; Clarke, M. F., Prospective identification of tumorigenic breast cancer cells. *Proceedings of the National Academy of Sciences* **2003,** *100* (7), 3983.

12. Collins, A. T.; Berry, P. A.; Hyde, C.; Stower, M. J.; Maitland, N. J., Prospective identification of tumorigenic prostate cancer stem cells. *Cancer Research* **2005,** *65* (23), 10946-10951.

13. Li, C.; Heidt, D. G.; Dalerba, P.; Burant, C. F.; Zhang, L.; Adsay, V.; Wicha, M.; Clarke, M. F.; Simeone, D. M., Identification of Pancreatic Cancer Stem Cells. *Cancer Research* **2007,** *67* (3), 1030.

14. Dalerba, P.; Dylla, S. J.; Park, I.-K.; Liu, R.; Wang, X.; Cho, R. W.; Hoey, T.; Gurney, A.; Huang, E. H.; Simeone, D. M.; Shelton, A. A.; Parmiani, G.; Castelli, C.; Clarke, M. F., Phenotypic characterization of human colorectal cancer stem cells. *Proceedings of the National Academy of Sciences* **2007,** *104* (24), 10158.

15. Morath, I.; Hartmann, T. N.; Orian-Rousseau, V., CD44: More than a mere stem cell marker. *The International Journal of Biochemistry & Cell Biology* **2016,** *81*, 166-173.
16. Orian-Rousseau, V., CD44 Acts as a Signaling Platform Controlling Tumor Progression and Metastasis. *Frontiers in Immunology* **2015,** *6*, 154.

17. Alvero, A. B.; Chen, R.; Fu, H.-H.; Montagna, M.; Schwartz, P. E.; Rutherford, T.; Silasi, D.-A.; Steffensen, K. D.; Waldstrom, M.; Visintin, I., Molecular phenotyping of human ovarian cancer stem cells unravels the mechanisms for repair and chemoresistance. *Cell Cycle* **2009,** *8* (1), 158-166.

18. Alvero, A. B.; Fu, H. H.; Holmberg, J.; Visintin, I.; Mor, L.; Marquina, C. C.; Oidtman, J.; Silasi, D. A.; Mor, G., Stem-like ovarian cancer cells can serve as tumor vascular progenitors. *Stem Cells* **2009,** *27* (10), 2405-2413.

19. Hassan, H.; El-Sheemy, M., Adult bone-marrow stem cells and their potential in medicine. *Journal of the Royal Society of Medicine* **2004,** *97* (10), 465-471.

20. Lu, M.; Glover, C. H.; Tien, A. H.; Humphries, R. K.; Piret, J. M.; Helgason, C. D., Involvement of tyrosine kinase signaling in maintaining murine embryonic stem cell functionality. *Experimental Hematology* **2007,** *35* (8), 1293-1302.

21. Palmqvist, L.; Glover, C. H.; Hsu, L.; Lu, M.; Bossen, B.; Piret, J. M.; Humphries, R. K.; Helgason, C. D., Correlation of murine embryonic stem cell gene expression profiles with functional measures of pluripotency. *Stem Cells* **2005,** *23* (5), 663-680.

22. Luo, L.; Zeng, J.; Liang, B.; Zhao, Z.; Sun, L.; Cao, D.; Yang, J.; Shen, K., Ovarian cancer cells with the CD117 phenotype are highly tumorigenic and are related to chemotherapy outcome. *Experimental and Molecular Pathology* **2011,** *91* (2), 596-602.

23. Zhang, S.; Balch, C.; Chan, M. W.; Lai, H.-C.; Matei, D.; Schilder, J. M.; Yan, P. S.; Huang, T. H.; Nephew, K. P., Identification and characterization of ovarian cancer-initiating cells from primary human tumors. *Cancer Research* **2008,** *68* (11), 4311-4320.

24. Hudson, L. G.; Zeineldin, R.; Stack, M. S., Phenotypic plasticity of neoplastic ovarian epithelium: unique cadherin profiles in tumor progression. *Clinical & Experimental Metastasis* **2008,** *25* (6), 643-655.

25. Jiang, H.; Lin, X.; Liu, Y.; Gong, W.; Ma, X.; Yu, Y.; Xie, Y.; Sun, X.; Feng, Y.; Janzen, V., Transformation of epithelial ovarian cancer stemlike cells into mesenchymal lineage via EMT results in cellular heterogeneity and supports tumor engraftment. *Molecular Medicine* **2012,** *18* (8), 1197-1208.

26. Strauss, R.; Li, Z.-Y.; Liu, Y.; Beyer, I.; Persson, J.; Sova, P.; Möller, T.; Pesonen, S.; Hemminki, A.; Hamerlik, P.; Drescher, C.; Urban, N.; Bartek, J.; Lieber, A., Analysis of Epithelial and Mesenchymal Markers in Ovarian Cancer Reveals Phenotypic Heterogeneity and Plasticity. *PLOS ONE* **2011,** *6* (1), e16186.

27. Gardi, N. L.; Deshpande, T.; Kamble, S.; Budhe, S.; Bapat, S. A., Discrete Molecular Classes of Ovarian Cancer Suggestive of Unique Mechanisms of Transformation and Metastases. *Clinical Cancer Research* **2013**.

28. Hu, Y.; Smyth, G. K., ELDA: Extreme limiting dilution analysis for comparing depleted and enriched populations in stem cell and other assays. *Journal of Immunological Methods* **2009,** *347* (1), 70-78.

29. Madajewski, B.; Boatman, M. A.; Chakrabarti, G.; Boothman, D. A.; Bey, E. A., Depleting Tumor-NQO1 Potentiates Anoikis and Inhibits Growth of NSCLC. *Molecular Cancer Research* **2016,** *14* (1), 14-25.

30. Li, Z., CD133: a stem cell biomarker and beyond. *Experimental Hematology & Oncology* **2013,** *2* (1), 17.

31. Landen, C. N.; Goodman, B. W.; Katre, A. A.; Steg, A. D.; Nick, A. M.; Stone, R.; Miller, L.; Vivas-Mejia, P. E.; Jennings, N. B.; Gershenson, D. M.; Bast, R. C.; Coleman, R. L.; Lopez-Berestein, G.; Sood, A. K., Targeting Aldehyde Dehydrogenase Cancer Stem Cells in Ovarian Cancer. *Molecular Cancer Therapeutics* **2010**.

32. Hamilton, T. C.; Young, R. C.; McKoy, W. M.; Grotzinger, K. R.; Green, J. A.; Chu, E. W.; Whang-Peng, J.; Rogan, A. M.; Green, W. R.; Ozols, R. F., Characterization of a human ovarian carcinoma cell line (NIH: OVCAR-3) with androgen and estrogen receptors. *Cancer Research* **1983,** *43* (11), 5379-5389.

33. Haley, J.; Tomar, S.; Pulliam, N.; Xiong, S.; Perkins, S. M.; Karpf, A. R.; Mitra, S.; Nephew, K. P.; Mitra, A. K., Functional characterization of a panel of high-grade serous ovarian cancer cell lines as representative experimental models of the disease. *Oncotarget* **2016,** *7* (22), 32810-32820.

34. Sutherland, R. M., Cell and environment interactions in tumor microregions: the multicell spheroid model. *Science* **1988,** *240* (4849), 177.

35. Tayama, S.; Motohara, T.; Narantuya, D.; Li, C.; Fujimoto, K.; Sakaguchi, I.; Tashiro, H.; Saya, H.; Nagano, O.; Katabuchi, H., The impact of EpCAM expression on response to chemotherapy and clinical outcomes in patients with epithelial ovarian cancer. *Oncotarget* **2017,** *8* (27), 44312-44325.

36. Soler, A. P.; Knudsen, K.; Tecson-Miguel, A.; McBrearty, F.; Han, A.; Salazar, H., Expression of E-cadherin and N-cadherin in surface epithelial-stromal tumors of the ovary distinguishes mucinous from serous and endometrioid tumors. *Human Pathology* **1997,** *28* (6), 734-739.

37. Ma, S.; Tang, K. H.; Chan, Y. P.; Lee, T. K.; Kwan, P. S.; Castilho, A.; Ng, I.; Man, K.; Wong, N.; To, K.-F.; Zheng, B.-J.; Lai, P. B. S.; Lo, C. M.; Chan, K. W.; Guan, X.-Y., miR-130b Promotes CD133+ Liver Tumor-Initiating Cell Growth and Self-Renewal via Tumor Protein 53-Induced Nuclear Protein 1. *Cell Stem Cell* **2010,** *7* (6), 694-707.

38. You, H.; Ding, W.; Rountree, C. B., Epigenetic regulation of cancer stem cell marker CD133 by transforming growth factor-β. *Hepatology* **2010,** *51* (5), 1635-1644.

39. Ferrandina, G.; Martinelli, E.; Petrillo, M.; Prisco, M. G.; Zannoni, G.; Sioletic, S.; Scambia, G., CD133 antigen expression in ovarian cancer. *BMC Cancer* **2009,** *9* (1), 221.

40. Turley, E. A.; Veiseh, M.; Radisky, D. C.; Bissell, M. J., Mechanisms of Disease: epithelial–mesenchymal transition—does cellular plasticity fuel neoplastic progression? *Nature clinical practice. Oncology* **2008,** *5* (5), 280-290.

CHAPTER 5
SUMMARY, CONCLUSIONS, AND OUTLOOK

5.1 Summary

The goal of this research was to investigate tumorigenesis in ovarian cancer using two-dimensional and three-dimensional cell culture systems as a function of the expression and activity of cytoprotective enzyme, NQO1, and cell phenotype (i.e., stem-like, epithelial, mesenchymal, or mixed). The expression of NQO1 in four established ovarian cancer cell lines was characterized in monolayer culture using immunochemical (i.e., western blot and ICC/IF) and gene expression (i.e., RT-qPCR) techniques. Following determination of enzyme expression, its activity was quantified using enzyme kinetic studies and visualized with confocal microscopy using a NQO1-activated fluorescent probe. Culture-time-dependent proliferation studies were then used to evaluate whether NQO1 expression and activity were contributing to the proliferative ability of each cell line. Next, an in vitro tumor model was employed to investigate the propensity of the studied cell lines to form spheroids under anchorage-independent culture conditions. A detailed investigation was carried out to determine if the observed expression and activity of the NQO1 in cell monolayers was correlated with spheroid/aggregate formation. In addition, NQO1 expression and activity in spheroids were evaluated using western blot, enzyme kinetics, and probe activation. Finally, an assessment of the cell phenotype in monolayers and spheroids was conducted using immunochemical techniques (i.e., western blot and ICC/IF), and the findings of those studies were then reviewed to assess whether they were linked to NQO1 and spheroid forming ability.

In the first chapter of this work, it was revealed that increased NQO1 expression and activity was associated with ovarian cancer cell lines derived from patients prior to administration of chemotherapy. For instance, the expression of NQO1 was observable in SHIN-3 and OVCAR-5 cells with western blot; whereas, it was undetectable in OVCAR-8 and OVCAR-3 cell lines. Similarly, the activity of NQO1 in SHIN-3 and OVCAR-5 (untreated cell lines) cells was increased compared to that in OVCAR-8 and OVCAR-3 (treated cell lines). In addition, the NQO1-activated fluorescent probe Q_3NTCy was capable of distinguishing between the studied cell lines as function of their individual NQO1activity levels, which supported the findings of the enzyme kinetics study that assessed enzyme activity.

Also, a direct relationship was observed between culture-time-dependent NQO1 activity and proliferation in SHIN-3 and OVCAR-5 cells (i.e., high NQO1 activity and highly proliferative), and OVCAR-3 cells (i.e., low NQO1 activity and low proliferative ability) which suggested that changes in NQO1 activity are reflective of number of daughter cells present at different stages of growth. For example, the highest NQO1 activity and proliferative ability was observed in SHIN-3 cells, while OVCAR-3 cells had the lowest activity and proliferative ability. On the other hand, proliferation studies on OVCAR-8 cells contradicted this trend because they had second highest rate of proliferation after SHIN-3, but the measured NQO1 activity for days 3-7 of culture was roughly 5-9X lower than that of SHIN-3 cells. Despite this noticeable difference in culture-time-dependent NQO1 activity and proliferation in OVCAR-8, it was concluded that relative to OVCAR-3 cells, each of the remaining cell lines displayed increased NQO1 activity and proliferative ability.

Next, I sought to determine the ability of each of cell line to produce multicellular tumor spheroids under growth conditions that did not promote cell attachment to the culture dish (anchorage-independent conditions). The results of this study were as follows: OVCAR-8 and SHIN-3 cells produced compact and semi-compact spheroids, respectively, while OVCAR-5 cells produced loose aggregates. OVCAR-3 cells did not produce spheroids or aggregates in this study. It was concluded that cell lines with increased NQO1 activity are capable of spheroid/aggregate formation. To further support this conclusion, a stable knockdown of NQO1 was conducted using OVCAR-5 cells. It was found that such NQO1-depleted OVCAR-5 cells were neither able to form spheroids, nor achieve the degree of aggregation observed in wild type OVCAR-5 cells. Also, NQO1 expression was found to be enhanced in spheroids relative to monolayers in OVCAR-8 based on the presence of protein bands in western blot studies, whereas such bands were undetectable monolayers.

In addition, the expression of tumor suppressor p53, which has been shown to be stabilized by NQO1, was evaluated in each of the cell lines.[1-2] It was found that SHIN-3 and OVCAR-8 cells had increased expression of the p53 protein, while expressing low expression of the p53 gene. In addition, faint p53 protein expression was observed in OVCAR-3, despite it having the highest expression of the p53 gene compared to the other cell lines. While an inverse relationship between expression of the p53 gene and protein was observed in OVCAR-8, SHIN-3, and OVCAR-3 cells, a direct relationship was observed in OVCAR-5 cells where p53 gene expression was low and subsequent protein expression was undetectable. After reviewing the findings of the p53 gene and protein expression study, my initial conclusion regarding the ability of the studied cell lines to form

spheroids under anchorage-independent conditions held true. Furthermore, my conclusion was modified so as to highlight that NQO1 activity and proliferative ability greater than or equal to that observed in OVCAR-8 cells and expression of the p53 protein greater than or equal to that observed in OVCAR-5 cells was unique to cell lines capable of spheroid or aggregate formation.

Also, NQO1 activity in day-5 and day-12 SHIN-3 and OVCAR-8 spheroids was comparable to that of their monolayer formats at day 1 and day 2 of culture. Also, it was found that the NQO1-activatable probe Q_3NTCy enabled visualization of NQO1 activity in SHIN-3 and OVCAR-8 spheroids in as little as 30-minutes. It was observed that prolonged exposure (> 30 minutes) to Q_3NTCy resulted in increased reporter formation within spheroids, but due to their thickness, reporter formation at a depth greater than 100 μm into spheroids was not observed. Thus, visualizing all of the active NQO1 in an intact spheroid using the Q_3NTCy probe is not possible.

Another goal of this work was to evaluate the presence of CSCs and cell phenotype in monolayer and spheroid cultures of the previously mentioned cell lines. The findings of these studies were then examined to determine whether they could be related to outcomes from the previously discussed NQO1 studies. Initially, the presence of four CSC markers (i.e., CD117, CD133, CD44, and ALDHA1), which have been previously associated with tumor initiation in ovarian cancer, were investigated in cell monolayers by western blot and immunocytochemistry.[3-10] It was found that of the four markers, only CD133, CD44, and ALDHA1 were present in one or more of the cell lines in this study. Specifically, it was observed that CD133 was highly expressed in monolayers of OVCAR-8, OVCAR-5, and OVCAR-3 relative to SHIN-3. However, upon examination of spheroid

cultures, CD133 expression was no longer observed for spheroids of OVCAR-8. It was concluded that increased CD133 expression may be necessary for initiation of spheroid formation, but it may be downregulated once the spheroid is formed. CD44 was found to be expressed in monolayers of SHIN-3, OVCAR-5, and OVCAR-8, but not in those of OVCAR-3. This observation served as yet another noticeable distinction between OVCAR-3 cells and the other cell lines, which displayed increased NQO1 activity and proliferative ability in addition to spheroid/aggregate forming ability.

Furthermore, when comparing CD44 presence in SHIN-3 and OVCAR-8 monolayers to that of their spheroids, it is found that CD44 expression remained constant. Therefore, not only does CD44 impact spheroid formation, but its constant expression in monolayers and spheroids. The last CSC marker evaluated was ALDHA1. ICC/IF analysis revealed that only SHIN-3 and OVCAR-3 cell monolayers contained ALDHA1, but the localization of the enzyme was different. Specifically, ALDHA1 was observed in the cytosol of SHIN-3 cells, but it was found in the nucleus of OVCAR-3 cells. Because the enzyme is primarily localized in the cytosol, its presence in the nucleus a cell is surprising; thus assessment of active ALDHA1 enzyme in nuclei should conducted.[4] Aside from this, it was observed that co-expression of ALDHA1 and CD44 (i.e., SHIN-3) or CD44 alone (i.e., in OVCAR-8 and OVCAR-5) will result in spheroid or aggregate formation, which implies that these CSC markers have a significant role in disease progression and survival.

Aside from CSC presence, I also evaluated the phenotypic nature of each cell line—specifically by evaluating the expression of biomarkers associated with the epithelial-to-mesenchymal transition (EMT), which has been linked to tumor formation.[11-13] It was determined that monolayer cultures of OVCAR-8 cells presented a purely mesenchymal

phenotype (i.e., only expression of Vimentin and N-cadherin detected), while OVCAR-3 was purely epithelial based on observed expression of both EpCAM and E-cadherin. On the contrary, co-expression of epithelial and mesenchymal markers was observed in monolayers of OVCAR-5 and SHIN-3 cells, with the former exhibiting a dominant mesenchymal nature and a dominant epithelial phenotype in the latter. This conclusion stemmed from ICC/IF being capable of detecting low and high levels of EMT markers in both cell lines, but only those with enhanced expression being detected by western blot. In transitioning from monolayer to spheroid culture, it was found that OVCAR-8 and SHIN-3 spheroids possessed epithelial and mesenchymal characteristics. This observation was surprising for OVCAR-8 spheroids, because neither epithelial marker was detected in monolayers, yet both were present in spheroids. Therefore, it was concluded that as with studies of NQO1 in monolayers and spheroids, protein expression in one culture system may not dictate whether that protein is expressed in a different culture model.

5.2 Conclusions and Outlook

The work detailed in this dissertation demonstrates the role of NQO1 in spheroid formation and cell phenotype in four human ovarian cancer cell lines. In addition, the influence of the enzyme on the proliferative ability of was also assessed. It was concluded that SHIN-3, OVCAR-5, and OVCAR-8 cells possessed enhanced NQO1 activity, were highly proliferative, and capable of spheroid/aggregate formation under anchorage-independent conditions. Further analysis revealed that while cancer stem cell markers were expressed in each cell line, CD44 presence was unique to OVCAR-5, SHIN-3, and OVCAR-8 cells in monolayers. In addition, a mixed or mesenchymal phenotype was observed in cell lines that expressed CD44. Therefore, it was concluded that expression

of cancer stem cell marker CD44, a mixed or mesenchymal phenotype, and enhanced NQO1 activity relative to OVCAR-3 cells provides a basis for spheroid/aggregate formation in vitro. In addition, cells possessing the aforementioned characteristics were found to be highly proliferative in monolayer culture. Figure 5.1 below was constructed to illustrate major findings in this work.

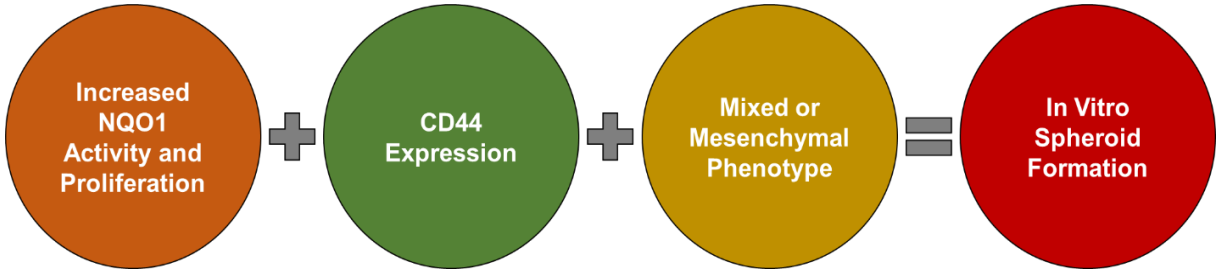

Figure 5.1. Visual representation of research findings.

The work presented in this document has the potential to serve as a template for characterizing cancer stem cells as a function of presence and the activeness of disease-associated enzymes because it could result in the development of new diagnostic and therapeutic targets. However, it is imperative that variations in the expression of cancer stem cell biomarkers between in vitro (i.e., traditional monolayer and anchorage independent/dependent spheroid culture), in vivo (i.e., mouse models), and ex-vivo (i.e., biopsied samples) systems are identified, so as to give researchers a better depiction of which models are suitable for evaluation of cancer cells. The rationale is based on it being reported that gene expression profiles in cell monolayers are not entirely reflective of what is observed once those cells are cultured spheroid models or in vivo.[14-15] Based on the findings presented in this dissertation, the expression of some cancer stem cell markers is not always affected by different culture conditions. Therefore, it is beneficial to assess

the expression and activity of enzymes present in cells that express said CSC markers. This would be advantageous for drug developers because constantly expressed CSC markers can serve as internal positive control or calibrator genes when comparing significant changes in gene expression of target molecules in samples, prior to and after treatment with anticancer agents or radiation therapy.

5.3 References

1. Asher, G.; Lotem, J.; Kama, R.; Sachs, L.; Shaul, Y., NQO1 stabilizes p53 through a distinct pathway. *Proceedings of the National Academy of Sciences* **2002,** *99* (5), 3099-3104.

2. Asher, G.; Lotem, J.; Cohen, B.; Sachs, L.; Shaul, Y., Regulation of p53 stability and p53-dependent apoptosis by NADH quinone oxidoreductase 1. *Proceedings of the National Academy of Sciences* **2001,** *98* (3), 1188-1193.

3. Martinez-Cruzado, L.; Tornin, J.; Santos, L.; Rodriguez, A.; García-Castro, J.; Morís, F.; Rodriguez, R., Aldh1 Expression and Activity Increase During Tumor Evolution in Sarcoma Cancer Stem Cell Populations. *Scientific Reports* **2016,** *6*, 27878-27878.

4. Tomita, H.; Tanaka, K.; Tanaka, T.; Hara, A., Aldehyde dehydrogenase 1A1 in stem cells and cancer. *Oncotarget* **2016,** *7* (10), 11018-11032.

5. Ferrandina, G.; Martinelli, E.; Petrillo, M.; Prisco, M. G.; Zannoni, G.; Sioletic, S.; Scambia, G., CD133 antigen expression in ovarian cancer. *BMC Cancer* **2009,** *9* (1), 221.

6. Curley, M. D.; Therrien, V. A.; Cummings, C. L.; Sergent, P. A.; Koulouris, C. R.; Friel, A. M.; Roberts, D. J.; Seiden, M. V.; Scadden, D. T.; Rueda, B. R., CD133 expression defines a tumor initiating cell population in primary human ovarian cancer. *Stem Cells* **2009,** *27* (12), 2875-2883.

7. Baba, T.; Convery, P.; Matsumura, N.; Whitaker, R.; Kondoh, E.; Perry, T.; Huang, Z.; Bentley, R.; Mori, S.; Fujii, S., Epigenetic regulation of CD133 and tumorigenicity of CD133+ ovarian cancer cells. *Oncogene* **2009,** *28* (2), 209.

8. Strauss, R.; Li, Z.-Y.; Liu, Y.; Beyer, I.; Persson, J.; Sova, P.; Möller, T.; Pesonen, S.; Hemminki, A.; Hamerlik, P.; Drescher, C.; Urban, N.; Bartek, J.; Lieber, A., Analysis of Epithelial and Mesenchymal Markers in Ovarian Cancer Reveals Phenotypic Heterogeneity and Plasticity. *PLOS ONE* **2011,** *6* (1), e16186.

9. Burgos-Ojeda, D.; Rueda, B. R.; Buckanovich, R. J., Ovarian cancer stem cell markers: Prognostic and therapeutic implications. *Cancer Letters* **2012,** *322* (1), 1-7.

10. Luo, L.; Zeng, J.; Liang, B.; Zhao, Z.; Sun, L.; Cao, D.; Yang, J.; Shen, K., Ovarian cancer cells with the CD117 phenotype are highly tumorigenic and are related to chemotherapy outcome. *Experimental and Molecular Pathology* **2011,** *91* (2), 596-602.

11. Nieto, M. A., Context-specific roles of EMT programmes in cancer cell dissemination. *Nature Cell Biology* **2017,** *19*, 416.

12. Chaffer, C. L.; San Juan, B. P.; Lim, E.; Weinberg, R. A., EMT, cell plasticity and metastasis. *Cancer and Metastasis Reviews* **2016,** *35* (4), 645-654.

13. Nieto, M. A.; Huang, Ruby Y.-J.; Jackson, Rebecca A.; Thiery, Jean P., EMT: 2016. *Cell* **2016,** *166* (1), 21-45.

14. Mueller-Klieser, W., Multicellular spheroids. *Journal of Cancer Research and Clinical Oncology* **1987,** *113* (2), 101-122.

15. Kunz-Schughart, L. A., Multicellular tumor spheroids: intermediates between monolayer culture and in vivo tumor. *Cell Biology International* **1999,** *23* (3), 157-161.

VITA

Milcah Jackson is native of Canton, MS. In August 2010, she pursed an undergraduate degree in Biochemistry with a minor in English at the University of Mississippi. She received her Bachelor of Arts (B.A., cum laude) degree in May 2014. In August 2014, she enrolled in the doctoral program in the Department of Chemistry at Louisiana State University in Baton Rouge, LA. In January 2015, she joined the research group of Prof. Robin L. McCarley. During her tenure, she was awarded the National Science Foundation Louis Stokes Alliance for Minority Participation (NSF-LSAMP) Bridge to the Doctorate Fellowship in 2014, and the National Science Foundation Graduate Research Fellowship (NSF-GRFP) in 2016. She plans to receive her Doctor of Philosophy degree (Ph.D.) at the summer 2019 commencement ceremony.